STATE WATER SURVEY DIVISION
LIBRARY COPY

REPORT OF INVESTIGATION NO. 28 1955

STATE OF ILLINOIS

WILLIAM G. STRATION, *Governor*

DEPARTMENT OF REGISTRATION AND EDUCATION

VERA M. BINKS, *Director*

RADAR BACK-SCATTERING FROM NON-SPHERICAL SCATTERERS

PART 1

CROSS-SECTIONS OF CONDUCTING PROLATES AND SPHEROIDAL FUNCTIONS

PART 11

CROSS-SECTIONS FROM NON-SPHERICAL RAINDROPS

BY

Prem N. Mathur and Eugam A. Mueller

STATE WATER SURVEY DIVISION

A. M. BUSWELL, *Chief*

URBANA ILLINOIS

(Printed by authority of State of Illinois)

179

STATE OF ILLINOIS

WILLIAM G. STRATTON, *Governor*

DEPARTMENT OF REGISTRATION AND EDUCATION

VERA M. BINKS, *Director*

RADAR BACK-SCATTERING FROM NON-SPHERICAL SCATTERERS

PART 1

CROSS-SECTIONS OF CONDUCTING PROLATES AND SPHEROIDAL FUNCTIONS

PART 11

CROSS-SECTIONS FROM NON-SPHERICAL RAINDROPS

BY

Prem N. Mathur and Eugene A. Mueller

STATE WATER SURVEY DIVISION

A. M. BUSWELL, *Chief*

URBANA, ILLINOIS

(Printed by authority of State of Illinois)

Definitions of Terms

Part I

b = semi minor axis of spheroid

a = semi major axis of spheroid

λ = wavelength of incident field

$\alpha = \frac{2\pi b}{\lambda}$ = = a measure of size of particle

$\xi, \eta, \phi,$ prolate spheroidal coordinates

e = eccentricity of ellipse

$S_{mn}(\eta)$ = angular spheroidal functions

P_{me}^{m} = Legendse polynomials

d_{n}^{mn} = expansion coefficients

$R_{mn}^{(m)}$ = radial spheroidal functions

J_{m+n} = spherical Bessel functions

$\bar{E}$ = electric field vector

$\bar{H}$ = magnetic field vector

σ = back scattering cross section

σ_g = geometric back scattering cross section

Part II

b = semi minor axis of spheroid

c = semi major axis of spheroid

S = Poynting vector

$\alpha = \frac{2\pi c}{\lambda}$ = measure of size of spheroid

λ = wavelength of the radiation

σ = back scattering cross section

$\ell, \ell_1, \ell_2, m, m_1, m_2, n, n_1, n_2,$ = direction no's of incident field and body coordinates

x, y, z = body coordinates

$\bar{E}$ = electric field

$\bar{H}$ = magnetic field

Ω = angle of polarization of scattered field in body coordinates

ϕ = angle of polarization of incident field in body coordinates

ϵ = dielectric constant of scatterer

TABLE OF CONTENTS

Appendices

ACKNOWLEDGEMENT

The authors wish to acknowledge the assistance of James Primm, D. M. Sen, Richard Duncan and Ruth Cipelle in computations and checking of the numerical work and F. A. Huff for reviewing the manuscript. Thanks are also due Douglas M. A. Jones and Lois Bivans for their suggestions regarding practical evaluations. Drafting was performed by Phillip Nuccio. This investigation was conducted under the supervision of G. E. Stout, Head, Meteorology Subdivision.

PART I

ABSTRACT

Studies were made of the scattering from non-spherical targets by making exact determination of the nose-on radar back scattering cross sections of conducting prolate spheroids of various sizes and shapes. The scattering coefficients and several complex prolate spheroidal functions appearing in the analysis have been computed. Numerical data, which are of importance in other similar studies of radar scattering, acoustic and ballastic scattering and antenna radiation problems involving prolates of dimensions below the resonance region, are reported.

Curves are given for the back scattered cross sections as a function of non-dimensional size and shape parameters for prolate spheroids. The results are compared with the Rayleigh-Gans first order approximation and Stevenson's third order approximation and the range of applicability of these approximations is evaluated.

The results indicate a substantial decrease in the radar echo as the shape of the equivolumetric targets vary from spherical to thin prolate spheroidal shapes. For a prolate of axis ratio b/a = 0.8 and α = 0.8, the ratio $\sigma_{prolate} / \sigma_{sphere}$ is about 1/2 and decreases to a value of approximately 1/200 for a prolate spheroid of axis ratio b/a = 0. 2, α = 0. 8.

Rayleigh-Gans first order approximation is not adequate for the size range $\alpha > 0.3$. However, Stevenson's third order solution yields results nearly identical with the exact values in the size range $\alpha < 1.0$.

INTRODUCTION

Development of Problem

In 1950, the Illinois State Water Survey initiated an investigation to determine the utility of radar for the quantitative measurement of rainfall over watersheds. Early in this investigation it became apparent that available data were insufficient to accurately determine the effects on radar-rainfall estimates, which arise from variations in the size and distribution of raindrops between and within storms. Because available techniques for the determination of storm drop size distribution were inadequate for the existing needs, a raindrop camera was designed and constructed. Development was completed in 1953 and routine observations made during 1953-54.

As raindrop data were collected, it became apparent that the majority of large drops within storms are non-spherical. Since these large drops contribute greatly to the reflectivity and attenuation from rain, a need was created for theoretical data to more accurately compute the reflectivity from storms.

Existing Solutions to Problem

Exact solutions of the problem of scattering of electromagnetic waves by non-spherical particles have been obtained only in a few cases. Contributions to this problem were made by Hertzfeld[1] and Moglich[2], who attacked the problem by methods of exact analysis. However, their solutions are formal ones and a great deal of work is required to reduce them to calculable forms. Schultz[3] obtained an exact solution for the spherical case of a conducting prolate with nose-on incidence. Even for this case the calculations are quite involved and tedious. Siegel, Gere, Marx and Sleator[4] have made a radar scattering study from this solution for a thin prolate (axis ratio 10;1).

Gans[5] and Rayleigh[6] obtained first-order solutions for the problem on the assumption that the characteristic dimensions of the scatterers are very small compared to the wavelength of the incidence radiation. This limitation of size is a serious one, and the results, while reasonable and useful, are of uncertain accuracy in detail. More recently, Stevenson[7] has extended these solutions to third-order terms. With the exception of the range of validity of this higher order approximation, his solution is quite general.

Scope of Investigation

To meet the existing need for more theoretical information, an investigation was undertaken to study the scattering of electromagnetic waves by non-spherical objects. This report covers the first part of this investigation, in which an evaluation was made of the range of applicability of the first-order Gans theory (presently in use) and the more recent third-order solution of Stevenson's against an exact solution for conducting prolates.

The second part of this report covers the development of formulas for back scattering and attenuation cross-sections for oblate and prolate raindrops, using Stevenson's field solutions. The results of this development are being used to make practical evaluations for raindrops at 3-cm wavelength in the size range, $\alpha = 0.1$ to $\alpha = 0.9$, from raindrop camera storm samples.

THEORY

Solutions of the scaler wave equation are required in several tields, including electromagnetic wave theory and elasticity theory. The desired solutions for the vector wave equation can be constructed [4,8] from solutions of the scaler wave equation of the form:

$$\nabla^2\psi + k^2\psi = 0 \tag{1}$$

The partial differential equation can be solved by the method of separation of variables using a coordinate system appropriate to the geometry of the problem.

Prolate Spheroidal Coordinates

The boundary value problems involving prolates may be treated in Prolate Spheroidal coordinates ξ , η , ϕ .

In this system the coordinate surfaces are two families of orthogenal surfaces of revolution. The surfaces of constant ξ are a family of confocal prolate spheroids, and the surfaces of constant η are a family of confocal hyperboloids of revolution (See Figure 1).

With the z-axis as the axis of revolution and ϕ the azimuthal angle measured about this axis, the equations of transformation from this system to Cartesian coordinates become:

$$\begin{aligned} x &= d/2\sqrt{(\xi^2 - 1)(1 - \eta^2)} \cdot \cos\phi \\ y &= d/2\sqrt{(\xi^2 - 1)(1 - \eta^2)} \cdot \sin\phi \\ z &= d/2\ \xi\eta \end{aligned} \tag{2}$$

where d is the interfocal distance FF' and ξ , η and ϕ vary in the range $1 \leq \xi \leq \infty$; $-1 \leq \eta \leq +1$ and $0 \leq \phi \leq 2\pi$

If 'a' is the semi-major axis, 'b' is the semi-minor axis and 'e' is the eccentricity of the generating ellipse, equation (2), along with the definition of eccentricity, yields:

$$e = (1 - b^2/a^2)^{1/2} = 1/\xi = d/2a \tag{3}$$

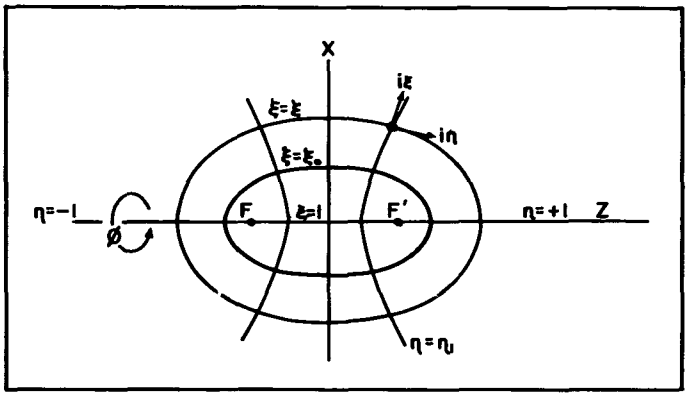

FIG. 1 - PROLATE SPHEROIDAL COORDINATES

The radial distance from any point (x, y, z) in space to the origin is

$$r = (x^2 + y^2 + z^2)^{1/2} = 1/2\ d\ (\xi^2 + \eta^2 - 1)^{1/2} \tag{4}$$

The relations between the unit vectors, i's,in cartesian and Prolate Spheroidal coordinated are as follows:

$$i_\eta = i_x\ (P.\ \cos\phi) + i_y\ (P.\ \sin\phi) + i_z\ (Q)$$

$$i_\xi = i_x\ (Q.\ \cos\phi) + i_y\ (Q.\ \sin\phi) - i_z\ (P)$$

$$i_\phi = i_x\ (-\ \sin\phi) + i_y\ (\cos\phi)$$

and (4)a

$$i_x = i_\eta\ (P.\ \cos\phi) + i_\xi\ (Q.\ \cos\phi) - i_\phi\ (\sin\phi)$$

$$i_y = i_\eta\ (P.\ \sin\phi) + i_\xi\ (Q.\ \sin\phi) + i_\phi\ (\cos\phi)$$

$$i_z = i_\eta\ (Q)\ -i_\xi\ (P).$$

where

$$P = -\eta(\xi^2 - 1)^{1/2}\ (\xi^2 - \eta^2)^{-1/2}$$

$$Q = \xi\ (1 - \eta^2)^{1/2}\ (\xi^2 - \eta^2)^{-1/2}$$

Basic Definitions

Parameters c, α. To present the results in a general form, it is convenient to represent the characteristic dimensions of the prolate

(semi-interfocal distance d or semi-major-axis a) by the non-dimensional parameters:

$$c = k\,d/2 = \pi\,d/\lambda \tag{5}$$

$$\alpha = k\,a = 2\pi a/\lambda \tag{6}$$

where k is the wave number $2\pi/\lambda$ and λ is the wavelength of the incident radiation.

Back-Scattering Cross Section. The back-scattering cross-section is defined as the ratio of the power radiated by an isotropic source, which is radiating with the same intensity as the particle does in the backward direction, to the incident energy density.

Geometrical Cross Section. To present the results in non-dimensional form, the back-scattering cross-section defined above is divided by a geometrical cross-section σ_G, obtained by the method of geometrical optics. σ_G is defined as:

$$\sigma_G = \pi\,R_1 \cdot R_2 \tag{7}$$

where R_1 and R_2 are the principal radii of curvature at the point of reflection. For the case of a prolate with nose-on incidence, $R_1 = R_2 = b^2/a$, and

$$\sigma_G = \pi \cdot b^4/a^2 \tag{8}$$

Scaler Wave Equation

The scaler Hemoltz's equation (Eq. 1) in prolate spheroidal coordinates ξ, η, ϕ becomes:

$$\frac{\partial}{\partial\eta}\left[(\eta^2-1)\frac{\partial\psi}{\partial\eta}\right] + \frac{\partial}{\partial\xi}\left[(\xi^2-1)\frac{\partial\psi}{\partial\xi}\right] + \left(\frac{1}{1-\eta^2} + \frac{1}{\xi^2-1}\right)\frac{\partial^2\psi}{\partial\phi^2} + c^2(\eta^2-\xi^2)\psi = 0 \tag{9}$$

where $c = k\,d/2$, $k = 2\pi/\lambda$ and λ is the wavelength. Equation (9) can be separated into three second order, linear, ordinary differential equations if we assume a solution of the form

$$\psi = R(\xi) \cdot S(\eta) \cdot \varphi(\phi) \tag{10}$$

The substitution of equation (10) into (9) yields:

$$\frac{d^2\psi}{d\phi^2} + m^2 \psi = 0 \tag{11}$$

$$\frac{d}{d\eta}(\eta^2-1)\frac{dS}{d\eta} + \left[A_{ml} - c^2\eta^2 - \frac{m^2}{\eta^2-1} \right] S = 0 \tag{12}$$

$$\frac{d}{d\xi}(\xi^2-1)\frac{dR}{d\xi} + \left[A_{ml} - c^2\xi^2 - \frac{m^2}{\xi^2-1} \right] R = 0 \tag{13}$$

where m, A_{ml} are the separation constants with m restricted to integral values to insure single values.

Solutions of Scaler Wave Equation

In order to obtain the solution of the wave equation, it is convenient to study the individual solutions of Equations (11), (12), and (13). The complete solution of the wave equation can then be formed by Equation (10).

The solution of Equation (11) is A sin $m\phi$ + B cos $m\phi$ where m is restricted to integral values and A and B are constants.

Angular Functions and their Integrals. Equation (12) may be satisfied by an expansion in terms of associated Legendre polynomials $P_n^{m+m(n)}$. The expansion for the angular functions of the first kind, which are regular in the range $-1 \leq \eta \leq 1$, according to Morse [10] is:

$$S_{ml}^{(1)}(\eta) = \sum_{n=0,1}^{\infty}{}' d_n^{ml} \quad P_{n+m}^{m}(\eta) \tag{14}$$

where d_n^{ml} are the expansion coefficients. Their numerical values for m = j, l = 3-j, with j taking values 0, 1, 2 and 3, have been tabulated in reference (9). The primes on the summation sign denote that the summation is to be taken over even values of n if l is even, and over odd values of n if l is odd. The associated Legendre functions are tabulated in reference (11).

For the special case $\eta = 1$, Equation (14) reduces to:

$$S_{ol}^{(1)}(1) = \sum_{n=0}^{\infty}{}' d_n^{ol} \quad ; \quad S_{ml}^{(1)}(1) = 0 \text{ for } \quad m \geq 1 \tag{15}$$

The angular functions corresponding to a given value of c are orthogenal in the interval (-1, 1). The orthogonality relation is:

$$I_1^{ml} = \int_{-1}^{+1} S_{ml}^{(1)}(\eta) \quad S_{kl}^{(1)}(\eta) \cdot d\eta = \begin{cases} 0 & \text{for } m \neq k \\ N_{ml} & \text{for } m = k \end{cases} \tag{16}$$

where $$N_{ml} = \sum_{n=0,1}^{\infty}{}' \frac{(2m+n)!}{n!\,(2m+2n+1)} \left(d_n^{ml}\right)^2$$

The numerical values of the normalizing factors N_{ml} for m = O, 1 = 0, 1, 2 and c = .1, .2, .4, .6 and 0.8 are given in Table XVI.

Other important integrals involving the angular spheroidal functions and their derivatives are:

$$I_2^{l2} = \int_{-1}^{+1} \eta (1-\eta^2)^{-\frac{1}{2}} S_{1l}^{(1)}(\eta)\, S_{0L}^{(1)}(\eta)\cdot d\eta \;;\; I_3^{l2} = \int_{-1}^{+1} \eta \cdot S_{0l}^{(1)}(\eta)\cdot S_{0L}^{(1)}(\eta)\cdot d\eta$$

and $$I_4^{l2} = \int_{-1}^{+1} (1-\eta^2) S_{0l}^{(1)\prime}(\eta)\cdot S_{0L}^{(1)}(\eta)\, d\eta \;;\; I_5^{l2} = \int_{-1}^{+1} (1-\eta^2)^{\frac{1}{2}} S_{1l}^{(1)}(\eta)\cdot S_{0L}^{(1)}(\eta)\, d\eta \qquad (17)$$

$$I_6^{l2} = \int_{-1}^{+1} \eta (1-\eta^2)^{\frac{1}{2}} S_{1l}^{(1)\prime}(\eta)\cdot S_{0L}^{(1)}(\eta)\cdot d\eta$$

where the primes on the angular functions denote the differentiation with respect to n. The values of these integrals, evaluated by Schultz [3] in terms of the expansion coefficients d_n^{ml}, are given in Appendix A.

Radial Functions. Equation (13) is satisfied by an expansion in spheroidal Bessel functions with coefficients involving the tabulated expansion coefficients, d_n^{ml}. These expressions, given by Stratton, Morse, Chu and Hunter [9] are:

$$R_{ml}^{(1)}(c,\xi) = \frac{(\xi^2-1)^{m/2}}{\xi^m \sum_{n=0,1}^{\infty}{}' d_n^{ml} \frac{(2m+n)!}{n!}} \sum_{n=0,1}^{\infty}{}' (i)^{l-n} d_n^{ml} \frac{(2m+n)!}{n!}\, j_{m+n}(c,\xi) \qquad (18)$$

where $j_{m+n}(c,\xi) = \sqrt{\frac{\pi}{2c\xi}}\, J_{m+n+\frac{1}{2}}(c,\xi)$, is the spherical Bessel function of the first kind. The cylindrical Bessel functions of half order, $J_{m+n+1/2}(c\xi)$, are tabulated in reference (12).

A second solution is obtained simply by replacing $j_{m+n}(c\xi)$ with the spherical Bessel function of the second kind, $n_{m+n}(c\xi)$. The expansion obtained is, however, slowly convergent when m is large or when ξ is equal to or nearly equal to one. An alternate expansion in terms of Legendre polynomials of the first and second kind, given by Stratton et al,[9] is more suitable to use. This expansion is given as follows:

$$R_{ml}^{(2)}(c,\xi) = G(c,m,l)\left\{ \sum_{n=-\infty}^{\substack{-2m-1 \\ \text{or} \\ -2m-2}}{}' \frac{d_n^{ml}}{\rho} \left[P_{-n-m+1}^{m}(\xi)\right] + \sum_{\substack{n=-2m+1 \\ \text{or} \\ -2m}}^{\infty}{}' d_n^{ml} \left[Q_{m+n}^{m}(\xi)\right] \right\} \qquad (19)$$

where for l even

$$G(c,m,l) = \frac{2\, c^{m-l}\, \Gamma\left(\frac{l+2m+1}{2}\right)}{\Gamma\left(\frac{l+2}{2}\right)\Gamma\left(m-\frac{1}{2}\right) d_{-2m}^{ml} \sum_{n=0}^{\infty}{}' d_n^{ml} \frac{(2m+n)!}{n!}} \qquad (20)$$

and, for l odd

$$G(c,m,l) = \frac{-8c^{m-2}\,\Gamma\left(\frac{l+2m+2}{2}\right)}{\Gamma\left(\frac{l+1}{2}\right)\Gamma(m-3/2)\,d_{l-2m}^{ml}\sum_{n=b}^{\infty}{}' d_n^{ml}\frac{(2m+n)!}{n!}} \tag{21}$$

The values of $\frac{d_n^{ml}}{P}$ are listed in reference (9). for negative values of n.

The derivatives of the radial functions are given by the expression·

$$R_{ml}^{(1)\prime}(c,\xi) = \frac{m\,R_{ml}^{(1)}(c,\xi)}{\xi(\xi^2-1)} + \frac{(1-\frac{1}{\xi^2})^{m/2}}{\sum_{n=0,1}^{\infty}{}' i^{l-n} d_n^{ml}\frac{(2m+n)!}{n!}}\sum_{n=0,1}^{\infty}{}' i^{l-n} d_n^{ml}\frac{(2m+n)!}{n!}\,j'_{m+n}(c\xi) \tag{22}$$

where

$$j'_{m+n}(c\xi) = \frac{d}{d\xi}(j_{m+n}) = \frac{c}{(2m+2n+1)}\left[(m+n)j_{m+n-1} - (m+n+1)j_{m+n+1}\right] \tag{23}$$

The primes on the radial functions $R_{ml}^{(\,)}$ denote the derivatives with respect to ξ

Also
$$R_{ml}^{(2)\prime}(c,\xi) = G(c,m,l)\cdot\left\{\sum_{n=-\infty}^{-2m-2\ \text{or}\ -2m-1}{}' \frac{d_n}{P}^{ml}\frac{d}{d\xi}\left[P_{-n-m-1}^{m}(\xi)\right] - \sum_{n=-2m+1\ \text{or}\ -2m}^{\infty}{}' d_n^{ml}\frac{d}{d\xi}\left[Q_{m+n}^{m}(\xi)\right]\right\} \tag{24}$$

The radiar functions of the first, second and fourth kind and their derivatives for m = 0, 1, l= 0, 1, 2 are computed for 16 combinations of ξ and c ; ξ =1.1, 1.1546, 1.2, 1. 3, and c = 0.1, 0.2, 0.4, 0.6 and 0.8. The numerical results are presented in tables I - VIII.

By analogy of Hankel functions, prolate spheroidal functions of the third and fourth kind may be formed as:

$$R_{ml}^{(3)}(c,\xi) = R_{ml}^{(1)}(c,\xi) + i\,R_{ml}^{(2)}(c,\xi) \tag{25}$$

$$R_{ml}^{(4)}(c,\xi) = R_{ml}^{(1)}(c,\xi) - i\,R_{ml}^{(2)}(c,\xi) \tag{26}$$

The asymptotic formulas for these functions for $c\xi \to \infty$ are:

$$R_{ml}^{(1)}(c,\xi) \simeq \frac{1}{c\xi}\cos\delta_{ml}\ ;\ R_{ml}^{(2)}(c,\xi) \simeq \frac{1}{c\xi}\sin\delta_{ml} \tag{27}$$

$$R_{ml}^{(3)}(c,\xi) \simeq \frac{1}{c\xi}e^{i\delta_{ml}}\ ;\quad R_{ml}^{(4)}(c,\xi) \simeq \frac{1}{c\xi}e^{-i\delta_{ml}}$$

where $$\delta_{ml} = \left(c\xi - \frac{m+l+1}{2}\pi \right) \tag{28}$$

The asymptotic behavior of the derivatives of these functions may be obtained by differenting the above equation :

$$R_{ml}^{(1)\prime}(c,\xi) \simeq -\frac{1}{\xi} \cdot \sin \delta_{ml} \tag{29}$$

$$R_{ml}^{(2)\prime}(c,\xi) \simeq \frac{1}{\xi} \cdot \cos \delta_{ml} \tag{30}$$

Solutions of Vector Wave equation

From the solutions of the scaler equation, solutions of the vector equation[8,14]

$$\nabla \times \nabla \times \bar{F} - \nabla(\nabla \cdot \bar{F}) - k^2 \bar{F} = 0 \tag{31}$$

can be obtained by using the formula

$$\bar{F}_1 = \nabla\psi ; \quad \bar{F}_2 = \nabla \times \bar{a}\psi ; \quad F_3 = \frac{1}{k} \nabla \times \bar{F}_2 \text{ or } \bar{F}_2 = \frac{1}{k} \nabla \times \bar{F}_3 \tag{32}$$

where a is a constant unit vector. Any pair of these vector solutions forms a complete set of orthogonal functions

SCATTERING CROSS-SECTIONS

Using the prolate spheroidal function theory, Schultz [3] has obtained an exact solution of scattering of electromagnetic waves by a conducting prolate for the case when the radar beam strikes the prolate nose-on. The orientation of the incident beam with respect to the coordinates of the prolate spheroid is shown in figure 2.

Note: Numerical values of the derivatives of the spherical Bessel Functions, $j_m' = \frac{d}{d\xi}(j_m)$, are reported in Table XV.

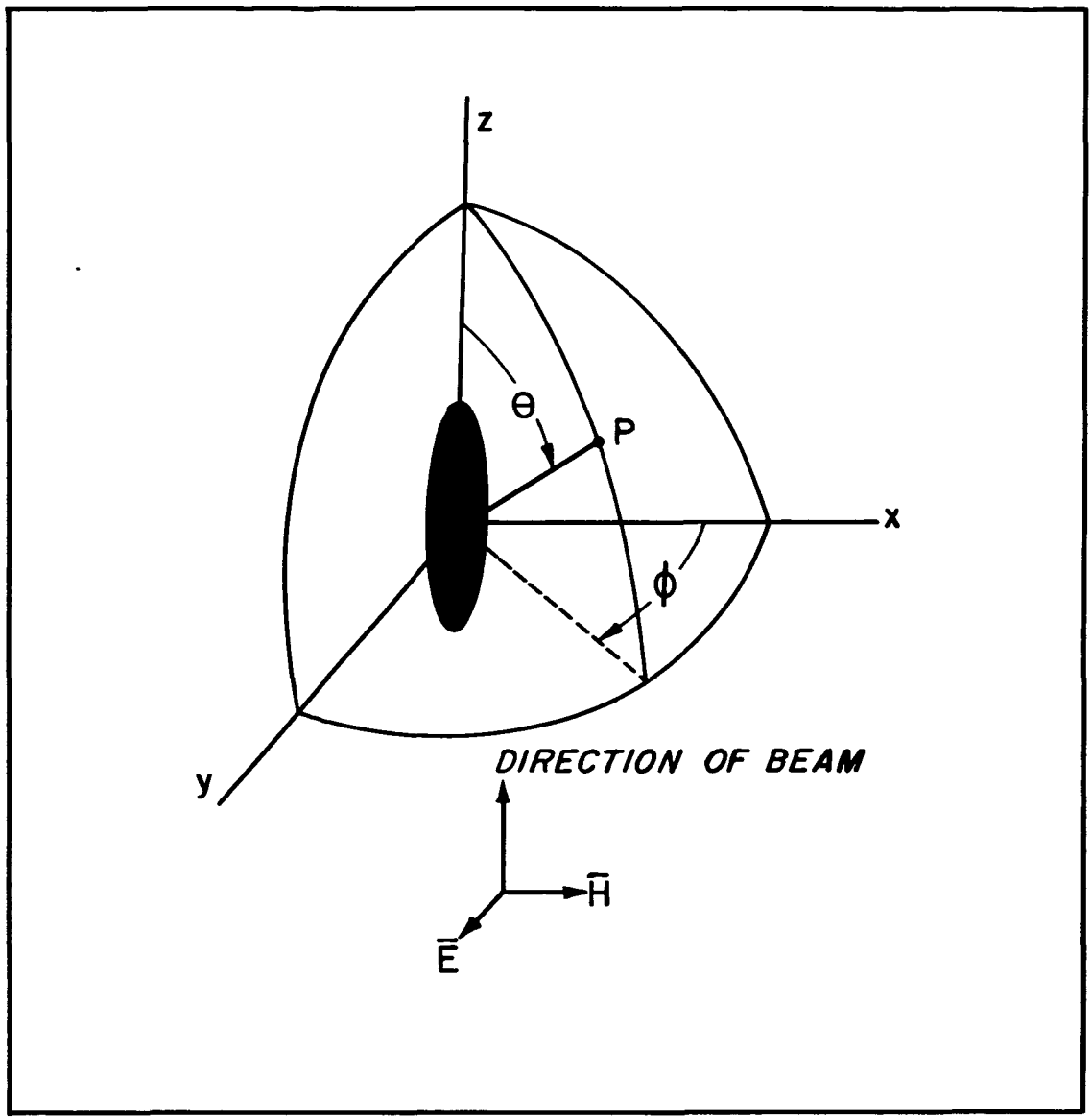

FIG. 2 - ORIENTATION OF THE SCATTERER AND THE INCIDENT FIELD IN BODY COORDINATES

The general expression for the scattering cross-section, $\sigma(\eta, \phi)$, from Schultz's solution [3] [4] is given as follows:

$$\frac{\sigma(\eta,\phi)}{4\pi a^2} = \left| \sum_{l=0,1}^{\infty} i^l \alpha_{0l} S_{0l}^{(1)}(\eta) \right|^2 \sin^2\phi + \left| \sum_{l=0,1}^{\infty} i^l \alpha_{0l} \eta S_{0l}^{(1)}(\eta) - i\beta_{1l}\sqrt{1-\eta^2}\, S_{1l}^{(1)}(\eta) \right|^2 \cos^2\phi \quad (33)$$

where α_{0l}, β_{1l} are obtained* from the solutions of the simultaneous equations;

$$\sum_{l=0}^{\infty} (\alpha_{0l} C_{Ll} + \beta_{1l} D_{Ll}) = \sum_{l=0}^{\infty} B_{Ll} \quad (34a)$$

$$\sum_{l=0}^{\infty} (\alpha_{0l} V_{Ll} + \beta_{1l} W_{Ll}) = \sum_{l=0}^{\infty} U_{Ll} \quad (34b)$$

and the coefficients C_{L1}, D_{L1}, B_{L1}, U_{L1}, V_{L1} and W_{L1} are functions of ξ, radial functions, their derivatives and boundary integrals of angular functions, etc. These coefficients are defined in appendix B, and their numerical values are given in tables X - XIII.

Radar Back-Scattering Cross Sections

For radar back-scattering cross-section, that is the scattering in the direction opposite to incident beam ($\eta = 1$), the expression for σ (Eq. 33) reduces to:

$$\sigma = 4\pi a^2 \cdot \left| \sum_{l=0}^{\infty}{}' i^l \alpha_{0l} S_{0l}^{(1)}(1) \right|^2 \quad (35)$$

or

$$\sigma/\sigma_G = 4\,(b/a)^4 \left| \sum_{l=0}^{\infty}{}' i^l \alpha_{0l} S_{0l}^{(1)}(1) \right|^2 \quad (36)$$

The corresponding expressions, based on Rayleigh - Gans [5, 6] Law and Stevenson's solution [7], are as follows:

Rayleigh - Gans;

$$\sigma/\sigma_G = \left(\frac{8\pi}{3}\right)^2 \left[\frac{1}{P'(1 - P'/4\pi)}\right]^2 \alpha^4 \quad (37)$$

where,

$$P' = \frac{2\pi}{e^2}\left[1 - \frac{b^2/a^2}{2e} \log_e \frac{1+e}{1-e}\right]$$

* The numerical values of these coefficients are reported in Table XIV,

Stevenson: $$\sigma/\sigma_G = 4 \cdot \left| A\alpha^2 + B\alpha^4 \right|^2 \qquad (38)$$

where, $A = 1/ab^2\ (K_1 - \bar{K}_2)$; $B = 1/a^3b^2\ (L_1 - N_2 - \bar{L}_2 + \bar{N}_1) - \frac{A}{30}\frac{b^2}{c^2}$

and K_1, $\bar{K}_2$, L., N etc., are functions of the semi-principal axes of the scatterer; the electrical properties of the scattering medium; and, the direction cosines which define the orientation of the incident field with respect to the coordinates of the scatterer, etc. The expressions for these functions are involved and are discussed in Part II[†] Only the numerical values of these coefficients* and the final results of this theory will be presented here.

Ballastic Scattering Cross-section

In ballastics for the case when the transmitter is on the major axis of the prolate and the receiver is on the ray with angles θ, ϕ ($\eta = \cos\theta$), the cross section can be computed from the equations (33) and (34).

Acoustic Scattering Cross-section

For the case of an acoustic plane wave obliquely incident on a prolate, the expression for the scattered wave (or acoustic pressure), satisfying the Neuman boundary condition, is:

$$\psi_s = -\psi_i \sum_{m,l}^{\infty} \left[\frac{2\, i^{m+l}}{N_{ml}} \cdot \epsilon_m \cdot \frac{R^{(1)\prime}_{ml}(c,\xi_o)}{R^{(3)\prime}_{ml}(c,\xi_o)} S^{(1)}_{ml}(\eta) \right. \qquad (39)$$
$$\left. S^{(1)}_{ml}(\cos\theta) \times R^{(3)}_{ml}(c,\xi) \cos m\phi \right]$$

where θ defines the angle between the direction of propagation of the incident wave, parallel to the x-z plane, and the positive z-axis (see figure 3), ψ_i is the incident wave and $\epsilon_o = 2$, $\epsilon_m = 1$ for $m > 0$. For the scattered field at large distances from the scatterer, the asymptotic relation (Eq. 2'6) may be used for $R^{(3)}_{ml}(c,\xi)$.

*See Table XVII

† Appendix D

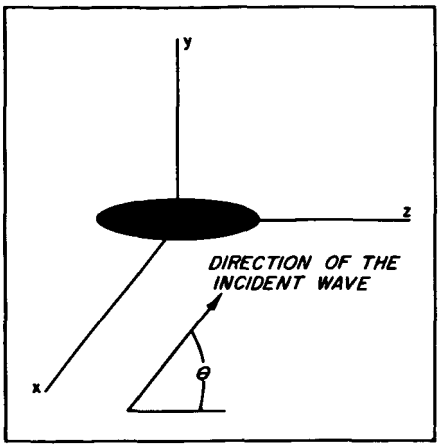

FIG. 3 - DIRECTION OF INCIDENCE OF PLANE ACOUSTIC WAVE IN THE BODY COORDINATES (Parallel to x-z Plane)

For the special case $\theta = o$ (Sohultz case), Equation (39) reduces to a much simpler form given by

$$\psi_s = -\psi_i \sum_{l=0}^{\infty} 2 i^l \left(\sum_{n=0}^{\infty}{}' d_n^{0l} \right) \cdot \frac{R_{0l}^{(1)\prime}(c,\xi)}{R_{0l}^{(3)\prime}(c,\xi_o)} S_{0l}^{(1)}(\eta) R_{0l}^{(3)}(c,\xi) \quad (40)$$

Since according to Equation (15), $S_{ml}^{(1)}(1) = 0$ for $m \geq 1$.

The corresponding expression for the back-scattering cross section is:

$$\frac{\sigma}{4\pi a^2} = \left| \frac{i}{c\xi_o} \sum_{l=0}^{\infty} A_{0l} \frac{R_{0l}^{(1)\prime}(c,\xi_o)}{R_{0l}^{(3)\prime}(c,\xi_o)} S_{0l}^{(1)}(1) \right|^2 \quad \text{where } A_{0l} = \frac{2i^l}{N_{0l}} \sum_{l=0}^{\infty}{}' d_n^{0l} \quad (41)$$

or in terms of tabulated coefficients B_{01}, C_{01}

$$\frac{\sigma}{4\pi a^2} = \left| \frac{i}{c\xi_o} \sum_{l=0}^{\infty} (B_{0l}^*/C_{0l}^*) S_{0l}^{(1)}(1) \right|^2 \quad (42)$$

where B_{0l}^*, C_{0l}^* are the complex conjugates of B_{0l}, C_{0l} respectively.

The numerical values of A_{01}, for 1 = 0, 1 and 2 and c = .1, .2 .4, .6 and .8 have been computed. These are reported in table XVI.

RESULTS AND CONCLUSIONS

The values of the radar back-scattering cross section, σ, computed from three different theories (Eqs. 36, 37 and 38) are presented in Figures 4,5 and 6 as a function of the non-dimensional parameter α. These figures correspond to three different shapes of Prolates (axis ratios b/a). Figure 7 represents a similar graph for prolates of axis ratio b/a = 0.1, obtained by Siegel et al[4].

In Figure 8, the ratio of $\sigma_{approx.}$ (obtained from Rayleigh-Gans or Stevenson's solution) to σ_{exact} (Schultz's exact solution) is plotted against the non-dimensional parameter α. The effect of the shape of the prolate spheroidal target on the radar echo is shown in Figure 9. The values of the back-scattering cross sections for the spheres which are used in Figure 9 correspond to those for equivolumetric spheres, and the curves are extrapolated to the axis ratio b/a = 0.2 with the aid of the data of reference (4).

The results indicate a substantial decrease in the values of the radar back-scattering cross sections as the shape of the equivolumetric scatterers vary from spherical to thin prolate spheroidal shapes. For prolate of axis ratio b/a = 0.8 and $\alpha = 0.8$, the ratio $\sigma_{sphere} / \sigma_{prolate}$ is about 1/2 and decreases to a value of approximately 1/200 for prolate spheroid of axis ratio b/a = 0.2 and $\alpha = .8$.

Figures 4 to 7 suggest that the Rayleigh-Gans first order solution is not adequate in the size range $\alpha > 0.3$. However, Stevenson's third order solution yields results nearly identical with the exact values in the size range $\alpha < 1.0$.

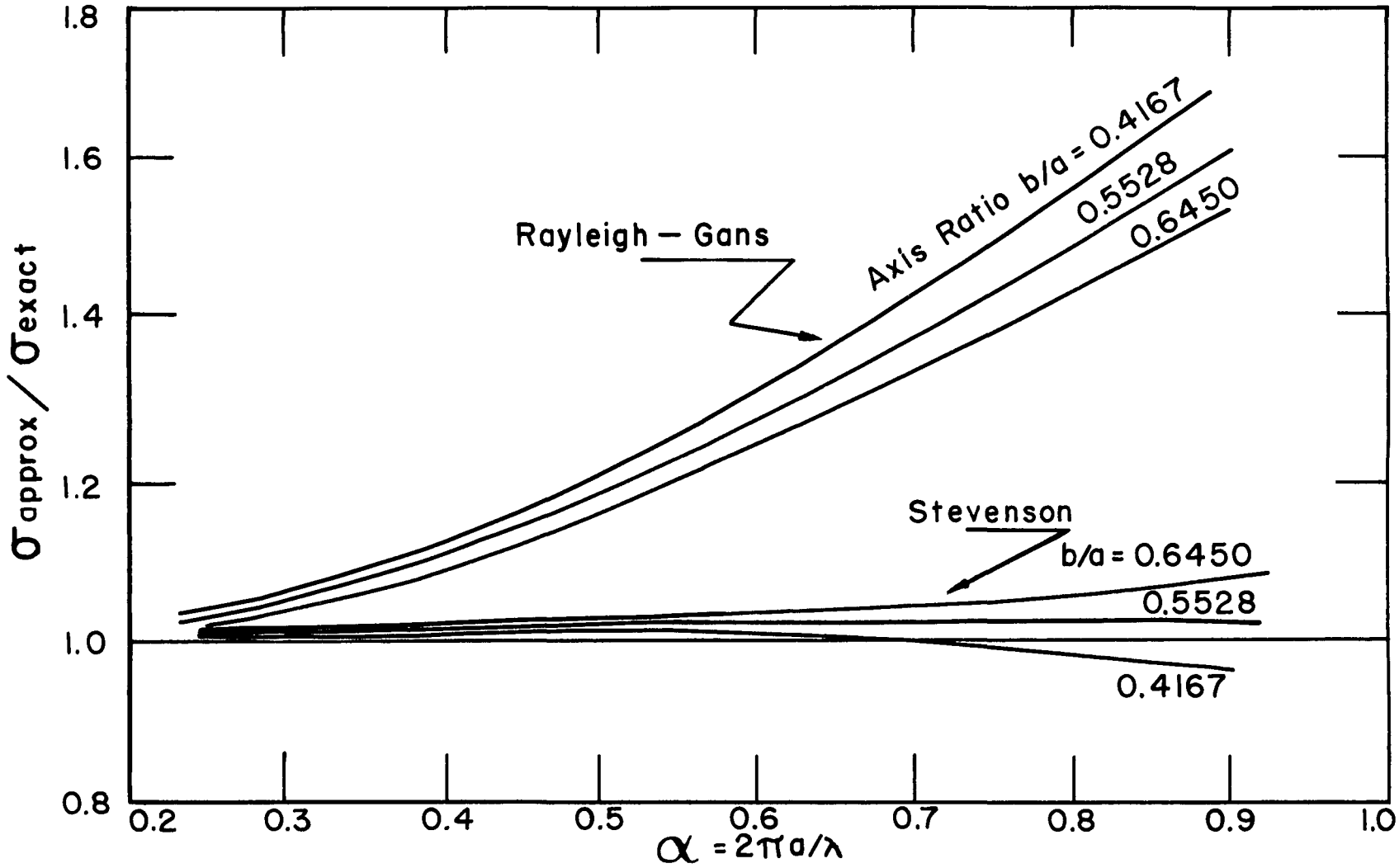

FIG. 4 - RADAR BACK SCATTERING CROSS SECTIONS FOR CONDUCTING PROLATES, NOSE-ON INCIDENCE, (b/a = 0.639)

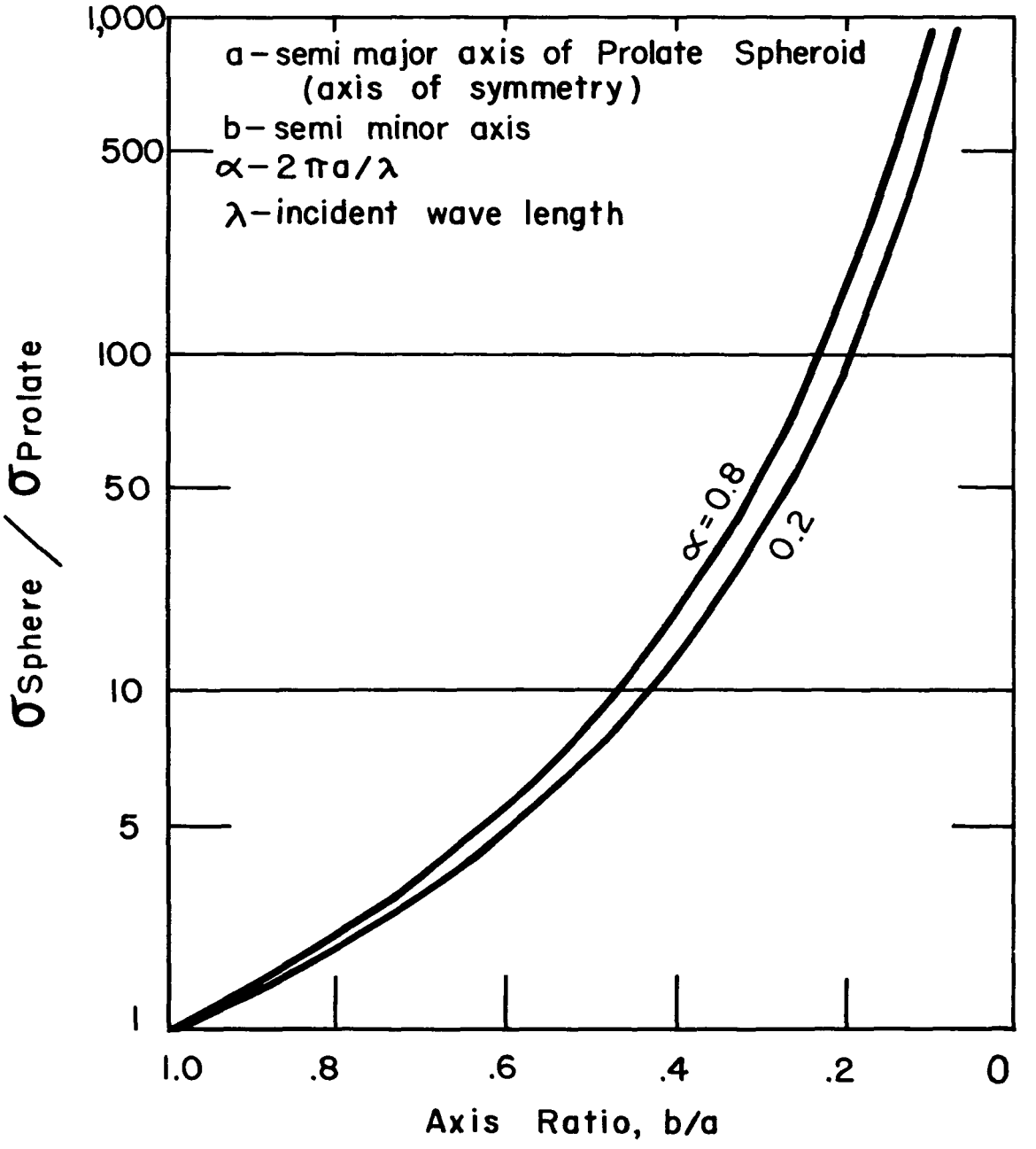

FIG. 5 - RADAR BACK SCATTERING CROSS SECTIONS FOR CONDUCTING PROLATES, NOSE-ON INCIDENCE, (b/a = 0.5528)

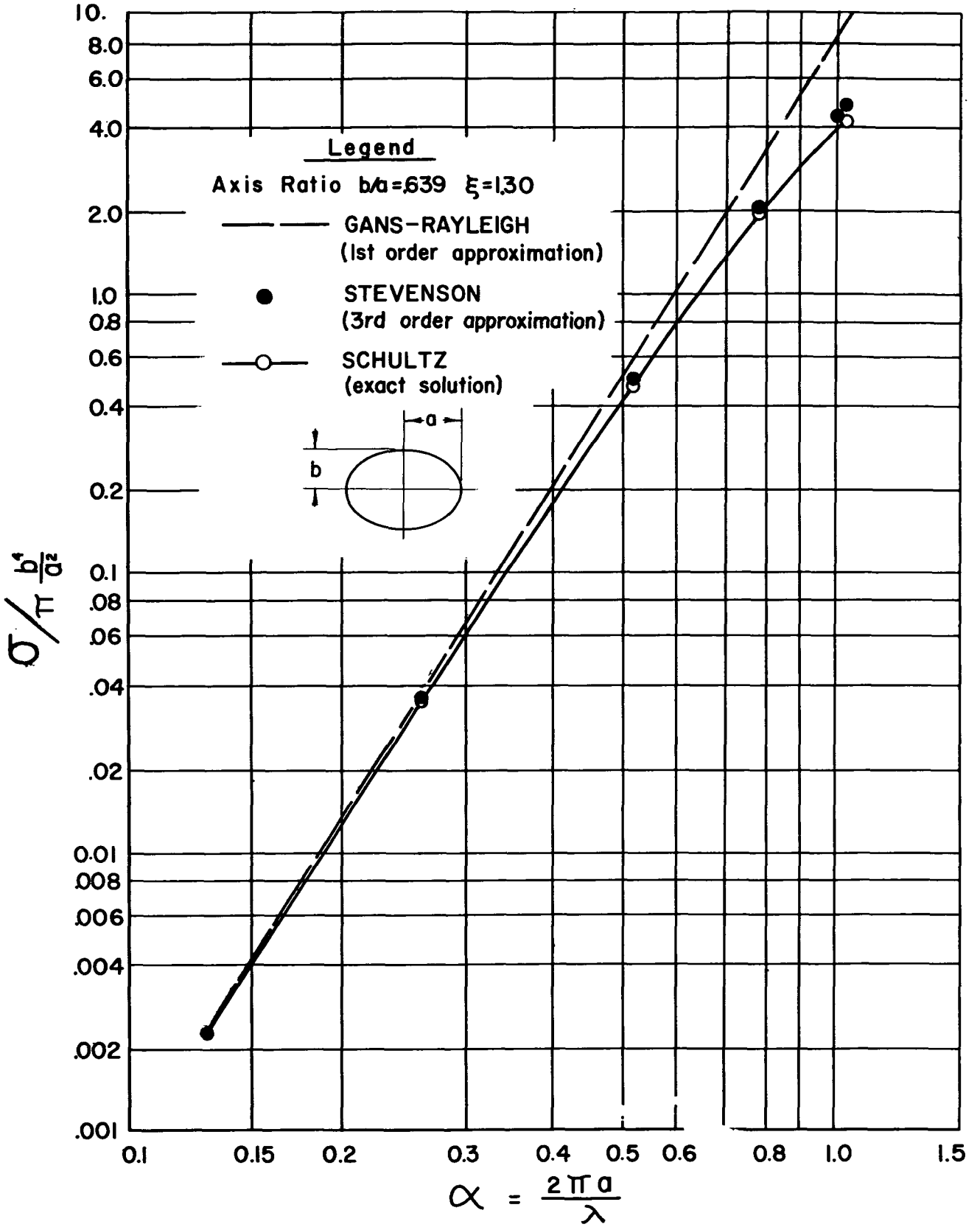

FIG. 6 - RADAR BACK SCATTERING CROSS SECTIONS FOR CONDUCTING PROLATES, NOSE-ON INCIDENCE, (b/a = 0.4167)

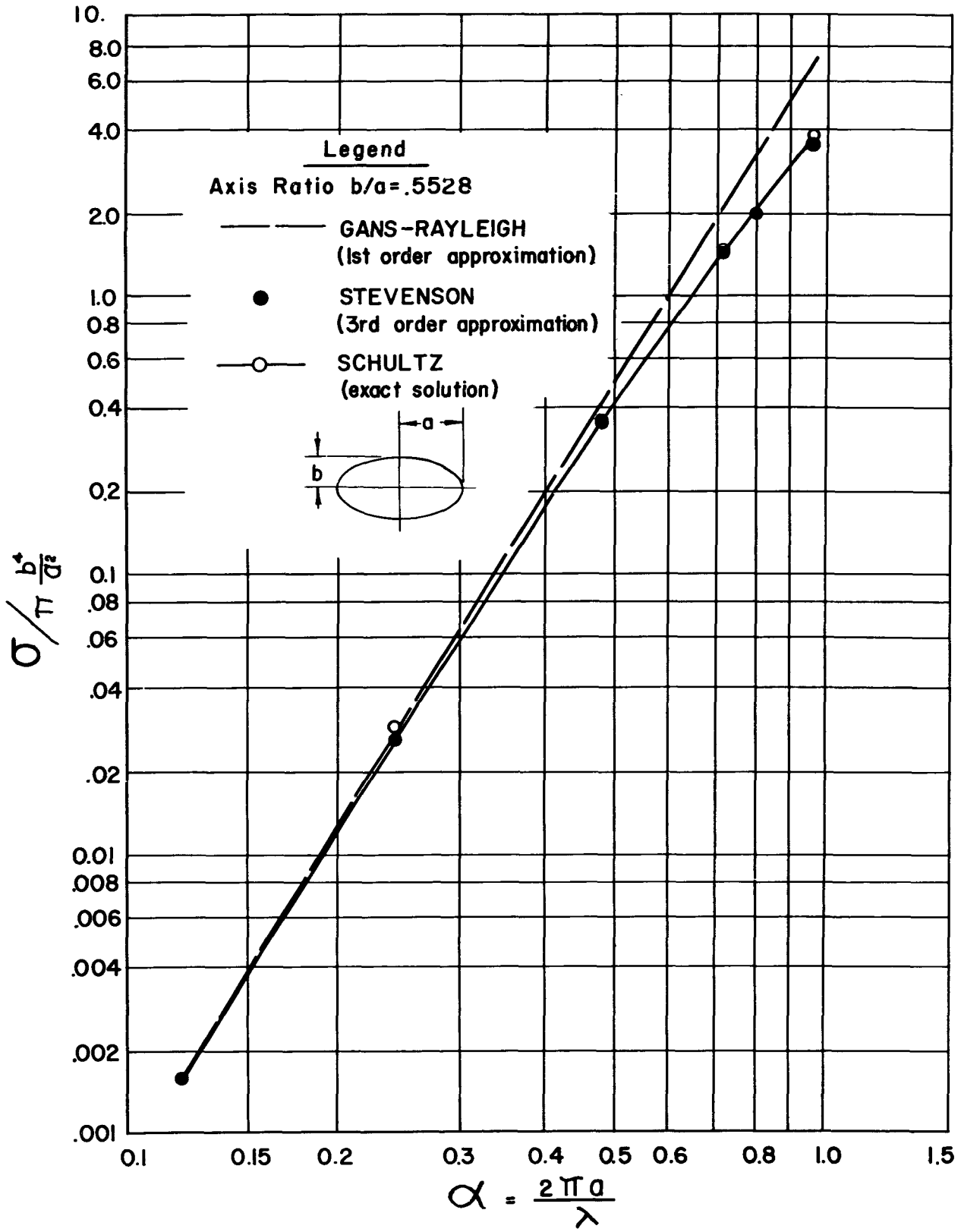

FIG. 7 - RADAR BACK SCATTERING CROSS SECTIONS FOR CONDUCTING PROLATES, NOSE-ON INCIDENCE, (b/a =0.1)

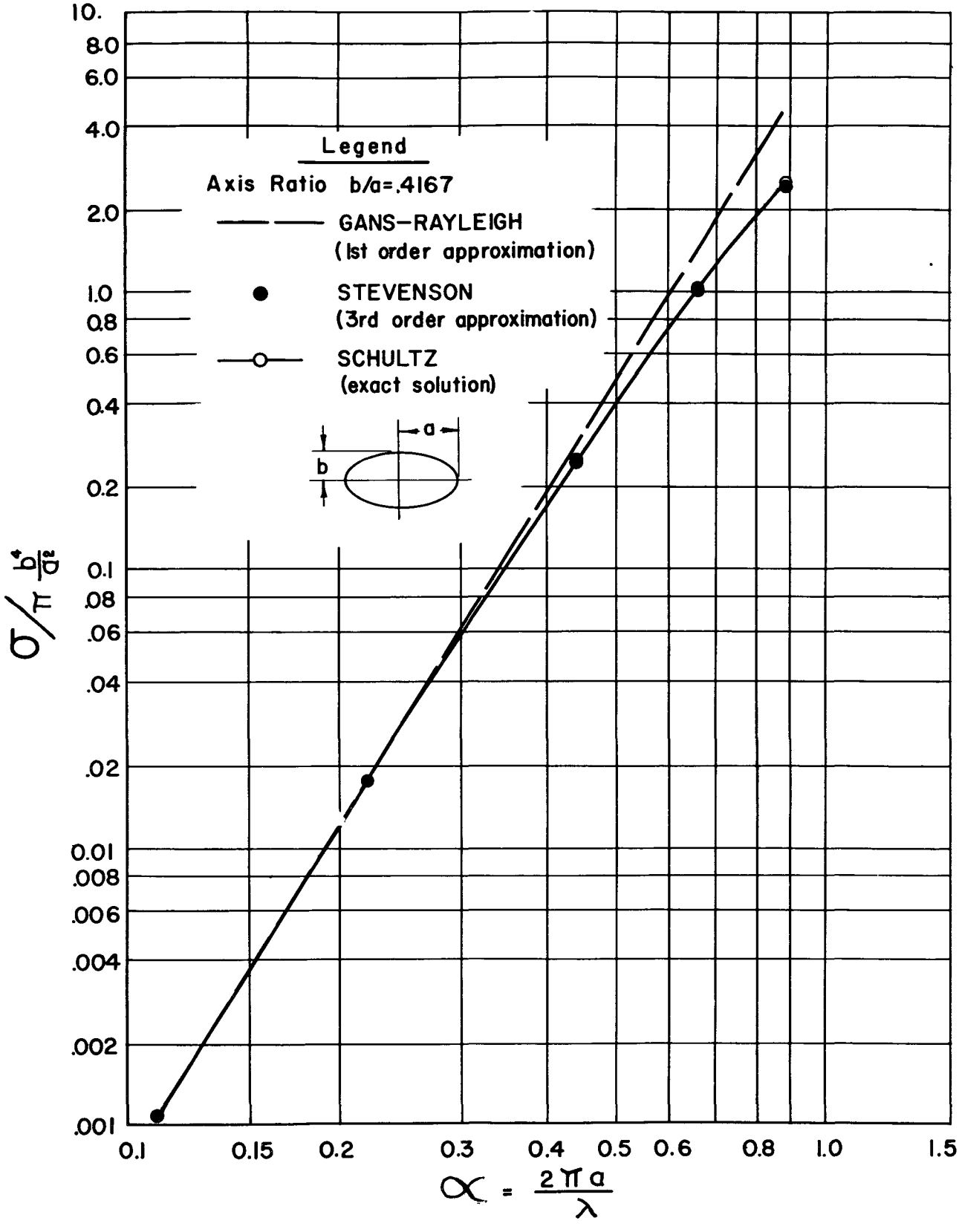

FIG. 8 - RATIO OF APPROXIMATE BACK SCATTERING TO SCHULTZ'S BACK SCATTERING FOR CONDUCTING PROLATES

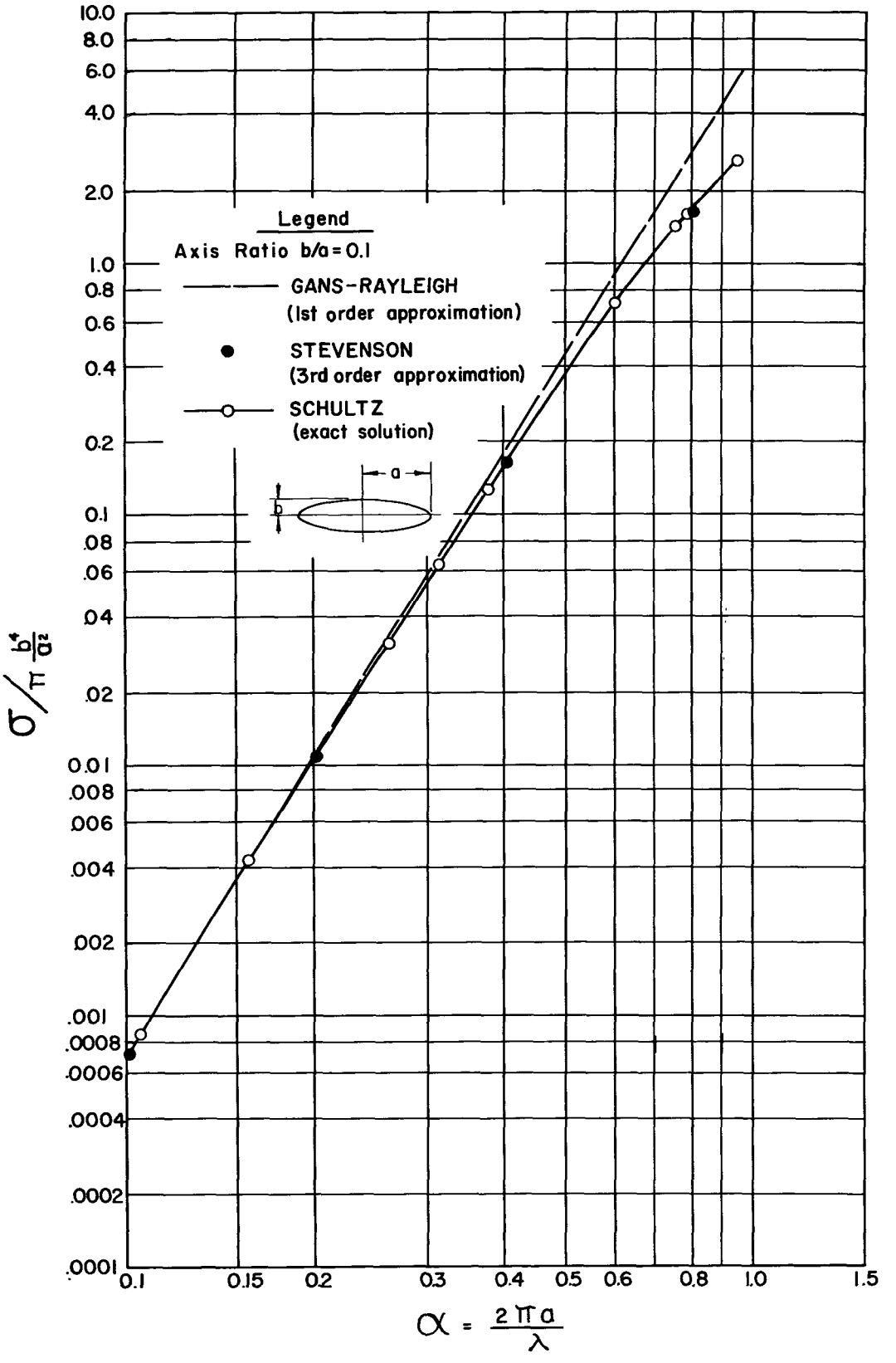

FIG. 9 - EFFECT OF THE SHAPE OF THE PROLATE SPHEROIDS ON THE BACK SCATTERED ECHO (Axis Ratio)

Part II

ABSTRACT

Several formulas for back-scattering and attenuation cross-sections are derived from Stevenson's field solutions. Detailed numerical evaluations of the scattering coefficients are made for various shapes of oblate and prolate water drops for radars of 3-cm and 10-cm wave length. Similar evaluation is made for conducting spheroids. Studies are extended to examine the depolarization from such drops. Various charts relating the scattering cross-section to the dimensions of the scatterer are presented in non-dimensional plots.

INTRODUCTION

Statement of Problem

As noted in Part 1 of this report, collection of data with a raindrop camera[15] during 1953-54 showed that the majority of large raindrops within storms are non-spherical. It is apparent that the electrical reflections from such non-spherical drops contribute substantially to the total radar reflectivity from a storm. To correlate quantitative data collected with the raindrop camera with the corresponding radar reception from a storm, a need was established for theoretical computations of the reflectivity for the various camera samples.

Scope of Investigation

The primary purpose of this study was to provide formulas for radar back-scattering cross-sections and forward scattering for raindrops at centimeter wave length. It was, however, believed that these formulas should be based on a more accurate theory than Gans[15] dipole approximation presently used in meteorological analysis.

In Part I, a detailed appraisal was made of the available solutions, for the scattering of electromagnetic waves by non-spherical particles, which are practical to evaluate. The results of this study indicated that a solution reported by Stevenson , which is essentially an extension of Gans' solution, predicts values of radar back-scattering cross-sections nearly identical to the exact values calculated from Schultz's theory[3] for the case of conducting prolates. The Gans theory for the same case was inadequate for drop size parameter $\alpha > 0.3$.

In the work, reported herein, the aforementioned formulas are derived for non-spherical raindrops from Stevenson's field solutions. The scattering coefficients are computed for several shapes of prolates and oblates ranging from extremely elongated prolates (rods) to extremely flat oblates (plates) and for the horizontal and vertical polarization of radar at 3-cm and 10-cm wave length. The study is extended to an examination of the depolarization effects from such drops.

THEORY

Since most radar applications are based on the transmission of short pulses of electromagnetic energy and echo pulses from a distant target, it is desirable to express the signal power returned as a function of radar values, characteristic parameters of the scatterer, and the distance between the scatterer and the receiver.

In the determination of such an echo, consider an isolated antenna radiating linearly polarized waves in the direction of maximum transmission. Since a distant target subtends sufficiently small angles measured from the energy source, the incident wave front is nearly plane. The problem of calculating the return echo is thus reduced to the problem of scattering of electromagnetic waves in the wave zone by a target of a given shape.

Radar Equation and Back-Scattering Cross-Section

If P_t is the total power transmitted by an isotropic antenna, then the power density, Si, (Radiated power per unit cross-sectional area) of the transmitted wave at a distance, R, is

$$S_i = \frac{P_t}{4\pi R^2} \tag{1}$$

The Power density of a directional radar can be represented by introducing a non-dimensional gain factor* (or antenna pattern factor), G, such that

$$S_i^{\gamma} = \frac{P_t \cdot G}{4\pi R^2} \tag{2}$$

---

* Gain factor G is the ratio of the power radiated by the directional antenna to the power radiated by an isotropic antenna having a total output, Pt.

The power scattered, P_s , from the incident radiation by an isotropic scatterer can be written as

$$P_s = S_i \cdot Q_s \tag{3)a}$$

and the corresponding power density, S_s, is

$$S_s^R = S_i \cdot Q_s \cdot \frac{1}{4\pi R^2} \tag{3)b}$$

where Q_s is the total scattering cross-section.

Since the scattering from raindrops is not isotropic and since the interest is in the back-scattered intensity, another non-dimensional gain factor, g, is employed for the backward direction of the scattered field such that

$$Q_s \cdot g = \sigma \tag{4}$$

and

$$S_s^R = S_i^Y \cdot \frac{\sigma}{4\pi R^2} \tag{5}$$

where S_s^R is the scattered power density in the direction opposite to the incident direction at a distance, R.

The symbol, σ, is now termed as the radar back-scattering cross-section, and represents the ability of the scattering object to reradiate power in the direction of the radar set. Therefore, it may be defined as the total power scattered by an isotropic source with intensity equal to the backward direction intensity of the original scatterer, divided by the incident energy density. Equation (5) may be rerranged as

$$\sigma = 4\pi R^2 \frac{S_s^R}{S_i^Y} \tag{6}$$

The power received by the radar from a single scatterer is

$$P_r = S_s^R \cdot A_r = S_s^R \cdot \left(\frac{\lambda^2 G}{4\pi} \right) \tag{7}$$

where A_r is the receiving cross-section of the antenna ($A_r = \frac{\lambda^2 G}{4\pi}$).

Substitution of Eqs. 2 and 5 in Eq. 7 yields

$$P_r = \frac{P_t \cdot G^2 \cdot \lambda^2}{(4\pi)^3 \cdot R^4} \sigma \tag{8}$$

Geometry and Parameters of Scatterers

Ellipsoid. The geometrical shape next to a sphere, in the order of analytical complexity, is the ellipsoid whose surface is defined by the equation

$$\frac{x^2}{a^2} + \frac{y^2}{b^2} + \frac{z^2}{c^2} = 1 \tag{9}$$

where a, b and c are the semi-principal axes of the triaxial ellipsoid. If two semi axes are equal (say a = b) the ellipsoid of revolution (or spheroid) is obtained. The axis of symmetry of this body is termed the figure axis. In the case under study (a = b), the semi axis, c , represents the figure axis. The equation of the spheroid becomes

$$\frac{(x^2 + y^2)}{b^2} + \frac{z^2}{c^2} = 1 \tag{10}$$

With the z-axis as the axis of symmetry (or c as the figure axis) the equation describes the surface of a prolate spheroid if c> a = b and an oblate spheroid if c < a = b (see Fig. 11). In the x-z or y-z plane, the equation represents an ellipse generating oblate or prolate surfaces.

Shape Parameter. The shape of prolate or oblate spheroid may be represented by the ratio of their semi-axes. .This ratio for prolate is chosen to be, b/c, and for oblate, c/b.

Parameter α . To obtain the results in general terms it is convenient to represent the size of the particles by normalizing it with respect to the wave length. The parameter α is the same as defined by Eq. 6 of Part I. This parameter may, however, be more generally defined as $\alpha = \frac{\pi}{\lambda}$ • where L. now represents any appropriate dimension of the prolate or oblate spheroid. For prolates the choice L = 2c is made, while for oblates the choice is L = 2b.

Electrical Properties of the Scatterer

Dielectric Constant and Magnetic Permeability. The scattered field intensity is influenced by the electrical properties (dielectric constant ϵ and magnetic permeability μ) of the scattering medium. If the scatterer is a perfect conductor, the dielectric constant is $\epsilon = m^2 \to \infty$ since the magnetic permeability is $\mu = 0$.

For water drops the dielectric constant is complex and depends on the incident wave length, λ , and the temperature. The value of

$(\epsilon)^{1/2}$ = m for water at 18°C, reported by Saxton[17], is 8.18-i 1.16 for a 3-cm wave, and for a 10-cm wave, $(\epsilon)^{1/2}$ m = 8.90-0.69 i. The magnetic permeability, μ, for this case is approximately unity.

Geometrical cross-section

It is customary to represent the radar cross-section in a non-dimensional form by normalizing it with an approximate geometric cross-section, σ_G, based on geometric optics. This is defined by Eq. 7 of Part I and is evaluated for a prolate spheroid at z-incidence (Eq. 8, Part I).

For y-incidence of the beam shown in Figure 11 (broad side incidence)

$$\sigma_G = \pi b^3/c \tag{11}$$

for both prolates and oblates.

Incidence of the Beam

The orientation of the radar beam, for an arbitrary incidence with respect to the body coordinates (x, y, z) of the scatterer, may be defined by a set of nine direction cosines according to the scheme:

	x	y	z
$\bar{n}$	l	m	n
E	l_1	m_1	n_1
H	l_2	m_2	n_2

(12)

where 1, m, n are the direction cosines of the poynting vector $\bar{n}$; l_1, m_1, n_1 define the direction of the electric field vector, E; and 12, m2, n2 refer to the magnetic field vector, H.

Z-Incidence. This refers here to the nose-on incidence. The direction of propagation of the beam is along the z-axis, with the electric field, E, parallel to the y-azis and the magnetic field, H, parallel to the x-axis. For this incidence

$$n = l_1 = m_2 = 1 \tag{13}$$

and all other direction cosines become zero. The only electric field which exists in the wave zone is the y-component.

Y-Incidence. This refers here to the case when the direction of propagation of the incident beam is along the y-axis of the body coordinates of the scatterer. Two different polarizations of the incident beam are considered.

A. Horizontal Polarization. This refers to the case when the electric vector is parallel to the x-axis and the magnetic vector is parallel to the z-axis (see Figure 11). The non-zero direction cosines for this case are, therefore

$$m = l_1 = n_2 = 1 \tag{14}$$

B. Vertical Polarization. For this case the beam is rotated 90 degrees anticlockwise from the horizontal position, such that the electric vector is parallel to the z-axis and the magnetic vector is parallel to the negative x-axis (see Figure 11). Consequently the non-zero direction cosines are

$$m = -l_2 = n_2 = 1 \tag{15}$$

Stevenson's Field Solutions

The radar back-scattering cross-sections are obtained from the wave zone scattered electric and magnetic vector fields. These fields are the solutions of the vector wave equation representing the combined Maxwell's equations, and satisfying a set of boundary conditions at the surface of the scatterer and at large distances from it.

An alternate method, assuming quasi-static field conditions at the scatterer, was employed by Gans[5] and extended by Stevenson' to solve the problem of the scattering of electromatic waves by ellipsoidal particles. It was shown by Stevenson that a formal solution can be obtained as a power series in α , each term of the series requiring only the solution of a standard problem in potential theory, instead of the general system of Maxwell's equation. The series can be carried out to as many terms as desired, although the calculation of successive terms becomes more involved.

For an electromagnetic plane wave of amplitude, E_o, incident on a dielectric ellipsoid (dielectric constant ϵ and permeability μ), Stevenson obtained the scattered field solution which may be written as

$$E_\theta = \eta H_\phi = \left(\frac{\partial P}{\partial \theta} + \frac{1}{\sin\theta} \frac{\partial \bar{P}}{\partial \phi} \right) \cdot \frac{E_o \cdot e^{ikR}}{R} \tag{16}$$

$$E_\phi = -\eta H_\theta = \left(\frac{1}{\sin\theta} \frac{\partial P}{\partial \phi} - \frac{\partial \bar{P}}{\partial \theta} \right) \cdot \frac{E_o \cdot e^{ikR}}{R} \tag{17}$$

where R, Θ and ϕ are the coordinates of a field point measured from the body coordinates x, y and z; η is the intrisic impedence ($\eta = \sqrt{\frac{\mu_o}{\epsilon_o}}$ for free space); and the quantities P and $\bar{P}$ are functions of surface harmonies, $S_j^{(m)}$, which may be defined as:

$$P = \sum_{s=2}^{\infty} k^s \sum_{j=1}^{s-1} \frac{(-1)^j}{j(j+1)} \cdot S_j^{(s-j-1)} \tag{18}$$

$$\bar{P} = \sum_{s=2}^{\infty} k^s \sum_{j=1}^{s-1} \frac{(-1)^j}{j(j+1)} \bar{S}_j^{(s-j-1)} \tag{19}$$

For a three-term series, the expansion for P reduces to

$$P = k^2 (K_1\alpha' + K_2\beta + K_3\gamma) + k^4 \left[(L_1\alpha' + L_2\beta + L_3\gamma) + (M_1\alpha'^2 + M_2\beta^2 + M_3\gamma^2) + (N_1\gamma\beta + N_2\gamma\alpha' + N_3\alpha'\beta) \right] - \frac{1}{30} \left[(K_1\alpha' + K_2\beta + K_3\gamma) \cdot (a^2\alpha'^2 + b^2\beta^2 + c^2\gamma^2) \right] \tag{20}$$

A similar expression is obtained for P by replacing the coefficients of α', β and γ of the above equation with the corresponding scattering coefficients refering to the magnetic field and indicated by bars. Thus

$$\bar{P} = k^2 (\bar{K}_1\alpha' + \cdots\cdots) + k^4 (\bar{L}_1\alpha' + \cdots) - \frac{1}{30} (\bar{K}_1\alpha' + \cdots\cdots) \tag{21}$$

Here α', β and γ are the direction cosines of the radius vector in body coordinates. The scattering coefficients K_j, L_j, $\bar{K}_j$, $\bar{L}_j$, N_j, $\bar{N}_j$ etc. with

j = 1, 2 and 3 are functions fo semi-axes (a, b, c); refractive indices; nine direction cosines 1, m, n, l_1, m_1, n_1 etc., and certain integrals. The defining expressions for these scattering coefficients are given in Appendix D. The special values of the integrals and other functions involved in these expressions are summarized in Appendix E.

BACK SCATTERING, FORWARD SCATTERING AND DEPOLARIZATION

General Formulas for Back-Scattering Cross Section.

The definition for σ is

$$\sigma = \frac{4\pi R^2 \cdot S_s^R}{S_i^Y} \tag{6}$$

The numerator on the right hand term of this equation represents the radial backward component of the poynting vector of the scattered wave integrated over a large** spherical surface of radius R.

The expression for S_s^R in terms of the field components is

$$S_s^R = \frac{1}{2} \mathcal{R}e \left(E_\theta H_\phi^* - E_\phi H_\theta^* \right)_{\theta=\pi} \tag{22}$$

and the corresponding value for S_i^Y for the incident beam is

$$S_i^Y = \frac{1}{2\eta} E_o^2 \tag{23}$$

Substituting Eqs. 16 and 17 in Eq. 22, and introducing the resulting expression for S_s^R in Eq. 6, the general formula obtained for 0" is obtained as

$$\sigma = 4\pi \left[\left(\frac{\partial P}{\partial \theta} + \frac{1}{\sin\theta} \frac{\partial \bar{P}}{\partial \phi} \right)_{\theta=\pi} \cdot \left(\frac{\partial P}{\partial \theta} + \frac{1}{\sin\theta} \frac{\partial \bar{P}}{\partial \phi} \right)^*_{\theta=\pi} + \left(\frac{1}{\sin\theta} \frac{\partial P}{\partial \phi} - \frac{\partial \bar{P}}{\partial \theta} \right)_{\theta=\pi} \cdot \left(\frac{1}{\sin\theta} \frac{\partial P}{\partial \phi} - \frac{\partial \bar{P}}{\partial \theta} \right)^*_{\theta=\pi} \right] \tag{24}$$

Case of Conducting Scatterer, Z-Incidenee.

For this case, the spherical coordinates are set up as shown in Figure 10. The z-axis is taken as the polar axis and the plane ϕ =0

** Radius of the sphere extends in the wave zone.

Note: the symbol "*" on the fields E and H and on the brackets of Eqs. 22 and 24 indicates complex conjugate.

as the x-z plane, so that the direction cosines α', β, and γ of a field point (x, y, z) in terms of spherical angular coordinates θ and ϕ are

$$\alpha' = \sin\theta \cdot \cos\phi \; ; \quad \beta = \sin\theta \cdot \sin\phi \; ; \quad \gamma = \cos\theta \tag{25}$$

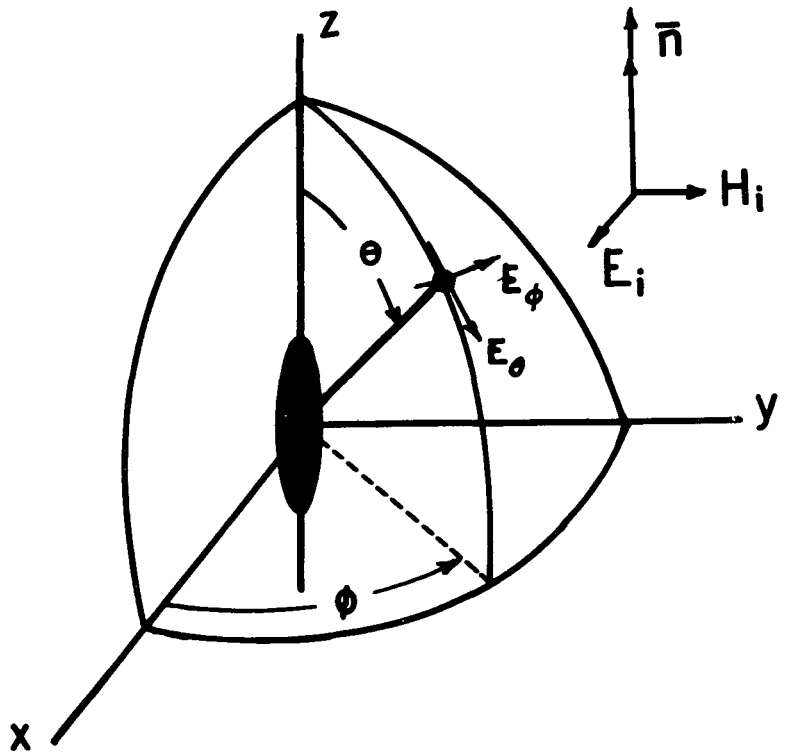

FIG. 10 - BODY COORDINATES

The values of these direction cosines and their derivatives with respect to θ and ϕ evaluated for the back scattered case ($\theta = \pi$) are

$$\alpha' = 0 \; ; \quad \beta = 0 \; ; \quad \gamma = -1 \; ;$$

$$\frac{\partial \alpha}{\partial \theta} = -\cos\phi \quad ; \quad \frac{1}{\sin\theta}\frac{\partial \alpha'}{\partial \phi} = -\sin\phi \quad ;$$
$$\frac{\partial \beta}{\partial \theta} = -\sin\phi \quad ; \quad \frac{1}{\sin\theta}\frac{\partial \beta}{\partial \phi} = \cos\phi \quad ; \qquad (26)$$
$$\frac{\partial \gamma}{\partial \theta} = 0 \quad ; \quad \frac{1}{\sin\theta}\frac{\partial \gamma}{\partial \phi} = 0$$

The calculations for the quantities appearing in Eq. 24 are involved but straight-forward. The steps are described briefly as follows: Differentiating P and $\bar{P}$ (Eqs. 20 and 21) with respect to θ and ϕ and substituting the values of α', β and γ and their derivatives from Eq. 26 the desired values of the terms appearing in Eq. 24 are obtained.

Substituting the values of these terms in Eq. 24 and rearranging the terms in powers of $\alpha = k.L$, the final formula for σ can be written in the non-dimensional form* as follows:

for prolates

$$\sigma/\sigma_G = \sigma/\pi b^4 = 4\left\{ \left| A\alpha^2 + B\alpha^4 \right|^2 + \left| \bar{A}\alpha^2 + \bar{B}\alpha^4 \right|^2 \right\} \qquad (27)$$

and for oblates

$$\sigma/\sigma_G = \sigma/\pi b^4 = 4\frac{c^4}{b^4}\left\{ \left| A\alpha^2 + \frac{c^2}{b^2}B\alpha^4 \right|^2 + \left| \bar{A}\alpha^2 + \frac{c^2}{b^2}\bar{B}\alpha^4 \right|^2 \right\} \qquad (28)$$

where
$$A = \frac{1}{b^2 c}(K_1 - \bar{K}_2) \; ; \; B = \frac{1}{(c^3 b^2)}\left[L_1 - N_2 - \bar{L}_2 + \bar{N}_1 \right] - \frac{A}{30}\frac{b^2}{c^2}$$
$$\qquad (29)$$
and
$$\bar{A} = \frac{1}{b^2 c}(\bar{K}_1 - K_2) \; ; \; \bar{B} = \frac{1}{(c^3 b^2)}\left[L_2 - N_1 + \bar{L}_1 - \bar{N}_2 \right] - \frac{\bar{A}}{30}\frac{b^2}{c^2} .$$

The values for the scattering coefficients K_1, K_2, L_1, L_2, etc. are to be evaluated from their general expressions given in Appendix B. For this particular case

$$l_1 = m_2 = n = 1, \quad l = l_2 = m = m_1 = n_1 = n_2 = 0 \qquad (30)$$

and $\epsilon \longrightarrow \infty$, $\mu = 1.0$. The resulting values ** of the scattering

---

* The final expression is independent of $\langle p$, as expected. The trignometric terms either cancel out or combine to form unity.

** The quantities P and I appearing in the following expressions are defined in Appendix B.

coefficients are:

$$K_1 = \frac{2}{3 I_a}$$

$$\bar{K}_2 = \frac{2}{3} \cdot \frac{b^2 c}{(P'/2\pi - 2)}$$

$$\frac{L_1}{b^2 c^3} = \frac{1}{15}\left(\frac{2\pi}{P'}\right)\left[\frac{8}{3}(b/c)^2 - \frac{7}{3}\right] + \frac{1}{15}\left(\frac{2\pi}{P'}\right)^2 \frac{b^2}{c^2}(I \times c)$$

$$\frac{\bar{L}_2}{b^2 c^3} = \frac{1}{15}\left(\frac{13}{16}\frac{b^2}{c^2} - \frac{11}{16}\right)\left(\frac{2\pi}{P'-4\pi}\right) + \frac{2}{15}\left(\frac{2\pi}{P'-4\pi}\right)^2$$
$$\times \left[\frac{b^2}{c^2}(I \times c) - e^2 \left(I_{bc} \cdot b^2 c^3\right)\right] \qquad (31)$$

$$\frac{N_2}{b^2 c^3} = \frac{(b^2/c^2 - 1)}{45}\left(\frac{2\pi}{P'-4\pi}\right) + \frac{1}{30} \cdot \frac{1}{I_{bc} b^2 c^3}\left(1 + \frac{P-P'}{P'-4\pi}\right)$$

$$\frac{\bar{N}_1}{b^2 c^3} = \frac{1}{45}\left(\frac{b^2}{c^2} - 1\right)\frac{2\pi}{P'} - \frac{(1/15)}{2 - (b^2 c^2 \cdot I_{bc})(b^2/c^2 + 1)} \cdot \left[e^2 + \frac{P}{P'}\right]$$

and $$L_2 = N_1 = \bar{L}_1 = \bar{N}_2 = 0$$

These formulas are valid for both horizontal and vertical polarization of the incident beam, but the values of the scattering coefficients* K_1, $\bar{K}_3$, L_1 etc. are different.

For the case of horizontal polarization, lj = m = n_2 (see Eq. 14) and the scattering coefficients for the dielectric spheroids (oblate, prolate drops) are:

$$\bar{K}_3' = 0 \quad ;$$

$$K_1' = \frac{K_1}{b^2 c} = \frac{2}{3}\left[\frac{2\pi(\epsilon-1)}{4\pi+(\epsilon-1)P'}\right] \quad ;$$

$$15L_1' = \frac{15L_1}{b^2c^3} = \left(\frac{2\pi}{4\pi+(\epsilon-1)P'}\right)\left\{(\epsilon-1)\left(\frac{2\,b^2/c^2-1}{3}\right)+\frac{P}{4\pi}\left(1-\frac{P}{P'}\right)\left(\frac{1}{2}-\frac{b^2}{2c^2}\right)\right.$$
$$\left. + \frac{\epsilon}{2}\left(1-b^2/c^2\right)\right\} + \left(\frac{2\pi}{4\pi+(\epsilon-1)P'}\right)^2\left\{(\epsilon-1)\left[(\epsilon-2)\frac{b^2}{c^2}(I.c)\right.\right. \qquad (31a)$$
$$\left. + \epsilon\, b^2/c^2\,\frac{P'}{2\pi} - 4\frac{b^2}{c^2}\right] + \epsilon^2\left(b^2/c^2+1\right) + \frac{P}{4\pi}\left(1-\frac{P}{P'}\right)\left[\frac{1}{2}(\epsilon-1)\right.$$
$$\left.\left. \times\left(b^2/c^2-1\right)\left(1+\frac{P}{P'}\right)\frac{P}{2\pi} + \left(\epsilon^2-2\epsilon\right)\left(b^2/c^2-1\right)\right]\right\} \quad ;$$

$$15\bar{L}_3' = \frac{15\bar{L}_3}{b^2c^3} = \frac{b^2}{2c^2}\cdot(1+\epsilon)$$

---

* The primes on the coefficients K_1, K_3, L_1, etc., refer to their non-dimensional form as defined in the above expressions.

Scattering Cross Sections for Non-Spherical Drops, Y-Incidence.

For the case of the radar beam (parallel to y-axis) striking vertically falling drops, the direction cosines of the field point x, y, z in terms of spherical angular coordinates θ and ϕ (see Figure 11) are

$$\alpha' = \sin\theta\cdot\cos\phi \qquad \beta = \cos\theta \qquad \gamma = \sin\theta\cdot\sin\phi \tag{32}$$

The values of these direction cosines and their derivatives evaluated at $\theta = \pi$ are

$$\begin{aligned} \alpha' &= 0 & \frac{\partial\alpha'}{\partial\theta} &= -\cos\phi & \frac{1}{\sin\theta}\frac{\partial\alpha'}{\partial\phi} &= -\sin\phi \\ \beta &= -1 & \frac{\partial\beta}{\partial\theta} &= 0 & \frac{1}{\sin\theta}\frac{\partial\beta}{\partial\phi} &= 0 \\ \gamma &= 0 & \frac{\partial\gamma}{\partial\theta} &= -\sin\phi & \frac{1}{\sin\theta}\frac{\partial\gamma}{\partial\phi} &= \cos\phi \end{aligned} \tag{33}$$

Differentiating the expressions for P and $\bar{P}$ with respect to θ and ϕ, making the evaluation with the aid of Eq. 32, substituting the resulting values in Eq. 24, and rearranging the terms in power of $\alpha = k L$ results in formulas for back-scattering cross-section, σ, as follows:

For prolate spheroids ($L = 2c$, $\alpha = 2\pi c/\lambda$)

$$\sigma/\sigma_G = \frac{\sigma}{\pi b^3/c} = 4\frac{b}{c}\left\{\left|\alpha^2(K_1'-\bar{K}_3') + \alpha^4\left[(L_1'-N_3'-\bar{L}_3'+\bar{N}_1') - \left(\frac{K_1'-\bar{K}_3'}{30}\right)\frac{b^2}{c^2}\right]\right|^2 + \left|\alpha^2(\bar{K}_1'+K_3') + \alpha^4\left[(L_3'-N_1'+\bar{L}_1'-\bar{N}_3') - \frac{(\bar{K}_1'+K_3')}{30}\frac{b^2}{c^2}\right]\right|^2\right\} \tag{34}$$

and for oblate spheroids ($L = 2b$, $\alpha = \frac{2\pi b}{\lambda}$)

$$\sigma/\sigma_G = \frac{\sigma}{\pi b^3/c} = 4\frac{c^3}{b^3}\left\{\left|\alpha^2(K_1'-\bar{K}_3') + \alpha^4\left[(L_1'-N_3'-\bar{L}_3'+\bar{N}_1')\frac{c^2}{b^2} - \frac{1}{30}(K_1'-\bar{K}_3')\right]\right|^2 + \left|\alpha^2(\bar{K}_1'+K_3') + \alpha^4\left[(L_3'-N_1'+\bar{L}_1'-\bar{N}_3')\frac{c^2}{b^2} - \frac{(\bar{K}_1'+K_3')}{30}\right]\right|^2\right\} \tag{35}$$

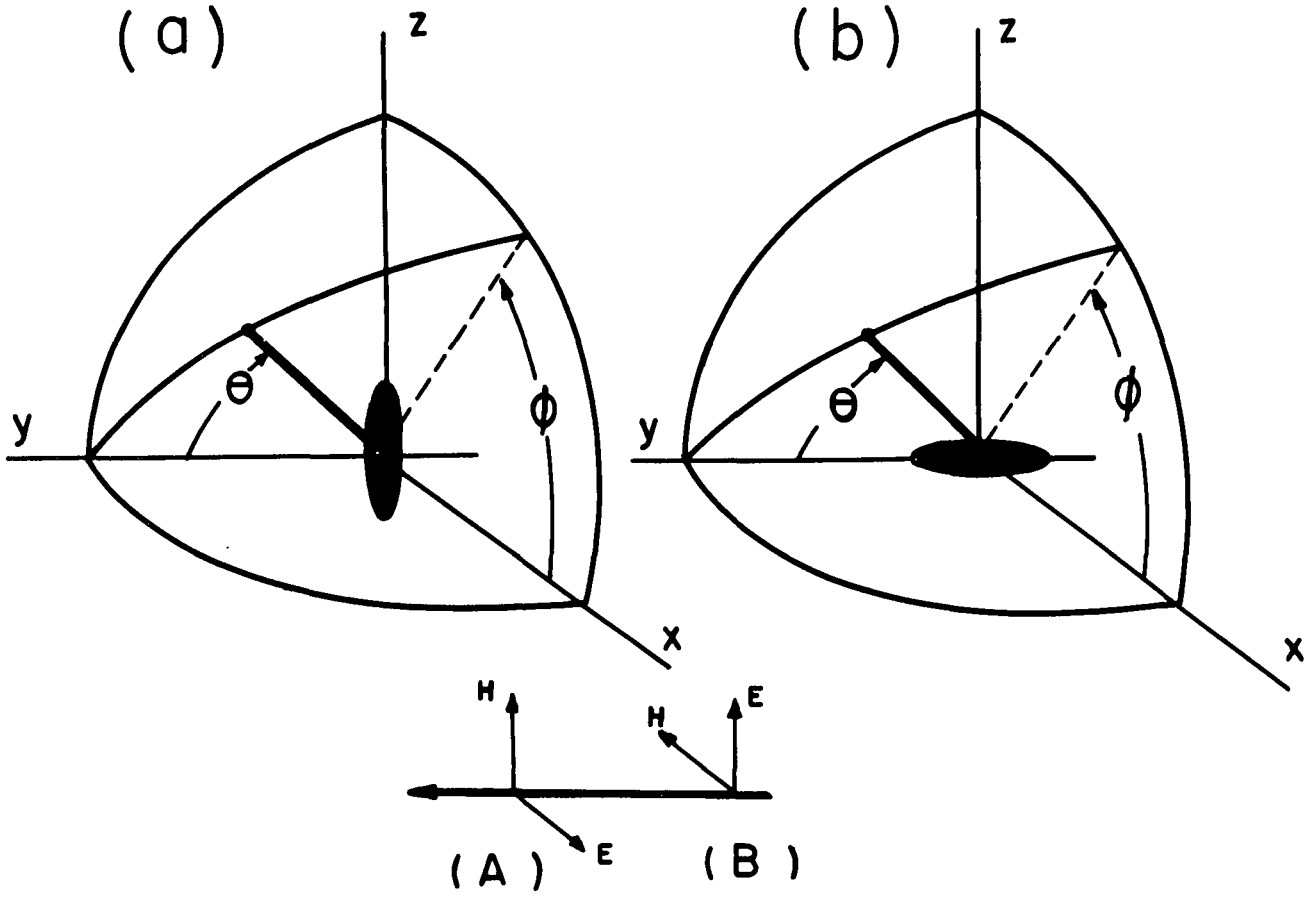

FIG. 11 - ORIENTATION OF THE FALLING DROPS AND THE RADAR BEAM IN BODY COORDINATES (Drops are a. Prolates, b. oblates. Radar Beam A. Horizontal Polarization B. Vertical Polarization)

$$15\bar{N}_1' = \frac{15\bar{N}_1}{b^2 c^3} = \frac{(\epsilon-1)}{3}\left(\frac{2\pi}{4\pi+(\epsilon-1)P'}\right)\left(b^2/c^2-1\right) + \frac{1}{2}\left(\frac{2\pi}{4\pi+(\epsilon-1)P'}\right)$$
$$\times\left\{\epsilon\left(1-b^2/c^2\right) + \frac{(\epsilon-1)}{2}\left(b^2/c^2-1\right)\cdot\left(1+\frac{P}{P'}\right)\frac{P'}{2\pi}\right\}$$
$$-\frac{1}{4}\left(b^2/c^2-1\right) \quad ;$$

$$15N_3' = \frac{15N_3}{b^2 c^3} = b^2/c^2\left[\frac{(\epsilon-1)}{\frac{(\epsilon-1)}{2(1-b^2/c^2)}\left[2-\left(\frac{3P'}{2\pi}\right)b^2/c^2\right]+2}\right]$$

(36)

and

$$\bar{K}_1' = K_3' = 0$$

$$L_3' = N_1' = \bar{L}_1' = \bar{N}_3' = 0$$

For the case of vertical polarization, using the conditions of Eq. 15, the expressions for the scattering coefficients for prolate and oblate water drops become as follows:

$$\bar{K}_1' = 0 \qquad K_3' = \frac{1}{b^2 c}K_3 = 2/3\ (\epsilon-1)\ F_3(\epsilon)\frac{1}{b^2 c}$$

where

$$F_3(\epsilon) = \frac{1}{[2+(\epsilon-1)P/2\pi]}$$

$$15\bar{L}_1' = \frac{15\bar{L}_1}{b^2c^3} = \frac{1}{2}\frac{b^2}{c^2}\left[\frac{\epsilon}{2}\left(1+\frac{c^2}{b^2}\right)-1\right] + \frac{1}{2}\frac{b^2}{c^2}\,G(\epsilon)\cdot\left(\frac{P'-P}{2\pi}\right)$$
$$\times\left[\frac{\epsilon(\epsilon-2)}{2}\left(\frac{c^2}{b^2}-1\right)+1\right] + \frac{1}{2}\,G(\epsilon)\left(\epsilon\left(\frac{b^2}{c^2}-1\right)\right)$$
$$G(\epsilon) = \left\{\left[(\epsilon-1)(1+b^2/c^2)\cdot\frac{1}{\epsilon^2}\left(\frac{3P'}{2\pi}-2\right)\right]+2\right\}^{-1}$$

$$15L_3' = \frac{15L_3}{b^2c^3} = F_3(\epsilon)\left\{(\epsilon-1)\left[\frac{6-5b^2/c^2}{3}+\epsilon\,\frac{b^2}{c^2}\right]\right\}$$
$$+ F_3^2(\epsilon)\left\{(\epsilon-1)\left[(\epsilon-2)\,Ixc + \epsilon\,\frac{c^2}{b^2}\,\frac{P}{2\pi} - \frac{4c^2}{b^2}\right]\right.$$
$$\left. + 2\frac{b^2}{c^2}\,\epsilon^2\right\} \qquad (37)$$

$$15N_1' = \frac{15N_1}{b^2c^3} = G(\epsilon)\left(\epsilon - b^2/c^2\right)$$

$$\bar{N}_3' = 0$$

and

$$K_1' = \bar{K}_3' = 0 \qquad L_1' = N_3' = \bar{L}_3' = \bar{N}_1' = 0$$

Expressions for the Scattered Electric Fields E_{s_x} and E_{s_z}

The expressions for these field components can be obtained easily by using the transformation of co-ordinate relations

$$E_{s_x} = -E_\theta \cos\phi - E_\phi \sin\phi$$
$$E_{s_z} = -E_\theta \sin\phi + E_\phi \cos\phi \qquad (38)$$

Evaluating E_Θ and E_Φ of Eqs. 16 and 17 as before and substituting the resulting values in the above equations, the following equations are obtained

$$E_{s_x} = \eta H_{s_z} = k^2(K_1 - \bar{K}_3) + k^4\left[L_1 - N_3 - \bar{L}_3 + \bar{N}_1 - \frac{b^2}{30}(K_1 - \bar{K}_3)\right] \qquad (39)$$

$$E_{s_z} = -\eta H_{s_x} = k^2(\bar{K}_1 + K_3) + k^4\left[L_3 - N_1 + \bar{L}_1 - \bar{N}_3 - \frac{b^2}{30}(\bar{K}_1 + K_3)\right] \qquad (40)$$

Thus, for horizontal polarization all scattering coefficients involved in Eq. 40, in view of Eq. 36, are zero, i. e., $E_{s_z} = 0$. Thus, only the x-component of the electric field is scattered back and has the same polarization as the incident field. Also, for vertical polarization, according to Eqs. 39 and 37, $E_{s_x} = 0$ and only the vertical component of the electric field is scattered back with the same polarization as the incident field. However, this is not true when the orientation of the electric field is intermediate between the two polarizations, (see Figures 21 and 22).

Extension of the Formulas to Obliquely Falling Drops

The formulas for the scattering cross-sections derived earlier can be easily extended to the case of obliquely falling drops, if the tilt of the drop is in the plane normal to the direction of propagation of the incident beam. In this case, consider the polarization of the incident beam (Electric field E) at an angle ϕ, (representing the tilt of the drop) which is intermediate between the horizontal and vertical polarization.

Resolving the incident electric field, E_i, into components along the x, z axes, the following relation is obtained

$$\tan\phi = E_{i_z} / E_{i_x} \qquad (41)$$

The radar back scattering cross-section, σ, for this case from Eq. 6 is

$$\sigma = 4\pi R^2 \frac{E_s^2}{E_i^2} = \frac{E_{s_x}^2 + E_{s_z}^2}{E_{i_x}^2 + E_{i_z}^2} \tag{42}$$

This may be written in a more appropriate form by combining Eqs. 41 and 42

$$\sigma = 4\pi R^2 \left(\frac{E_{s_x}^2}{E_{i_x}^2} \cos^2 \phi + \frac{E_{s_z}^2}{E_{i_z}^2} \sin^2 \phi \right) \tag{43}$$

or according to the definition of

$$\sigma = \sigma_x \cos^2 \phi + \sigma_z \sin^2 \phi \tag{44}$$

where σ_x represents the back-scattering cross-section for the case of horizontal polarization and σ_z for vertical polarization.

Depolarization

The angle of polarization, Ω, of the scattered field with respect to the body coordinates may be written as

$$\Omega = \tan^{-1} \frac{E_{s_z}}{E_{s_x}} \tag{45}$$

or

$$\Omega = \tan^{-1} \sqrt{\frac{\sigma_z}{\sigma_x}} \cdot \tan \phi$$

since

$$E_{s_x} = \sqrt{4\pi R^2} E_{i_x} \cdot \sqrt{\sigma_x} = \sqrt{4\pi R^2 \sigma_x} \cdot E_i \cos\phi$$

and

$$E_{s_z} = \sqrt{4\pi R^2} E_{i_z} \cdot \sqrt{\sigma_z} = \sqrt{4\pi R^2 \sigma_z} \cdot E_i \sin\phi \qquad (46)$$

Thus, if the incident electric field is polarized at an angle, ϕ , the scattered field will be polarized at an angle, Ω .

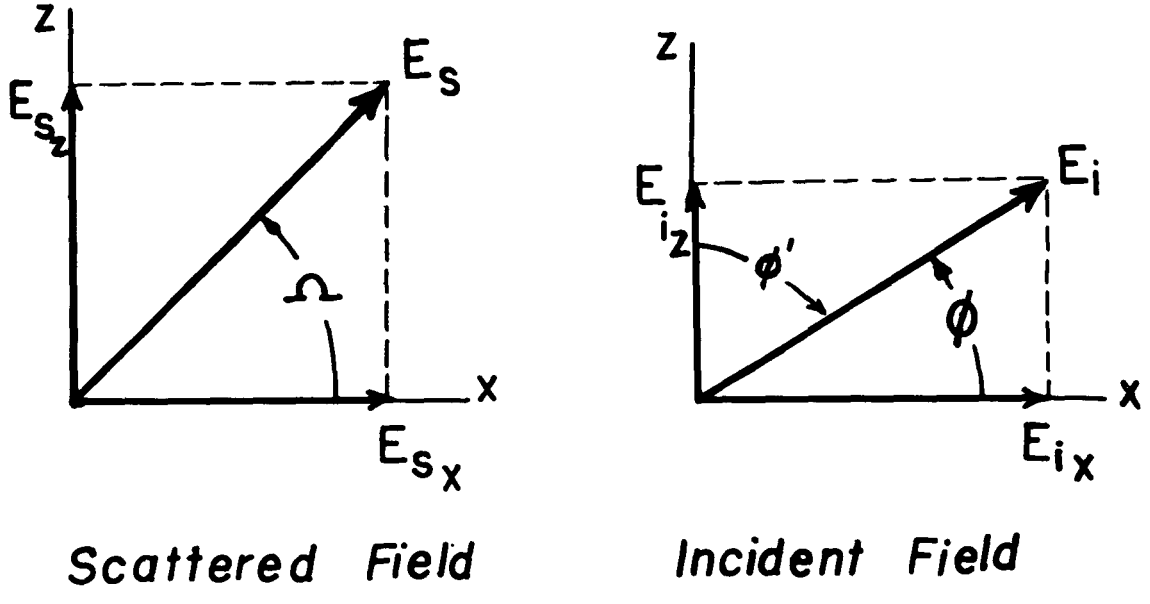

FIG. 12 - SCATTERED FIELD, INCIDENT FIELD

Forward-Scattering Cross-Section Q_s

The scattering cross-section, Q_s, according to the definition of Eq. 3 is

$$Q_s = P_s / S_i \tag{47}$$

where P_s is the total power scattered by the scatterer and represents the radial poynting vector* integrated over a sphere of large distance, R, i. e.

$$P_s = \frac{1}{2} \mathcal{R}e \int_0^{\pi} \int_0^{2\pi} (E_\theta H_\phi^* - E_\phi H_\theta^*) R^2 \cdot \sin\theta \cdot d\theta \cdot d\phi \tag{48}$$

Calculations of this integral, for the case of Stevenson's solution, are involved. Only the steps are described and final results are presented here.

Differentiating P and $\bar{P}$ with respect to 8 and ϕ, and substituting these differentials in Eqs. 16 and 17 provides the required field components appearing in the integral. By carrying out the integration and rearranging the terms it can be shown that

$$Q_s = \left(\frac{8\pi}{3}\right) \sum_{j=1}^{3} \left[(k^2 K_j + k^4 L_j)^2 + (k^2 \bar{K}_j + k^4 \bar{L}_j)^2 \right] + \sum_{j=1}^{3} \left[q_j (M_j M_m + \bar{M}_j \bar{M}_m) + P_j (M_j^2 + \bar{M}_j^2) \right] \tag{49}$$

where P_j and q_j are constants of integration and m takes values in cyclic order with j.

RESULTS, CONCLUSIONS AND RECOMMENDATIONS

From the formulas derived in the text, values of the scattering coefficients K_j, $\overline{K}_j$, L_j, $\overline{L}_j$, etc. of Eqs. 36 and 37 were computed for both prolate and oblate raindrops for a 3-cm wave for horizontal and vertical polarization, and for a 10-cm wave for horizontal polarization. The data are presented in Tables XVIII to XXIII inclusive. The shapes of the drops denoted by the appropriate values of the axis ratios (b/c for prolates and c/b for oblates) is represented by the first column of these tables.

Using these tables the radar back-scattering cross-sections were computed for non-spherical raindrops for the above mentioned cases. The results are summarized in Figures 13 to 18. These figures show the variation of the ratio σ/σ_e with α, with the shape of the drops (axis ratio) as a parameter. The charts for oblates, however, differ slightly in that the ordinate is multiplied by $(c/b)^3$ to present a wider spread between the curves of different oblates (c/b values).

Calculations were also made for the radar back-scattering cross-sections for oblates and prolates at Z-incidence. The results are presented in Figures 19 and 20.

Figures 21 and 22 show the depolarization angle of the back-scattered field measured from the horizontal incident field as a function of the orientation of the drops. The angle ϕ' is measured from the vertical axis to the major axis of the drop. Figures 23 and 24 show the back-scattering cross-section of a tilted drop, normalized with respect to the back scattering cross-section of the untilted drop ($\phi' = 0$), as a function of the tilt angle ϕ'

In making the practical evaluation in Part I and Part II it was the conclusion of the authors that an exact solution,based on spheroidal function theory for dielectric spheroids, would be limited in its application to raindrop analysis, considering the choice of variables required in such an analysis and the labor that would be involved in the numerical evaluation. Stevenson's solution in this respect is less tedious to calculate and allows arbitrary choice of the drop orientation and incident field conditions, the drop shape (even includes a triaxial ellipsoid $a \neq b \neq c$), and the electric properties of the scattering medium. Since this solution is in the form of a power series, an extension of the present formulas and numerical results, based on a three-term solution, can easily be made. It may, however, be emphasized again that the check of the accuracy of this theory has been made only indirectly;

that is, only for the case of conducting prolate spheroids since there is no exact solution available at present for dielectric spheroids. Therefore, the results are based on the assumption that the behavior of the dielectric spheroids (like in the case of spheres)* is not radically-different from those of conducting spheroids. It would be desirable in future to: (1) check this theory directly against an exact solution for dielectric spheroids, if and when such a solution is developed, and (2) if necessary, extend the present results to more terms of the series.

* See discussion of reference 16, page 613.

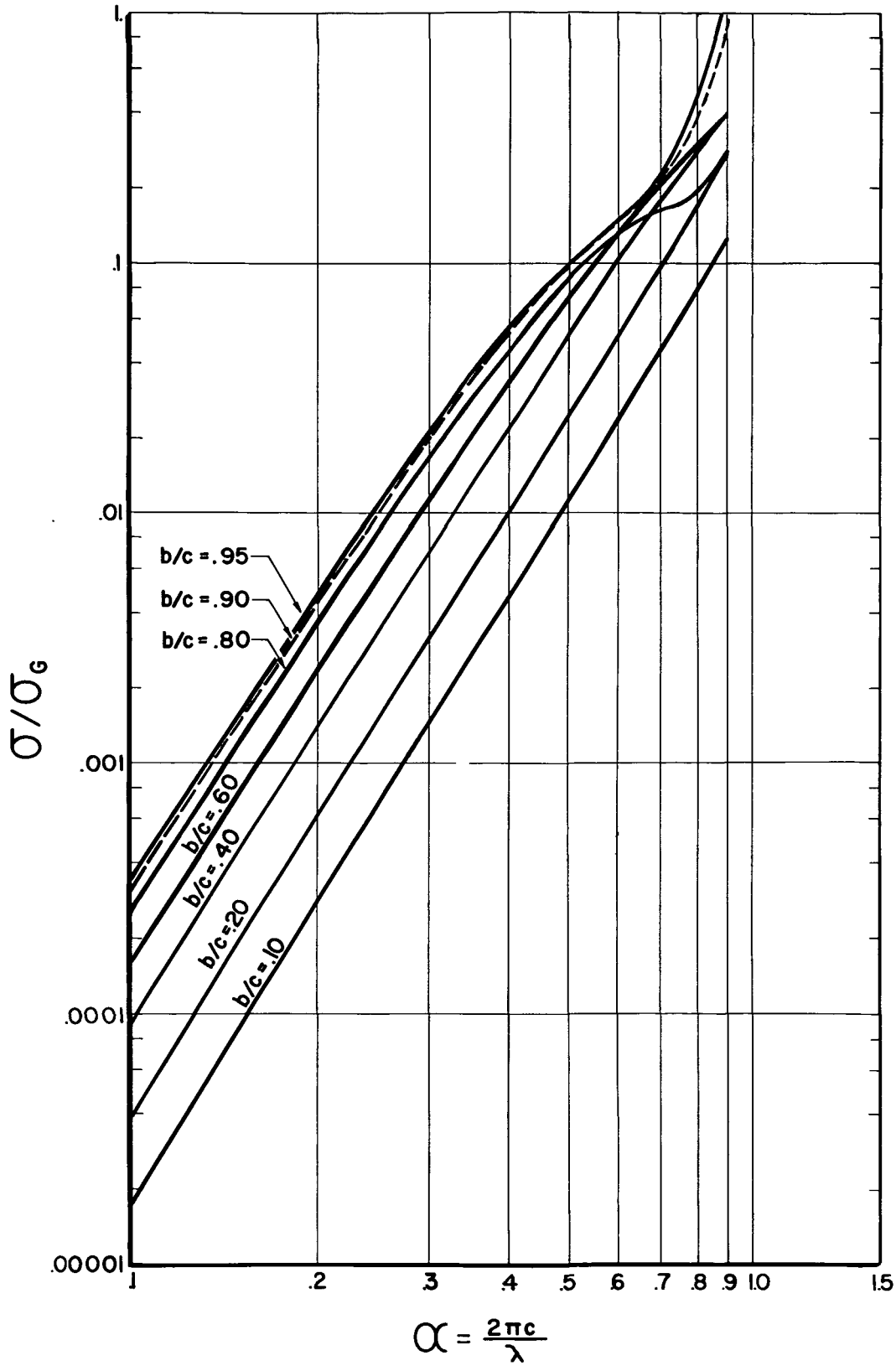

FIG. 13 - RADAR BACK-SCATTERING CROSS-SECTIONS FOR FALLING PROLATE DROPS AT 3 CM WITH HORIZONTAL POLARIZATION

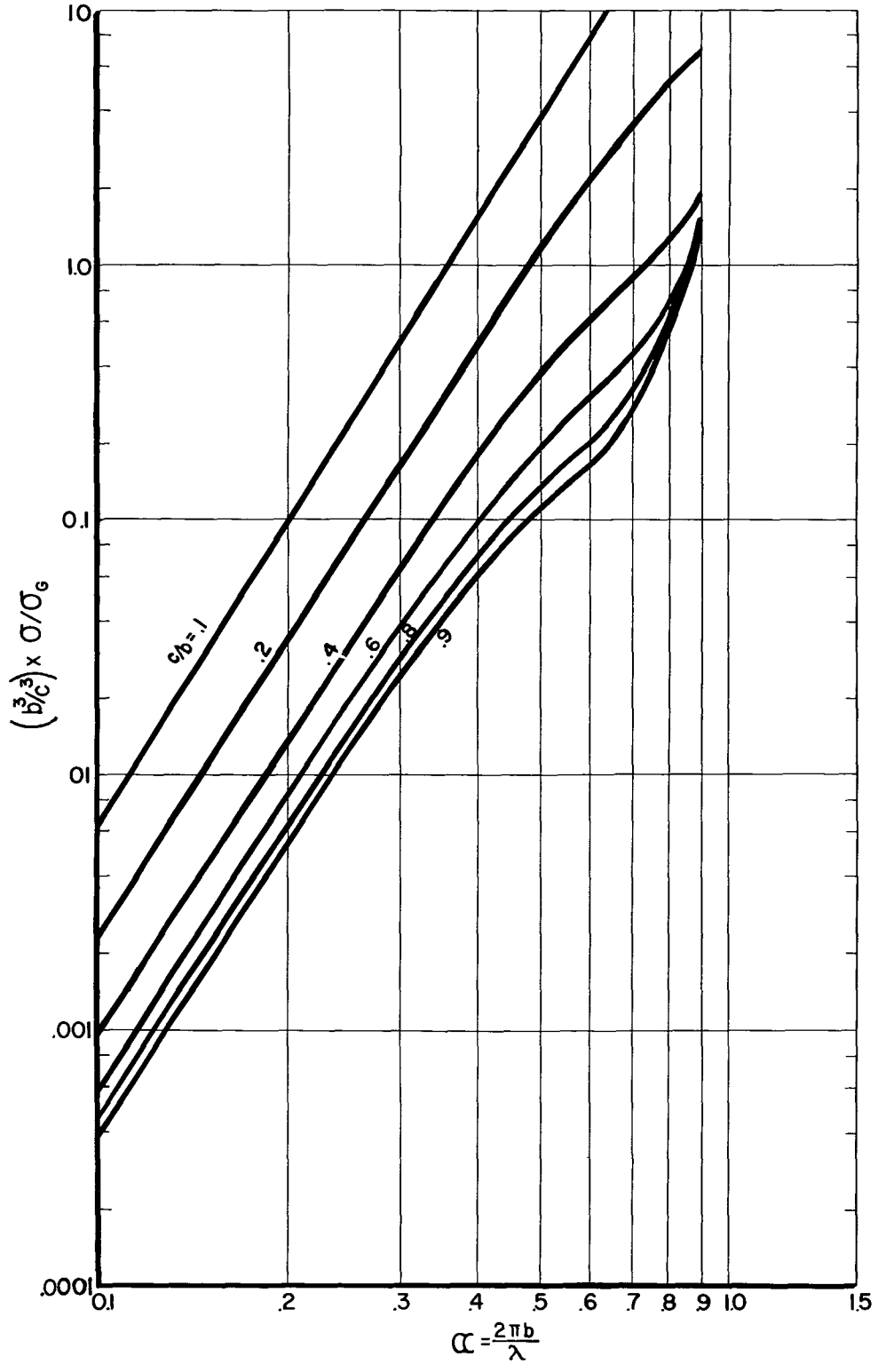

FIG. 14 - RADAR BACK-SCATTERING CROSS-SECTIONS FOR FALLING OBLATE DROPS AT 3 CM WITH HORIZONTAL POLARIZATION

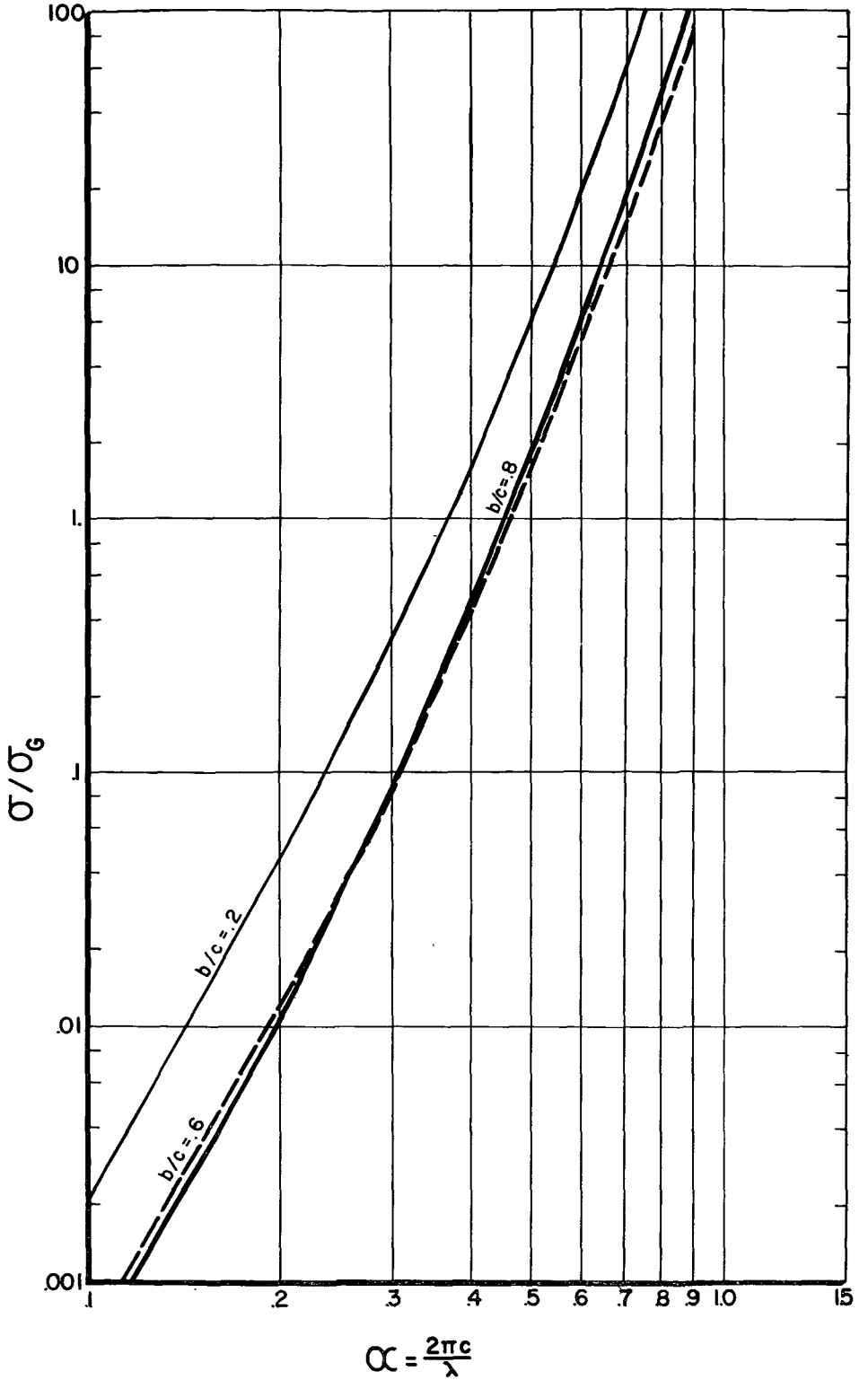

FIG 15 - RADAR BACK-SCATTERING CROSS-SECTIONS FOR FALLING PROLATE DROPS AT 3 CM WITH VERTICAL POLARIZATION

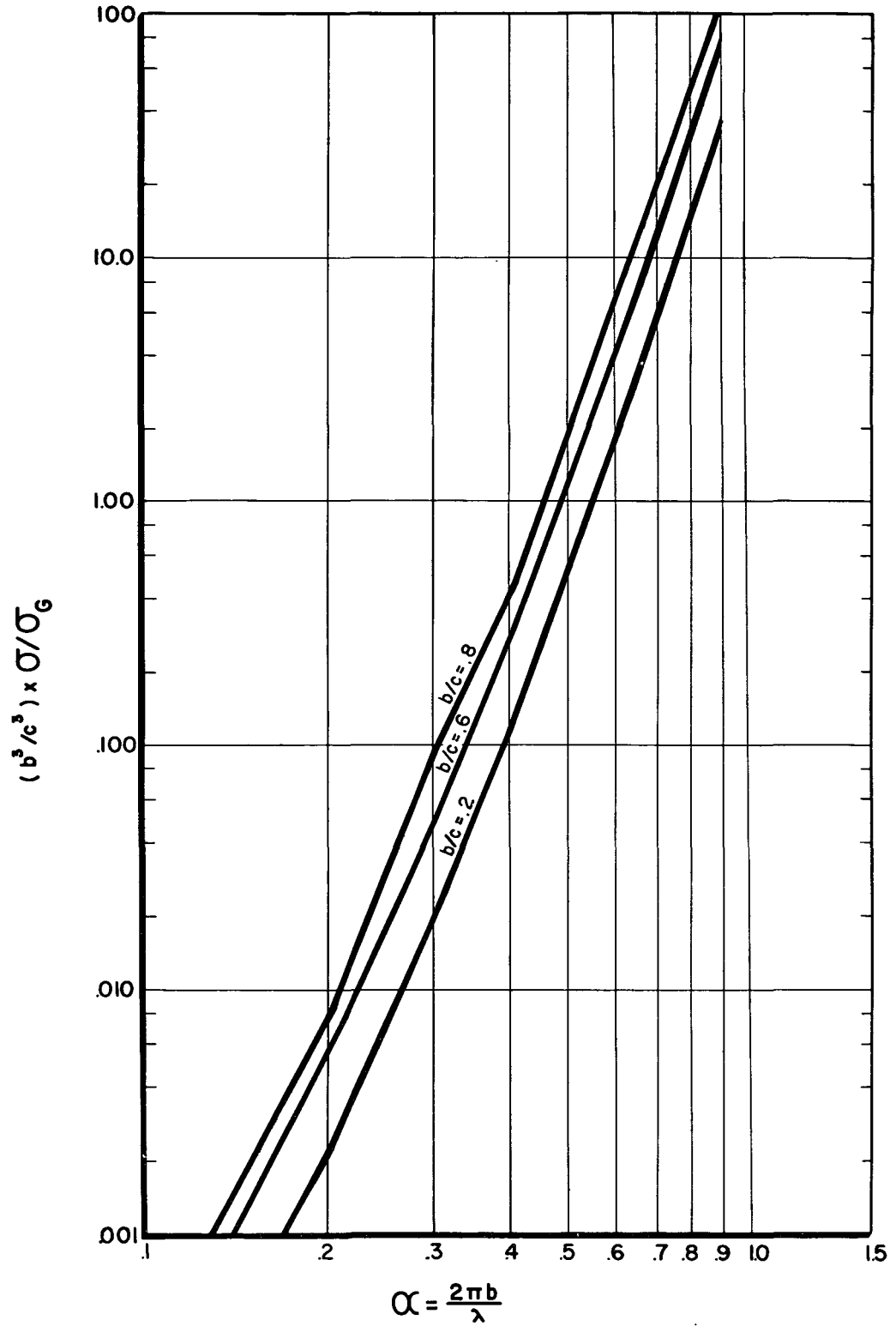

FIG. 16 - RADAR BACK-SCATTERING CROSS-SECT IONS FOR FALLING OBLATE DROPS AT 3 CM WITH VERTICAL POLARIZATION

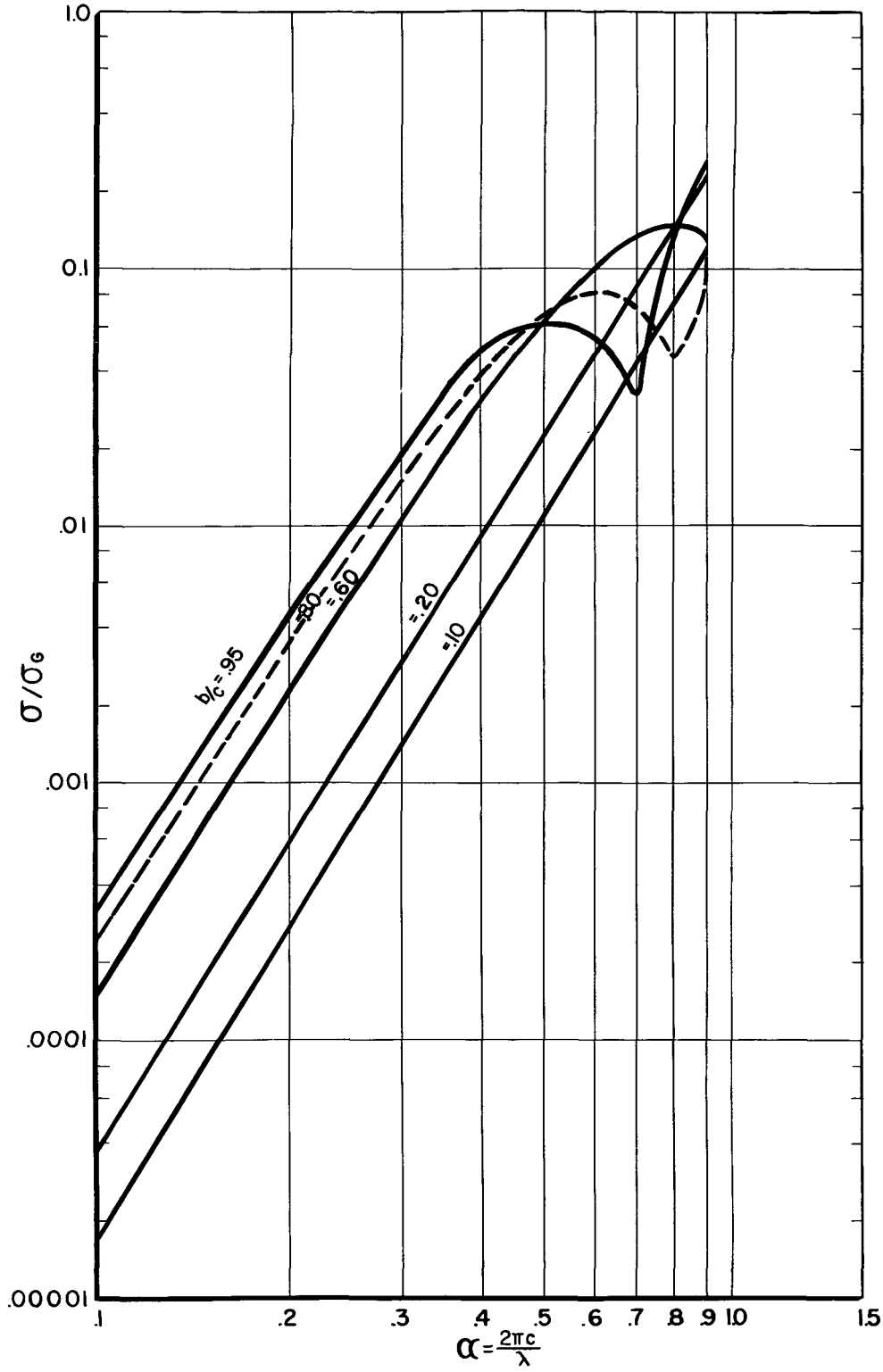

FIG. 17 - RADAR BACK-SCATTERING CROSS-SECTIONS FOR FALLING PROLATF DROPS AT 10 CM WITH HORIZONTAL POLARIZATION

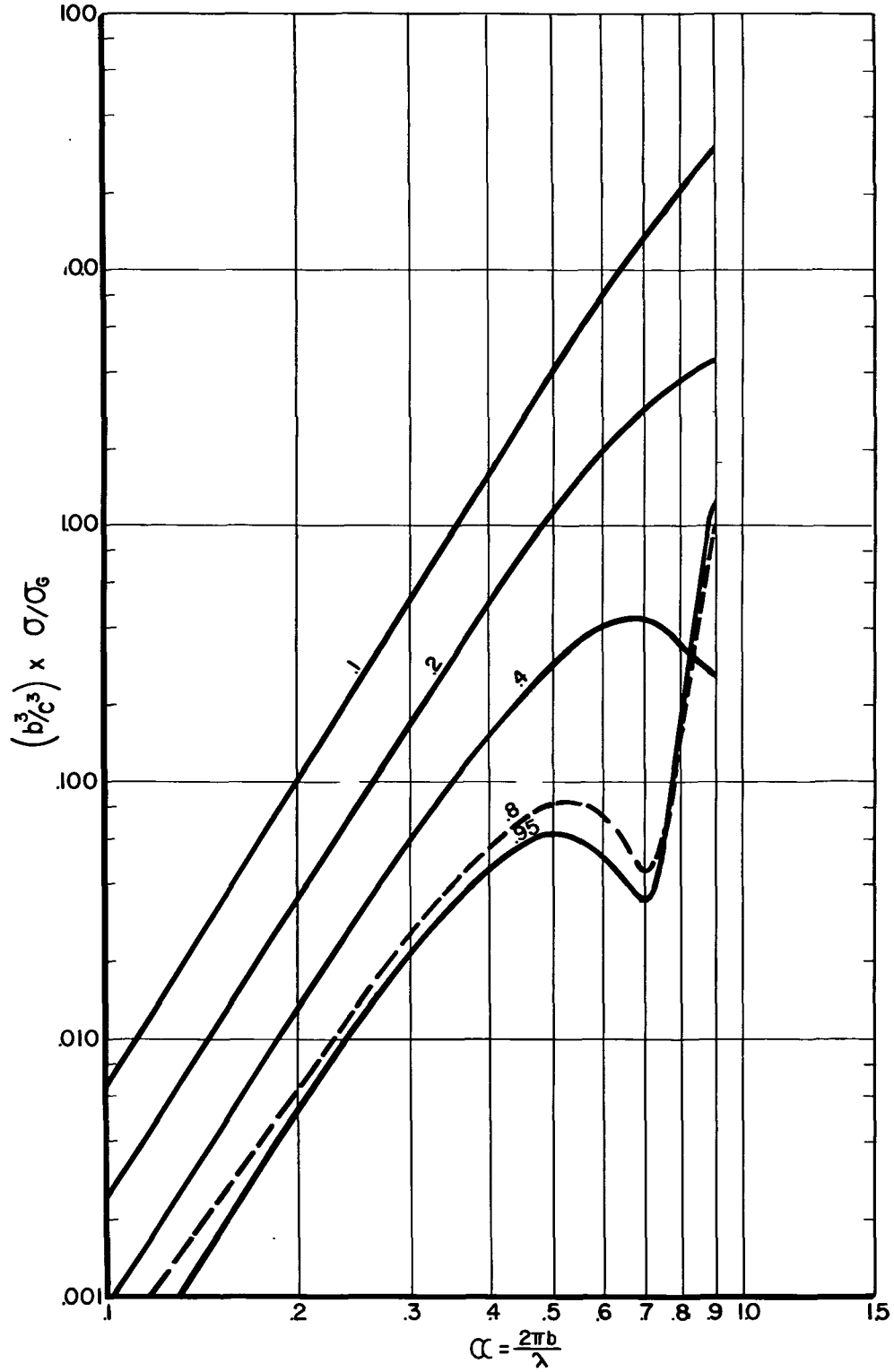

FIG. 18 - RADAR BACK-SCATTERING CROSS-SECTIONS FOR FALLING OBLATE DROPS AT 10 CM WITH HORIZONTAL POLARIZATION

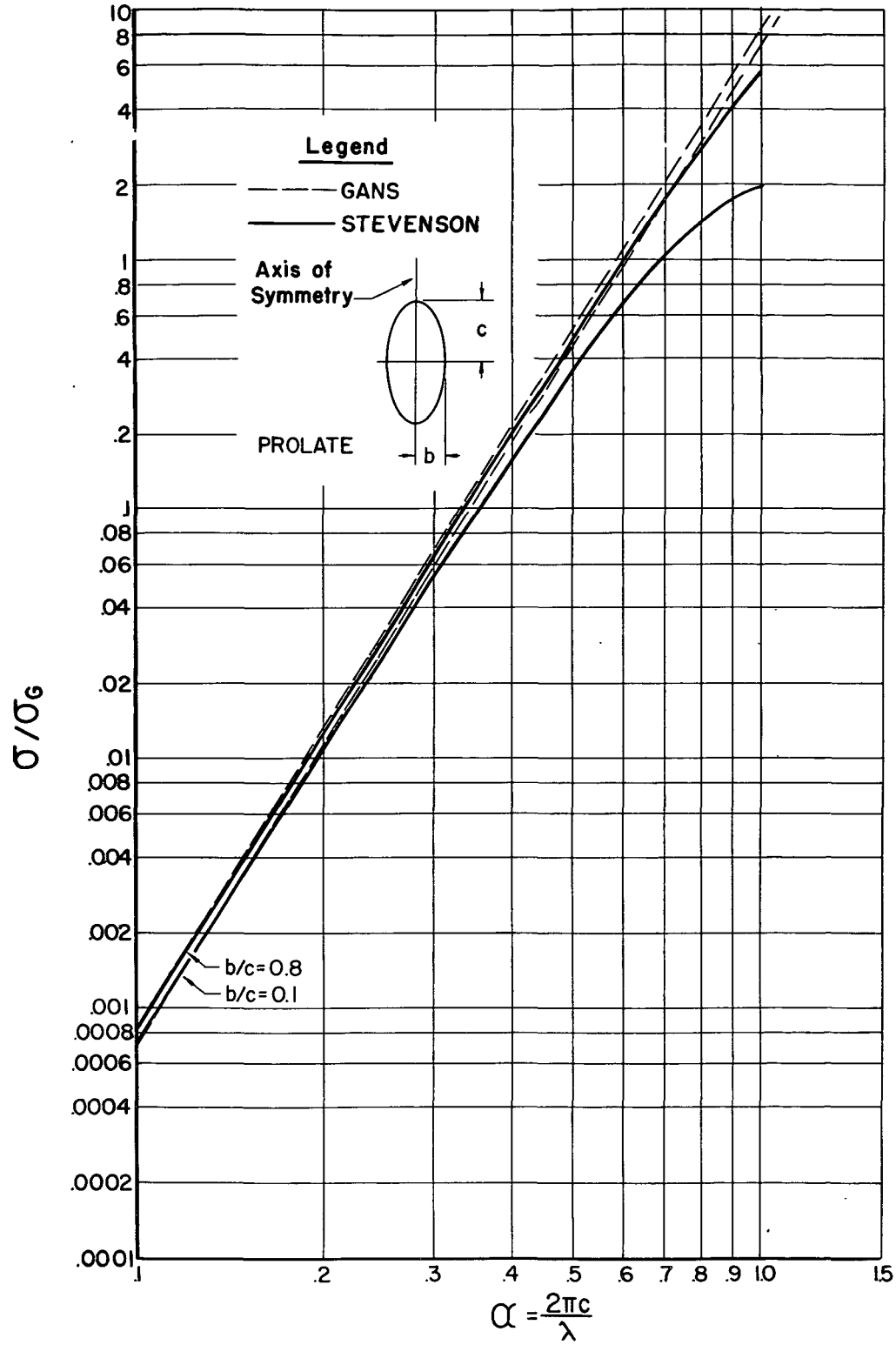

FIG. 19 - RADAR BACK-SCATTERING CROSS-SECTIONS FOR CONDUCTING OBLATES (Z-Incidence)

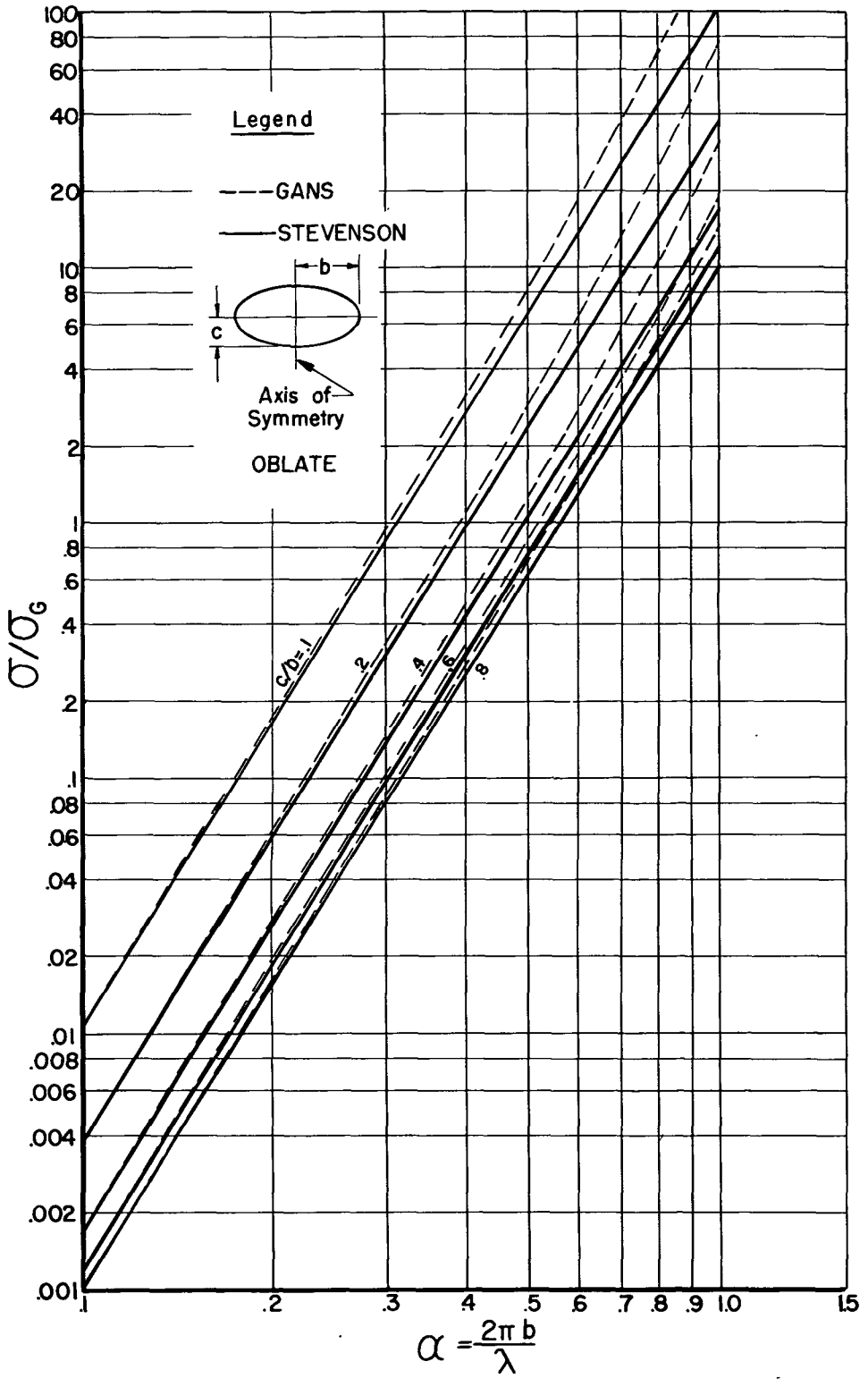

FIG. 20 - RADAR BACK-SCATTERING CROSS-SECTIONS FOR CONDUCTING PROLATES (Z -Incidence)

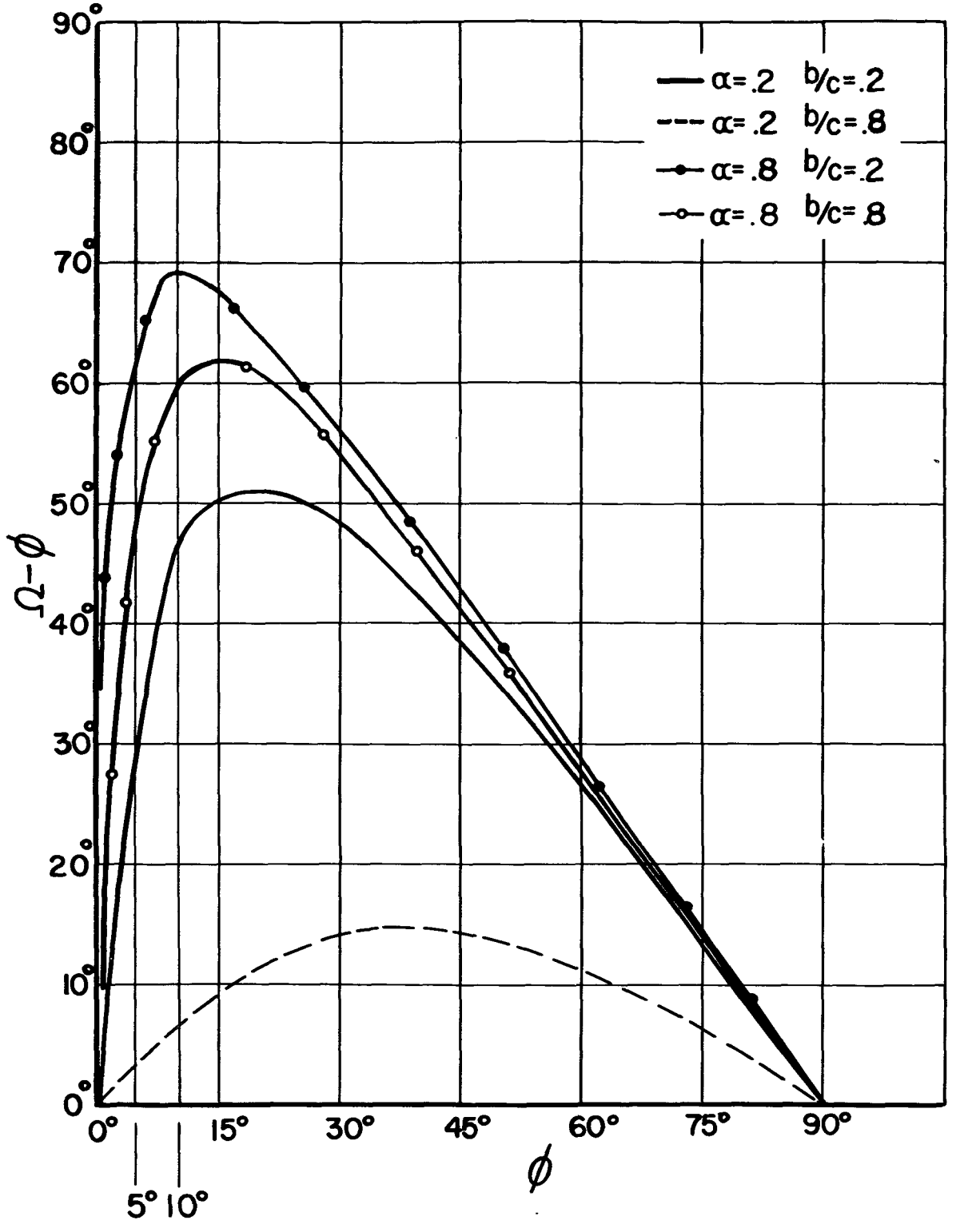

FIG. 21 - POLARIZATION OF THE FIELD SCATTERED FROM PROLATES

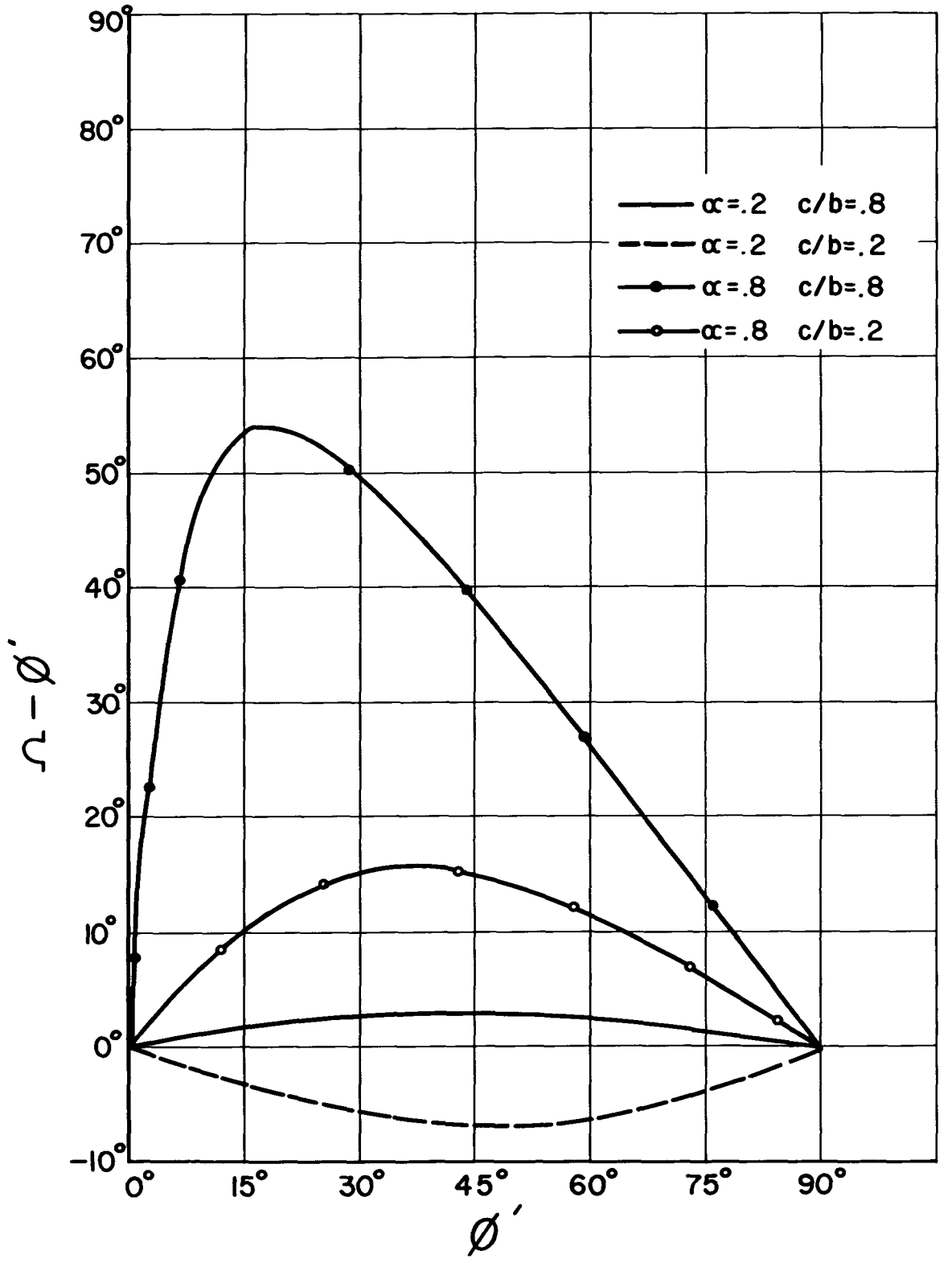

FIG. 22 - POLARIZATION OF THE FIELD SCATTERED FROM OBLATES

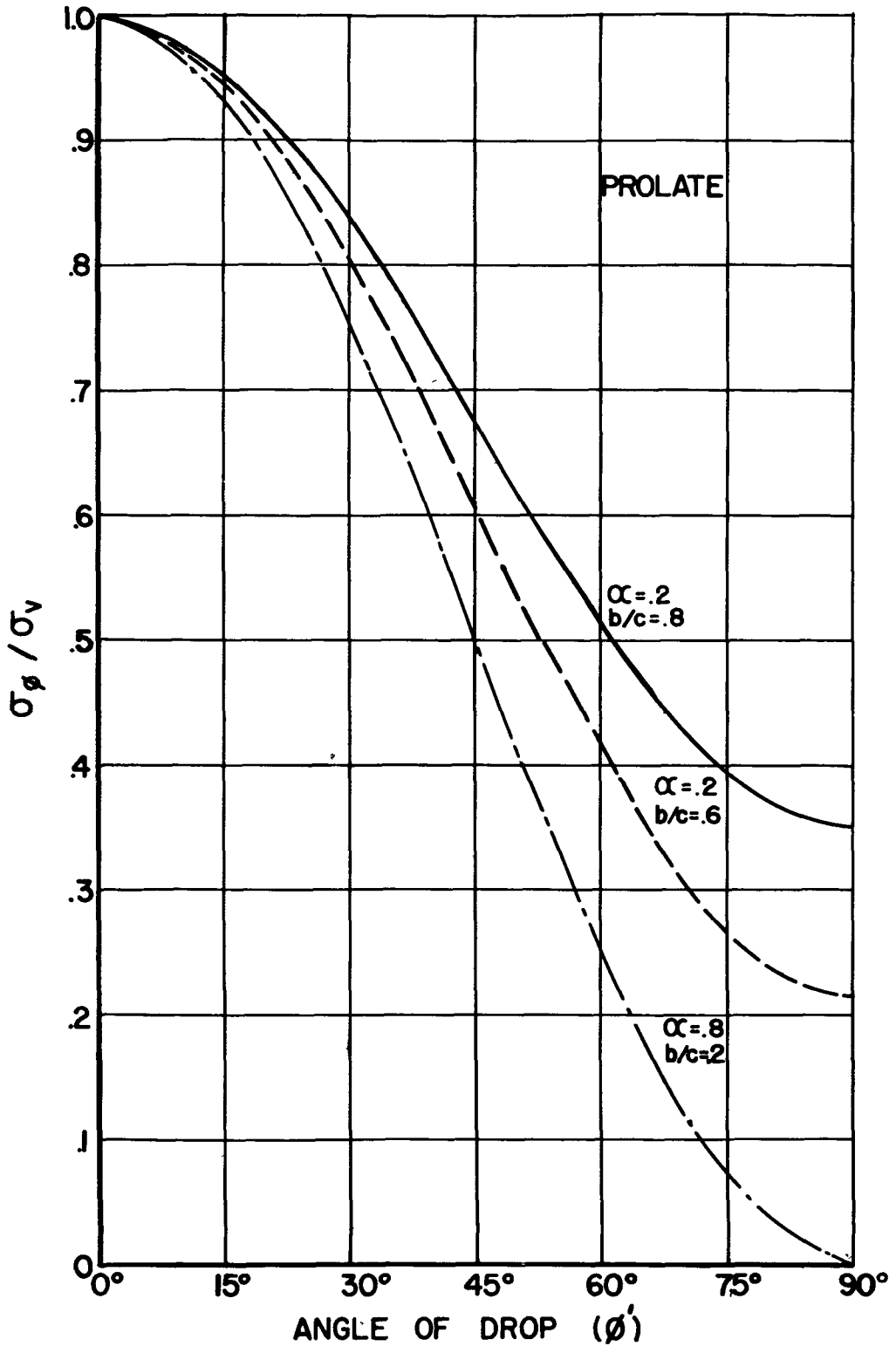

FIG. 23 - RATIO OF THE BACK-SCATTERING CROSS-SECTION FOR TILTED DROPS TO THE BACK-SCATTERING CROSS-SECTION FOR NON-TILTED DROPS, AXIS RATIO 0-8

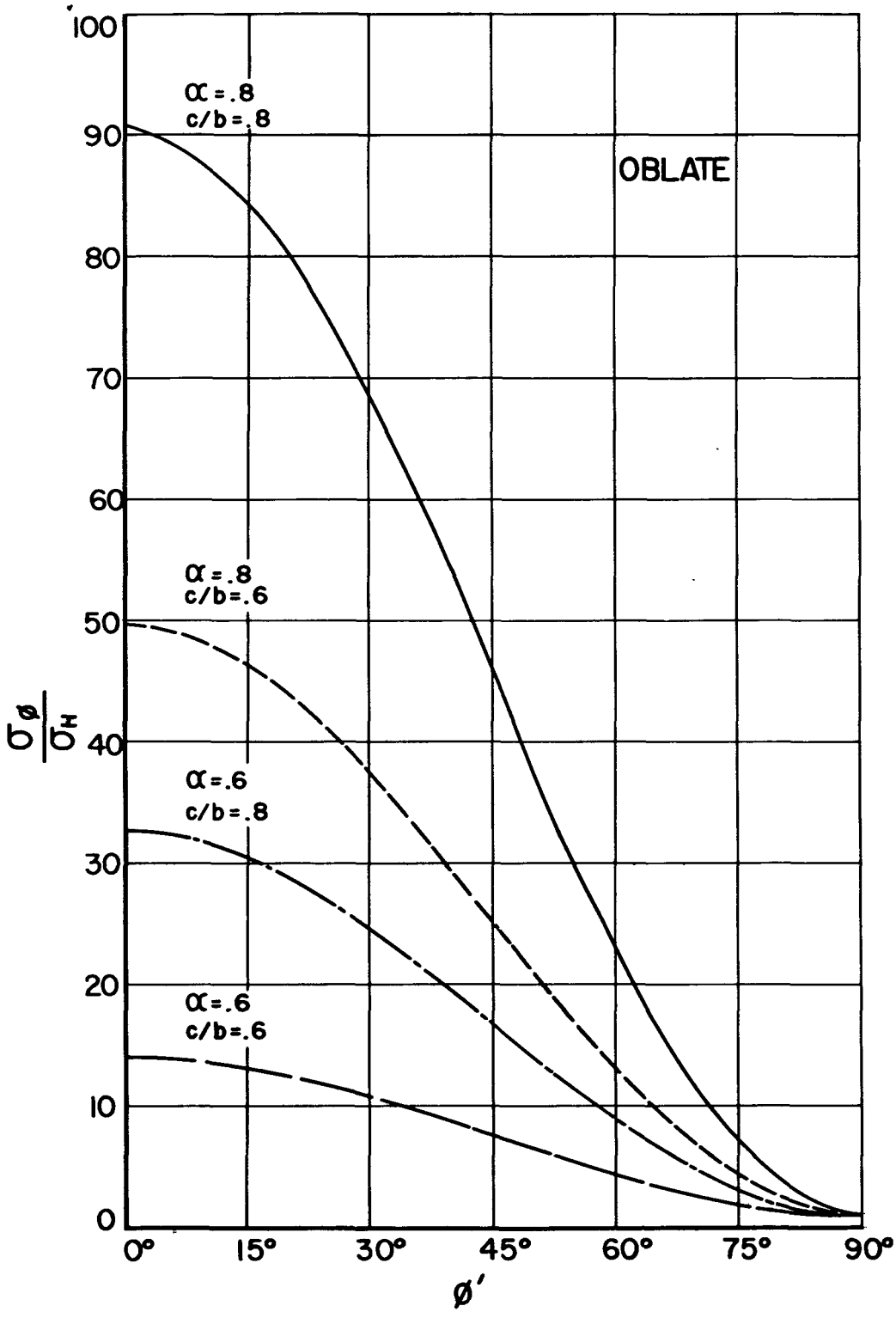

FIG. 24 - RATIO OF THE BACK-SCATTERING CROSS-SECTION FOR TILTED DROPS TO THE BACK-SCATTERING CROSS-SECTION FOR NON-TILTED DROPS, AXIS RATIO 0.2

REFERENCES

1. Herzfeld, "Uber die Beugung von elektro-magnetischen Wellen an gestreckten, Vollkommen leitenden Rotationsellipsoiden", Wiener Ber Wien Akademi der Wissenschaften, V. 1. 120, 1911, pp. 1587.

2. Moglich, F., "Beugungserschieinungen an Korpern von Ellipsoidischer Gestalt", Annalen der Physik, Vol. 83, 1927, pp. 609.

3. Schultz, F. V., Scattering by a Prolate Spheroid, Report UMM-42, Aeronautical Research Center, University of Michigan, March, 1950.

4. Siegel, K. M., Gere, B. H., Marx, I., Sleatator, F. B., The Numerical Determination of Radar Cross-Section of a Prolate Spheroid, Report UMM-126, University of Michigan, October 1953.

5. Gans, R., "Uber die Form ultramikroskopischer Goldteilchen", Ann. der Phys. 1912, Vol. 137, pp. 881-990.

6. Rayleigh, Lord, Phil. Mag., Vol. 44, pp. 28 (1897).

7. Stevenson, A. F., "Electromagnetic Scattering by an Ellipsoid in the Third Approximation", Jo. App. Phys. Vol.24, No. 9, September 1953, pp. 1143-1151.

8. Hansen, W. W., "A New Type of Expansion in Radiation Problems", Physical Reviews, Vol. 47, 1935, pp. 139.

9. Stratton, J. A., Morse, P. M., Chu, L. J., and Hunter, R. A., Elliptic Cylinder and Spheroidal Wave Functions, Wiley & Sons Inc., New York, 1941.

10. Morse, P. M., "Additional Formulae for Spheroidal Functions" Proc. Mat. Acad. Sci., Vol. 21, 1935, pp. 56.

11. Mathematical Tables Project, National Bureau of Standards Tables of Associated Legendre Functions, Columbia University Press, New York, 1945.

12. Mathematical Tables Project, National Bureau of Standards Tables of Associated Legendre Functions, Columbia Press, New York, 1947.

13. Ritz, J. F., "On the Differentiability of Asymptotic Series", Bulletin of Am. Math. Soc., Vol. 29, 1918, pp. 225.

14. Stratton, J.S., Electromagnetic Theory, McGraw-Hill, New York, 1941.

15. Jones, D.M.A., and Dean, L. A., A Raindrop Camera, Research Report No. 3, Illinois State Water Survey, under contract DA-36-039 SC-42446, U. S. Army Signal Corps Engineering Laboratories, Fort Monmouth, N. J., December 1953.

16. Kerr, D. E., Editor, Propogation of Short Waves Radiation Laboratory Series, McGraw-Hill Co. Vol. 13, 1951, pp. 31.

17. Saxton, J. A., The Dielectric Properties of Water at Wavelengths from 2 mm to 10 cm and Over the Temperature Range 0° to 40° C. National Physical Laboratory (British) Paper No. RRB/C 115, March 1945.

APPENDIX A

The values of the integrals I_n^{Ll} of equation (17) evaluated by Schultz[3,4] in terms of tabulated prolate spheroidal coefficients are:

$$I_1^{Ll} = N_{0l} \quad \text{for } L=l$$

$$= 0 \quad \text{for } L \neq l$$

$$I_2^{Ll} = -2\mu_{L,l+1}\left[\sum_{n=0}^{\infty}\mu_{n,l}\cdot\frac{n+1}{2n+3}\cdot d_n^{ll}\cdot d_{n+1}^{0L} + \sum_{n=0}^{\infty}\sum_{p=n+1}^{\infty}\mu_{L,P}\cdot\mu_{L,N}\, d_n^{0L}\cdot d_p^{ll}\right.$$

where $\mu_{ij} = 0$ for $i+j$ odd & equal to one for $i+j$ even.

$$I_3^{Ll} = \sum_{n=1}^{\infty}{}' \frac{n+1}{n(n+2)}\cdot\left[d_{\frac{n-1}{2}}^{0l}\; d_{\frac{n+1}{2}}^{0L} + d_{\frac{n+1}{2}}^{0l}\; d_{\frac{n-1}{2}}^{0L}\right]$$

$$I_4^{Ll} = \sum_{n=1}^{\infty}{}' \frac{n+1}{n(n+2)}\left[(n+3)\, d_{\frac{n+1}{2}}^{0l}\cdot d_{\frac{n-1}{2}}^{0L} - (n-1)\, d_{\frac{n-1}{2}}^{0l}\cdot d_{\frac{n+1}{2}}^{0L}\right]$$

$$I_5^{Ll} = \sum_{n=0,2_{(even)}}^{\infty}{}' \frac{n+2}{2(n+1)(n+3)}\left[n\, d_{\frac{n}{2}-1}^{ll}\cdot d_{\frac{n}{2}+1}^{0L} - (n+4)\, d_{\frac{n}{2}}^{ll}\cdot d_{\frac{n}{2}}^{0L}\right]$$

$$I_6^{Ll} = 2\mu_{l,n}\left\{\sum_{n=0}^{\infty}\frac{(n+1)^2}{(2n+1)(2n+3)}\cdot\left[(n+2)\, d_n^{ll}\cdot d_n^{0L} + n\cdot d_{n-1}^{ll}\cdot d_{n+1}^{0L}\right]\right.$$

$$-\sum_{n=0}^{\infty}\mu_{l,n}\frac{d_n^{0L}}{(2n+1)}\left[\frac{n(n-1)}{2n-1}\cdot d_{n-2}^{ll} + \frac{(n+1)^2}{2n+3}\, d_n^{ll} + n\, d_n^{ll}\right]$$

$$\left.-\sum_{n=0}^{\infty}\sum_{p=0}^{\infty}\mu_{l,n}\,\mu_{l,p}\cdot d_n^{0L}\cdot d_p^{0l}\right\}$$

The numerical values of these integrals have been computed for c = .1, .2, .4, .6, and .8 for all combinations of the values of l = 0, 1, 2 and L = 0, 1, 2. The data are reported in table IX.

APPENDIX B

The general expressions for the scattering coefficients appearing in simultaneous equations (34a) and (34b) are as follows:

$$B_{Ll} = \left(\frac{i}{c\xi}\right) \cdot A_{ol} \cdot (\xi^2 - 1)^{1/2} \cdot R_{ol}^{(-1)\prime}(c,\xi) \cdot I_1^{Ll}$$

$$C_{Ll} = (\xi^2 - 1)^{1/2} \cdot R_{ol}^{(4)\prime}(c,\xi) \cdot I_1^{Ll}$$

$$D_{Ll} = -R_{1l}^{(4)}(c,\xi) \cdot I_2^{Ll}$$

$$U_{Ll} = \left(\frac{i}{c\xi}\right) \cdot A_{ol}\left[(\xi^2 - 1)\ R_{ol}^{(1)\prime}(c,\xi) \cdot I_3^{Ll} + \xi\, R_{ol}^{(1)}(c,\xi) \cdot I_4^{Ll}\right]$$

$$V_{Ll} = (\xi^2 - 1)\ R_{ol}^{(4)\prime}(c,\xi) \cdot I_3^{Ll} + \xi\, R_{ol}^{(4)}(c,\xi) \cdot I_4^{Ll}$$

$$W_{Ll} = -\xi(\xi^2 - 1)^{1/2} \cdot R_{1l}^{(4)\prime}(c,\xi)\, I_5^{Ll} + (\xi^2 - 1)^{1/2} \cdot R_{1l}^{(4)}(c,\xi) \cdot I_6^{Ll}$$

$$A_{ol} = \frac{2i^l}{N_{ol}} \cdot \sum_{n=0,1}^{\infty}{}' d_n^{ol}$$

These coefficients have been computed for different combinations of $l = 0, 1, 2$ and $L = 0, 1, 2$ and for each combination of $\xi = 1.1, 1.2, 1.3$ and $c = .1, .2, .4, .6$ and $.8$. The numerical data are reported in tables X - XIII.

APPENDIX C

The scattering coefficients α_{0l}, β_{1l} appearing in the infinite system of simultaneous equations (Eqs. 34a, 34b) decrease very rapidly[4] with increasing mode l as long as l is greater than the characteristic dimension times the wave number ($\alpha = ka$). In the range of α below the resonance region, it is sufficient to truncate the equations series after four or five terms*. The determinantal solution of α_{0l}, β_{1l} for three terms of the series are given as follows:

$$\alpha_{00} \times G = \begin{vmatrix} B_{00} & 0 & D_{01} \\ B_{22} & C_{22} & D_{21} \\ U & V_{12} & W_{11} \end{vmatrix} \quad \alpha_{01} \times H = \begin{vmatrix} B_{11} & D_{10} & D_{12} \\ U_{01} & W_{00} & W_{02} \\ U_{21} & W_{20} & W_{22} \end{vmatrix} \quad \alpha_{02} \times G = \begin{vmatrix} C_{00} & D_{00} & D_{01} \\ 0 & B_{22} & D_{21} \\ V_{10} & U & W_{11} \end{vmatrix}$$

$$\alpha_{03} \times H = \begin{vmatrix} C_{11} & B_{11} & D_{10} \\ V_{01} & U_{01} & W_{00} \\ V_{21} & U_{21} & W_{20} \end{vmatrix} \quad \beta_{11} \times H = \begin{vmatrix} C_{11} & B_{11} & D_{12} \\ V_{01} & U_{01} & W_{02} \\ V_{21} & U_{21} & W_{22} \end{vmatrix} \quad \beta_{12} \times G = \begin{vmatrix} C_{00} & 0 & B_{00} \\ 0 & C_{22} & B_{22} \\ V_{10} & V_{12} & U \end{vmatrix}$$

$$\beta_{13} \times H = \begin{vmatrix} C_{11} & D_{10} & B_{11} \\ V_{01} & W_{00} & U_{01} \\ V_{21} & W_{20} & U_{21} \end{vmatrix} \qquad G = \begin{vmatrix} C_{00} & 0 & D_{01} \\ 0 & C_{22} & D_{21} \\ V_{10} & V_{12} & W_{11} \end{vmatrix} \qquad H = \begin{vmatrix} C_{11} & D_{10} & D_{12} \\ V_{01} & W_{00} & W_{02} \\ V_{21} & V_{20} & W_{22} \end{vmatrix}$$

and $\quad U = U_{10} + U_{12}$

The numerical values of the scattering coefficient α_{0l} for $l = 0$, 1 and 2 are presented in table IX.

---

* Since in the present computations α is less than one, the scattering coefficients corresponding to $l \geq 3$ were neglected. This termiriation affected the values of σ in the sixth significant figure after the decimal.

APPENDIX D

The general expressions for the scattering coefficients involved in Eqs. 20 and 21 are as follows:

$$K_1 = \frac{2}{3}(\epsilon-1) f_1(\epsilon) l_1 \quad ; \qquad D_1$$

$$15 L_1 = f(\epsilon)\left\{(\epsilon-1) l_1 \left[\frac{1}{3}(6a^2-b^2-c^2) - (a^2 l^2 + b^2 m^2 + c^2 n^2)\right] + \epsilon (b^2 mn^2 - c^2 nm^2)\right\} + f^2(\epsilon) l_1 \left\{(\epsilon-1)\left[(\epsilon-2) I + \epsilon a^2 I_a - \frac{4a}{bc}\right] + \epsilon^2 \mu (b^2 - c^2)/(a b c)\right\} + f_1(\epsilon)\cdot g(\mu)$$

$$\times\left\{(I_b - I_c)\left[\frac{\mu}{2}(b^2+c^2)(mn^2 + nm^2) - mn_2 b^2 - nm_2 c^2\right] - \epsilon\mu (b^2-c^2)(mn^2 + nm^2)/(abc)\right\} + f^2(e)\, g_1(\mu)\, l_1$$

$$\times\left\{(I_b - I_c)\left[(\epsilon-1) k_1(\mu) + \epsilon\mu (\epsilon\mu - 2)(b^2 - c^2)/(a b c)\right]\right\} \qquad D_2$$

$$15 M_1 = \frac{\epsilon-1}{3Q}\left[(\epsilon-1)(I_{ab}\, nn' + I_{ac}\, nm' - 2 I bc\, l l_1) + \frac{2\epsilon}{abc\sum a^2 b^2} \times (2a^2 l l_1 - b^2 m_1 m - c^2 n n_1)\right] \qquad D_3$$

$$15 N_1 = -\frac{1}{3}(\mu-1) f_1(\mu)(b^2 - c^2) l_2 + g_1(\epsilon)\left[(\epsilon/2)(b^2+c^2) \times (mn_1 + n m_1) - b^2 m n_1 - c^2 n m_1\right] + f_1(\mu)\cdot g_1(\epsilon) \times l_2 \left[\epsilon\mu (b^2 - c^2)/(abc) - (\mu-1) k_1(\epsilon)\right] \qquad D_4$$

The expressions for the undefined functions and integrals involved in Eqs. D_1 to D_4 are as follows:

$$f_1(\epsilon) = \left((\epsilon - 1)\ I_a + \frac{2}{a\,b\,c} \right)^{-1} \quad ; \quad I_a = \int_0^\infty \frac{du}{(a^2+u)\ R(u)}$$

$$R(u) = \left[(a^2+u) + (b^2+u) + (c^2+u) \right]^{1/2} \quad ;$$

$$I = \int_0^\infty \frac{du}{R(u)} \quad , I_a = \int_0^\infty \frac{du}{(a^2+u)\ R(u)}$$

$$I_{ab} = \int_0^\infty \frac{du}{(a^2+u)(b^2+u)\ R(u)}$$

$$g_1(u) = \left[(u-1)(b^2+c^2) I_{bc} + \frac{2}{a\,b\,c} \right]^{-1}$$

$$Q = (\epsilon-1)^2 \left(I_{ab}\ I_{bc} + I_{bc}\ I_{ca} + I_{ca} I_{ab} \right) \frac{4\epsilon(\epsilon-1)}{a\,b\,c}$$

$$\times \left(J + \frac{\Sigma a^2}{\Sigma a^2 b^2} J' \right) + \frac{4\epsilon^2}{a^2 b^2 c^2 (\Sigma a^2 b^2)}$$

$$J = \int_0^\infty \frac{du}{\left[R(u)\right]^3} = \left(I_{ab} - I_{ac} \right) / \left(c^2 - b^2 \right)$$

$$J' = \int_0^\infty \frac{u\,du}{\left[R(u)\right]^3} = I_{ab} - C^2 J \qquad \text{etc.}$$

$$\sum a^2 = a^2 + b^2 + c^2 \qquad \sum a^2 b^2 = a^2 b^2 + b^2 c^2 + c^2 a^2$$

$$k_1(\epsilon) = b^2 I_b - c^2 I_c - (\epsilon/2)(b^2+c^2)(I_b - I_c)$$

and the remaining scattering coefficients K_2, K_3, L_2, L_3 etc. of Eqs. 20 and 21 are obtained by cyclic permutations of a, b, c; l, m, n; l_1, m_1, n_1 ; l_2, m_2, n_2

The scattering coefficients referring to magnetic field $\bar{K}_j$, $\bar{L}_j$, $\bar{M}_j$ and $\bar{N}_j$ (j = 1, 2, 3) are obtained from the corresponding K_j, L_j etc. by making the following substitution

$$l_1,\ m_1,\ n_1 \longrightarrow l_2,\ m_2,\ n_2 \quad ;$$

$$l_2,\ m_2,\ n_2 \longrightarrow -l_1, -m_1, -n_1 \quad ; \quad \epsilon \longleftrightarrow \mu .$$

APPENDIX E

Special values of the functions shape factors and integrals involved in the expressions for the scattering coefficients described in Appendix D and in the text are as follows:

$$I_a = \frac{1}{b^2 c} \cdot \frac{P'}{2\pi} \quad ; \quad I_c = \frac{1}{b^2 c} \cdot \frac{P}{2\pi} \qquad P = 4\pi - 2P'$$

where $$P' = \frac{2\pi}{e^2}\left[1 - \frac{b^2/c^2}{2e} \log_e \frac{1+e}{1-e}\right]$$ for prolates

and $$P' = \frac{2\pi}{e^2}\left[\frac{b/c}{e} \sin^{-1} e - b^2/c^2\right]$$ for oblates;

also

$$I_{bc} = \frac{1}{b^2 c} \cdot \frac{3}{2\pi e^2}\left(P' - \frac{4\pi}{3}\right) ;$$

$$I = \frac{1}{ce} \log_e \frac{1+e}{1-e} \quad \text{(for prolates)} ;$$

$$I = \frac{1}{c\sqrt{b^2/c^2 - 1}} \sin^{-1}(e) \quad \text{(for oblates)} :$$

Various relations connecting the integrals are

$$I_a + I_b + I_c = 2/(abc)$$

$$a^2 I_a + b^2 I_b + c^2 I_c = I$$

$$I_{ab} = (I_a - I_b)/(b^2 - a^2)$$

and

$$3I_{aa} + I_{ab} + I_{ac} = \frac{2}{a^3 bc}$$

$$3a^2 I_{aa} + b^2 I_{ab} + c^2 I_{ac} = 3 I_a$$

TABLE I

RADIAL SPHEROIDAL FUNCTIONS

c	ξ	(1) $R_{01}(c,\xi)$	(1) $R_{01}(c,\xi)$	(1) $R_{02}(c,\xi)$	(2) $R_{00}(c,\xi)$	(2) $R_{01}(c,\xi)$	(2) $R_{02}(c,\xi)$
0.1	1.1	.99953	.036615	.(3)5864*	-15.1860	-203.0500	-7.9210×10^{3}
	1.2	.99915	.039916	.(3)7394	-11.9450	-132.2400	-4.2870×10^{3}
	1.3	.99875	.043317	.(3)9185	-10.1290	-97.7920	$-2,761 0 \times 10^{3}$
0.2	1.1	.99638	.073087	.(2)2339	- 7.5446	- 51.2740	-993.0827
	1.1546	.99556	.076624	.(2)2660	- 6.5256	- 39.7550	-671.8480
	1.2	.99480	.079630	.(2)2920	- 5.9110	- 33.5270	-538.2389
	1.3	.99320	.086234	.(2)3612	-4.9920	-24.8900	-347.1258
0.4	1.1	.98561	.144720	.(2)9275	- 3.6810	- 13.3140	-125.8000
	1.2	.97944	.157290	.011740	- 2.8280	- 8.8240	- 68.5000
	1.3	.97288	.169790	.014373	- 2.3470	- 6.6380	- 44.4000
0.6	1.1	.96808	.213700	.020744	- 2.3400	- 6.2643	- 37.9900
	1.2	.95350	.231160	.026080	- 1.7520	- 4.2222	- 20.9230
	1.3	.93990	.248110	.031700	- 1.4110	- 3.2260	- 13.7200
0.8	1.1	.94435	.278260	.036660	- 1.6360	- 3.7640	- 16.5250
	1.2	.92070	.299310 <	.045690	- 1.1660	- 2.5822	- 9.2340
	1.3	.89530	.318970	.055240	- .8840	- 1.9947	- 6.1600

* Numbers in parenthesis refer to the number of zeros between the decimal point and the first significant figure. Thus . (3)5864 = . 0005864.

TABLE II

RADIAL SPHEROIDAL FUNCTIONS

c	ξ	$R_{00}^{(4)}(c,\xi)$	$R_{01}^{(4)}(c,\xi)$	$R_{02}^{(4)}(c,\xi)$
0.1	1.1	. 99953+i15. 1860	. 0366l5+i205. 0500	. (3)5864+i7. 9210xl0^3
	1.2	.99915+i11.9450	.039916+i132.2400	. (3)7394+i4.2870xl0^3
	1.3	. 99875+i110. 1290	. 043317+i 97. 7920	.(3)9185+i2. 76l0xl0^3
0.2	1.1	.99638+i 7.5446	.073087+i 51.2740	. (2)2339+i993.0827
	1.1546	.99556+i6.5256	.076624+i39.7550	. (2)2660+i671. 8480
	1.2	.99480+i5.9110	.079630+i33.5270	. (2)2920+i538. 2389
	1.3	.99320+14.9920	.086234+i24.8900	. (2)36l2+i347. 1258
0.4	1.1	.98561+i3.6810	.144720+i13.3140	.(2)9275+i125.8000
	1.2	.97944+i2.8280	.157290+i8.8240	.011740+i68.5000
	1.3	.97288+i2.3470	.169790+i6.6380	.014373+i44.4000
0.6	1.1	.96808+i2.3400	,213700+i6.2643	.020744+i37.9900
	1.2	.95350+i1.7520	.231160+i4.2222	.026080+i20.9230
	1.3	.93990+i 1.4110	.248110+i3.2260	.031700+i13.7200
0.8	1.1	.94435+i 1.6360	.278260+i3.7640	.036660+i16.5250
	1.2	.92070+i1.1660	. 299319+i2.5822	.045690+i9.2340
	1.3	.89530+i0.8840	. 318970+i1.9947	.055240+i6.1600

TABLE III

DERIVATIVES OF RADIAL SPHEROIDAL FUNCTIONS

c	ξ	$R^{(1)\prime}_{00}(c,\xi)$	$R^{(1)\prime}_{01}(c,\xi)$	$R^{(1)\prime}_{02}(c,\xi)$	$R^{(2)\prime}_{00}(c,\xi)$	$R^{(2)\prime}_{01}(c,\xi)$	$R^{(2)\prime}_{02}(c,\xi)$
0.1	1.1	-.003664	.033225	.001263	47.7110	1.1160×10^{3}	6.1620×10^{4}
	1.2	-.003993	.033198	.001596	22.8040	459.00	2.1529×10^{4}
	1.3	-.004315	.033178	.001731	14.5600	260.00	1.0738×10^{4}
0.2	1.1	-.014588	.065806	.005840	24.0070	277.3110	7.7103×10^{3}
	1.1546	-.015240	.065733	.006118	15.1530	163.3070	4.1639×10^{3}
	1.2	-.015943	.065620	.006354	11.5184	113.7713	2.6954×10^{3}
	1.3	-.017266	.065405	.006875	7.3829	64.2501	1.3451×10
0.4	1.1	-.058140	.125650	.023110	12.3010	70.6200	968.2189
	1.2	-.063200	.124370	.024970	5.9920	29.1000	339.0446
	1.3	-.068210	.121500	.026920	3.9000	16.5100	169.5008
0.6	1.1	-.129490	.177150	.050580	8.5080	31.9460	289.0000
	1.2	-.140026	.172440	.055640	4.2240	13.2960	101.4230
	1.3	-.150280	.167310	.059690	2.7930	7.5590	50.8400
0.8	1.1	-.226560	.213450	. 086910	6.7307	18.5440	123.1200
	1.2	-.243740	.202530	.092847	3.4386	7.7734	43.5700
	1.3	-.259770	.190660	.098170	2.3339	4.5110	21.8800

TABLE IV

DERIVATIVES OF RADIAL SPHEROIDAL FUNCTIONS

c	ξ	$R^{(4)\prime}_{00(c,\xi)}$	$R^{(4)\prime}_{01(c,\xi)}$	$R^{(4)\prime}_{02(c,\xi)}$
0.1	1.1	-.003664-i47.7110	. 033225-il. Il60x10^{3}	.001263-i6. 1620x10^{4}
	1.2	-.003993-i22.8040	.033198-i459.0000	.001596-i2. 1529x10^{4}
	1.3	-.004315-i14.5600	.033178-i260.0000	.001731-i1.0738x10^{4}
0.2	1.1	-.014588-i24.0070	.065806-i277.3110	.005840-i7. 7103x10^{3}
	1.1546	-.015240-i15.1530	.065733-i163.3070	.006118-i4. I639x10^{3}
	1.2	-.015943-i11.5184	.065620-i113.7713	.006354-i2. 6954x10^{3}
	1.3	-.017266-i7.3829	.065405-i64.2501	.006875-i1. 3451x10^{3}
0.4	1.1	-.058140-i12.3010	.125650-i70.6200	.023110-i968.2189
	1.2	-.063200-i5.9920	.124370-i29.1000	.024970-i339.0446
	1.3	-.068210-i3.9000	.121500-i16.5100	.026920-i169.5008
0.6	1.1	-.129490-i8.5080	.177150-i31.9460	.050580-i289.0000
	1.2	-.140026-i4.2240	.172440-i13.2960	.055640-i101.4230
	1.3	-.150280-i2.7930	.167310-i7.5590	.059690-i50.8400
0.8	1.1	-.226560-i6.7307	.213450-i18.5440	.086910-i123.1200
	1.2	-.243740-i3.4386	. 202530-i7.7734	. 092847-i 43.5700
	1.3	-.259770-i2.3339	.190660-i4.5110	.098170-i21.8800

TABLE V

RADIAL SPHEROIDAL FUNCTIONS

c	ξ	$R^{(1)}_{10}(c,\xi)$	$R^{(1)}_{11}(c,\xi)$	$R^{(1)}_{12}(c,\xi)$	$R^{(2)}_{10}(c,\xi)$	$R^{(2)}_{11}(c,\xi)$	$R^{(2)}_{12}(c,\xi)$
0.1	1.1	.01526	.(3)3660	.(5)4400	-254.900	-3136.50	-1.9605×10^{6}
	1.2	.02207	.(3)5297	.(5)7800	-155.330	-1587.70	-8.3643×10^{5}
	1.3	.02769	.(3)7223	.(4)1180	-108.300	-999,900	-4.5867×10^{5}
0.2	1.1	.03050	.001344	.(4)3520	-64.0938	-393.482	-1.2292×10^{4}
	1.1546	.03837	.001773	.(4)4961	-53.9700	-256.770	-8.374×10^{3}
	1.2	.04409	.002104	.(4)6250	-38.3466	-199.291	-5.2511×10^{3}
	1.3	.05519	.002867	.(4)9420	-27.3350	-124.760	-2.8839×10^{3}
0.4	1.1	.06070	.005326	.(3)2810	-16.3700	-50.180	-773.880
	1.2	.08753	.008400	.(3)498	-10.0949	- 25.543	-331.680
	1.3	.10920	.01138	.(3)7478	-7.08100	- 16.070	-182.660
0.6	1.1	.90966	.01188	.001103	-7.48800	- 14.860	-154.530
	1.2	.12968	.01868	.001660	-4.70600	- 7.670	- 66.576
	1.3	.16090	.02516	.002492	-3.41400	- 4.860	- 36.836
0.8	1.1	.11905	.02088	.002210	-4.38700	- 6.490	- 50.600
	1.2	.16968	.03224	.003895	-2.80000	- 3.386	-21.950
	1.3	.20933	.04397	.006910	-2.07700	- 2.188	- 12.781

TABLE VI

RADIAL SPHEROIDAL FUNCTIONS

c	ξ	$R_{10}^{(4)}(c,\xi)$	$R_{11}^{(4)}(c,\xi)$	$R_{12}^{(4)}(c,\xi)$
.1	1.1	.01526+i255.000	. (3)336+i3. 137x10^3	. (5)440+i1. 9605x10^6
	1.2	.02207+i155.300	. (3)530+il. 588x10^3	. (5)780+i8. 3643x10^5
	1.3	.02769+i108.300	.(3)722+i1.000x10^3	. (4)118+i4.5867x10^5
.2	1.1	.03050+i64.090	.001344+i393.50	. (4)352+i1. 2292x10^4
	1.1546	.03837+i53.970	.001773+i256.77	. (4)496+i8.374x10^3
	1.2	.04410+i38.347	. 002100+i 199. 30	. (4)625+i5. 2511x10^3
	1.3	.05519+i27.335	. 002867+i 125. 000	. (4)942+i2.8839x10^3
.4	1.1	.06070+i16.370	.005330+i50.180	. (3)281+i773.88
	1.2	.08750+i10.094	.008400+i25.540	.(3)498+i331.68
	1.3	.1092+i7.081000	. 01138+i16. 070	. (3)748+il82.66
.6	1.1	.09066+i7.49000	. 01188+i14. 860	.001103+i154.53
	1.2	.12968+i4.71000	.01868+i7.670	.00166+i66.5760
	1.3	.16090+i3.41400	.02516+i4.860	.002492+i36.836
.8	1.1	.11905+i4.38700	. 02090+i6.4900	.002210+i50.600
	1.2	.16970+i2.80000	.03220+i3.3860	.003895+i21.950
	1.3	.20930+i2.07700	.04400+i2.1880	. 006910+il2. 781

TABLE VII

DERIVATIVES OF RADIAL SPHEROIDAL FUNCTIONS

c	ξ	$(1)'$ $R_{10(c,\xi)}$	$(1)'$ $R_{11(c,\xi)}$	$(1)'$ $R_{12(c,\xi)}$	$(2)'$ $R_{10(c,\xi)}$	$(2)'$ $R_{11(c,\xi)}$	$(2)'$ $R_{12(c,\xi)}$
0.1	1.1	.07990	.001980	.(4)2930	1.7793×10^{3}	2.7952×10	2.14667×10^{7}
	1.2	.06016	.001880	.(4)3650	613.080	8.6300×10^{3}	5.769×10^{6}
	1.3	.05210	.001970	.(4)4290	320.163	4.080×10	2.43167×10^{6}
0.2	1.1	.15950	.008250	.(3)2612	443.267	3.497×10^{3}	1.34316×10^{5}
	1.1546	.13260	.007664	.(3)2790	298.300	1.700×10^{3}	6.8481×10
	1.2	.11980	.007495	.(3)2904	152.696	1.0804×10^{3}	3.61087×10^{4}
	1.3	.10339	.007587	.(3)3411	79.7370	511.217	1.5225×10^{4}
0.4	1.1	.31580	.032660	.001648	111.048	439.800	8.4326×10^{3}
	1.2	.23440	.029680	.002310	38.1930	136.010	2.2701×10^{3}
	1.3	.20030	.029850	.002697	19.9800	64.4600	958.640
0.6	1.1	.46749	.063340	.007630	49.1000	130.899	1.6760×10^{3}
	1.2	.34240	.068220	.007570	16.9700	40.5800	452.000
	1.3	.28960	.086570	.008120	8.94600	19.2740	191.400
0.8	1.1	.60680	.126240	.015220	27.8690	55.7630	545.400
	1.2	.43660	.111930	.017960	9.60900	17.3290	147.615
	1.3	.35860	.112100	.021750	5.11300	8.25000	62.6880

TABLE VIII

DERIVATIVES OF RADIAL SPHEROIDAL FUNCTIONS

c	ξ	$R^{(4)}_{10(c,\xi)}$	$R^{(4)}_{11(c,\xi)}$	$R^{(4)}_{12(c,\xi)}$
.1	1.1	.0799-il.779x10^{3}	.00148-i2.7952x10^{4}	.(4)293-i2.14667x10^{7}
	1.2	.06016-i613.000	.00188-i.6300x10^{3}	.(4)365-i5.7691x10^{6}
	1.3	.0521-i320.000	.00197-i4.080x10^{3}	.(4)430-i2.43167x10^{6}
.2	1.1	.1595-i443.300	.00825-i3.498x10^{3}	.(3)2612-il.34316x10^{5}
	1.1546	.1326-i298.300	.007664-i1.700x10^{3}	.(3)2790-i6.8481x10^{4}
	1.2	.1198-i152.700	.0075-il.0804x10^{3}	.(3)2904-i3.61087x10^{4}
	1.3	.1034-i79.740	.00759-i511.22	.(3)3411-i1.5225x10^{4}
.4	1.1	.3158-i111.05	.03266-i439.80	.00165-i8.4326x10^{3}
	1.2	.2344-i38.193	.02970-H36.00	.00231-i2.2701x10^{3}
	1.3	.2003-i19.980	.02990-i64.460	.002697-i958.64
.6	1.1	.4675-i49.100	.06334-i130.90	.00763-il.676x10^{3}
	1.2	.3424-i16.970	.06822-i40.580	.00757-i452.000
	1.3	.2896-i8.9460	.08657-i19.270	.00812-i191.400
.8	1.1	.6068-i27.869	.12620-i55.760	.01522-i545.400
	1.2	.4366-i9.6090	.11190-i17.330	.01796-i147.615
	1.3	.3586-i5.1130	.1121-i8.25000	.02175-i62.6880

TABLE IX

NUMERICAL VALUES OF

INTEGRALS OF ANGULAR SPHEROIDA FUNCTIONS

c	I_1^{00}	I_1^{11}	I_1^{22}	I_2^{01}	I_2^{10}	I_2^{12}	I_2^{21}	I_3^{01}	I_3^{10}	I_3^{12}
.1	1.9978	.66590	.40024	-1.9979	-.6664	-1.9987	-.8002	.6656	.6656	.2666
.2	1.9911	.66346	.40080	-1.9888	-.6634	-1.9954	-.8006	.6624	.6624	.2666
.4	1.9652	.65408	.40339	-1.9542	-.6538	-1.9784	-.8026	.6499	.6499	.2665
.6	1.9234	.63879	.40762	-1.8976	-.6377	-1.9447	-.8058	.6297	.6297	.2662
.8	1.8684	.61777	.41360	-1.8279	-.6178	-1.9152	-.8095	.6029	.6029	.2661

c	I_3^{21}	I_4^{01}	I_4^{10}	I_4^{12}	I_4^{21}	I_5^{00}	I_5^{02}	I_5^{11}	I_5^{20}	I_5^{22}
.1	.26657	1.3322	-.(3)889	.79985	-.2665	-1.3326	.(3)302	-.7994	.2665	-.6858
.2	.26661	1.3280	-.003538	.79943	-.2662	-1.3302	.(2)121	-.7997	.2659	-.6868
.4	.26649	1.3137	-.013925	.80166	-.2662	-1.3214	.(2)489	-.7905	.2636	-.6898
.6	.26618	1.2899	-.030550	.80352	-.2655	-1.3056	.010940	-.7745	.2591	-.6950
.8	.26612	1.2582	-.052380	.80721	-.2654	-1.2900	.018410	-.7519	.2531	-.7018

c	I_6^{00}	I_6^{02}	I_6^{11}	I_6^{20}	I_6^{22}
.1	.66649	-1.9994	.3995	.26669	.74268
.2	.66421	-1.9979	.3980	.26688	.7452
.4	.65813	-1.9914	.3937	.26774	.7403
.6	.64755	-1.9806	.3857	.26970	.7370
.8	.63455	-1.9671	.3758	.27103	.73283

$$I_n^{01} = I_n^{10} = I_n^{02} = I_n^{20} = I_n^{12} = I_n^{21} = 0$$

with $n = 1, 5, 6$ and

$$I_n^{00} = I_n^{02} = I_n^{11} = I_n^{20} = I_n^{22} = 0$$

with $n = 2, 3, 4$

TABLE X

DETERMINANTAL COEFFICIENTS

c	ξ	B_{00}	B_{11}	B_{22}	C_{00}	C_{11}	C_{22}
0.1	1.1	-0. 03049i	-0.27650	-0. 01053i	-0. 00335-i43.672	0. 01019-i342. 37	0. (3)2310-il3330
	1.2	-0. 04407i	-0.36660	-0. 01766i	-0. 00529-i30.226	0. 01474-i203.80	0. (3)4240-i57l6
	1.3	-0. 05505i	-0.42340	-0. 02213i	-0. 00686-i24. 163	0. 01847-i144. 55	0. (3)5750-i3570
0.2	1.1	-0. 06038i	-0.27314	-0. 02436i	-0. 01331-i21. 907	0. 02001-i84. 317	0. 001073-il416. 3
	1.2	-0. 08754i	-0.36130	-0. 03516i	-0. 02106-il5. 220	0. 02887-i50. 070	0. 001688-i716. 69
	1.3	-0. 10959i	-0.41627	-0. 04398i	-0. 02857-i12.212	0. 03604-i35.410	0. 002289-i447. 84
0.4	1.1	-0. 11795i	-0.25764	-0. 04819i	-0. 05236-i11. 077	0. 03785-i21.27	0. 004270-i179. 00
	1.2	-0. 1701i	-0.33830	-0. 06 060i	-0. 08233-i7. 8109	0. 05425-i12. 69	0. 006690-i91. 000
	1.3	-0.21223i	-0.38208	-0. 08609i	-0. 1132-i6. 36600	0. 06634-i9. 015	0. 009016-i57. 000
0.6	1.1	-0. l6940i	-0.23735	-0. 07085i	-0. 11406-i7.4960	0. 05212-i9. 397	0. 009450-i54. 000
	1.2	-0.24305i	-0.30648	-0. 11091i	-0. 17850-i5. 3858	0. 07340-i5. 66l	0. 015040-i27.420
	1.3	-0. 30140i	-0.34375	-0. 12815i	-0.23990-i4.4590	0. 08920-i4. 030	0.020210-117.210
0.8	1.1	-0.212331	-.20854	-0. 09187i	-0. 19403-i5. 7634	. 06043-i5.2770	0. 016460-i23. 340
	1.2	-0. 30303i	-.26251	-0. 13020i	-0. 30210-i4. 2620	. 08301-i3. 2020	0. 025460-il1. 953
	1.3	-0. 37330i	-.28565	-0.159lli	-0.40320-i3.6223	. 09786-i2. 3265	0. 033730-i7. 5180

TABLE XI

DETERMINANTAL COEFFICIENTS

c	ξ	D_{01}	D_{10}	D_{21}	D_{12}	U_{01}
0.1	1.1	0.(3)6713+i6268	0.01017+i170.0	0.(3)269+12510	0. (5)88+i3. 9185x10^{6}	-1.5899
	1.2	0.001059+i31730	0.01471+il03. 5	0. (3)424+il271	0. (4)1559+il. 6718x10^{6}	-1.8386
	1.3	0.001443+i19980	0.01845+i72.18	0.(3)578+18000	0. (4)2358+i0. 9194x10^{6}	-2.0830
0.2	1.1	0.002673+i782.6	0.02023+i42.52	0.00108+i31500	0. (4)7024+i0. 02453x10^{6}	-1.5821
	1.2	0.004176+i396.4	0.02926+i25.44	0.00168+il59560	0. (3)1247+il. 0478x10^{4}	-1.8270
	1.3	0.005702+i248.6	0. 03660+i18. 13	.00230+il00. 100	0. (3)1881+i0. 5754x10^{4}	-2.0645
0.4	1.1	0.010416+i98.06	0.03970+i10. 70	0.00428+i40.274	0. (3)5559+il. 531	-1.5489
	1.2	0.016420+i49.91	0. 05721+i6. 600	0.00674+i20.498	0. (3)9852+i656	-1.7783
	1.3	0.022240+i31.40	0.07139+i4.630	0.00914+i12.898	0. (2)148+i36l0	-1.9998
0.6	1.1	0.022540+i28.20	0.05781+i4.776	0. 00957+il 1. 97	0.00214+i30100	-1.4949
	1.2	0.035450+i14. 56	0.08270+i3.004	0.01505+i6.180	0.003228+i1290	-1.7013
	1.3	0.047740+i9.220	0.12600+i2.177	0.02027+i3.916	0.004862+i71.6	-1.8924
0. 8	1.1	0.038200+i11.86	0.07360+i2.710	0.01692+i5.254	0.00423+i96.91	-1.4219
	1.2	0.058860+i6. 189	0. 10484+il. 730	0. 02607+i2. 741	0. 00747+i42. 04	-1.5991
	1.3	0.080430+i4.000	0.12930+i1.283	0.03560+il. 771	0.01321+i24.48	-1.7547

TABLE XII

DETERMINANTAL COEFFICIENTS

c	ξ	$U_{10}+U_{12}$	U_{21}	V_{01}	V_{10}	V_{12}	V_{21}
.1	1.1	-0. 035l94i	0.2421	0. 0583+i143. 31	-0. 00149-i6.684	0. (3)476+i3,520	-0. 008876-i122
	1.2	-0. 05600i	0.2219	0. 0735+i76. 970	-0. 00224-i6. 691	0. (3)897+il, 598	-0. 008867-i96. 13
	1.3	-0. 07300i	0.2057	0. 09026+i49, 90	-0. 00312-i6. 699	0.00127+1896	-0. 008910-i81. 71
.2	1.1	-0. 08094i	0.2419	0. 1160+i36. 00	_0.00591-i3. 366	0. 00239+i441.60	-0. 01773-130. 54
	1.2	-0. 11067i	0.2219	0. 146l+i20.27	-0. 00887-i3. 378	0. 00355+i200. 14	-0. 01774-i24. 06
	1.3	-0. 14425i	0.2042	0. 1785+i13.60	-0. 01246-i3. 392	0. 00502+il 13. 31	-0. 01792. i20.43
.4	1.1	-0.15899i	0.2415	0.2263+i9.603	-0. 02302.il. 735	0. 00947+i56. 70	-0.03535^17.850
	1.2	-0.21850i	0.2235	0.2834+i5. 590	-0. 03444-il. 761	0. 01422+i26. 16	-0. 03568-i6. 231
	1.3	-0.28265i	0.2107	0.3444+i3.931	-0. 04820-il. 791	0.0200+i15.093	-0. 03641-i5. 334
.6	1.1	-0.23242i	0.2401	0. 3267+i4. 664	-0. 04965-i1.216	0. 02116+i17. 43	-0. 05252-i3. 679
	1.2	-0. 3l797i	0.2242	0.4056+i2.854	-0. 07375-il. 235	0. 03167+i8.296	-0. 05346-i2. 902
	1.3	-0.40842i	0.2126	0.4888+i2. 125	-0. 10260-il. 270	0.04410+i5.227	-0. 05490-i2. 502
.8	1.1	-0.2995i	0.2391	0.4121+i2.861	-0. 08310-i0. 947	0.03740+i7.794	-. 06927-i2. 135
	1.2	-0.40475i	0.2265	0. 5056+il. 846	-0. 12270-il. 015	0. 055l2+i3.843	-. 07159-il. 732
	1.3	-0. 51500i	0.2191	0. 6011+il. 386	-0. 16900-il. 056	0. 07600+i2. 187	-0.7509-i1.516

TABLE XIII

DETERMINANTAL COEFFICIENTS

c	ξ	W_{00}	W_{11}	W_{22}	W_{02}	W_{20}
0.1	1.1	0.05834-il, 117	0.(3)85-il0,690	0. (4)117-i6. 753963x10^6	-0. (5)403-il, 793, 186	-0.00886+i270.2
	1.2	0.07358-i581.65	0.001214-i5, 071	0. (4)239-i2. 737731x10^6	-0. (4)1034-il, 108, 052	-0. 00886+i157. 5
	1.3	0.09030-i400.46	0.001943-i3, 187	0. (4)391-il. 516644x10^6	-0. (4)196-i760,978	-0.00886+i116.2
0.2	1.1	0.11623-i277.74	0.003562-i1,335	0.(3)102-i41,886.9	-0. (4)324-ill, 166	-0.01765+167.Z6
	1.2	0.14636-il45.38	0.005316-i634.4	0. (3)1898-il7, 143. 0	-0. (4)833-i6,926	-0.01754+i59.20
	1.3	0.17903-i99.460	0.007486-i399.0	0.(3)310-i9,505.00	-0.(3)1564-i4767	-0.0175+128.98
0.4	1.1	0.22867-i68.969	0. 01397-i166. 00	0.(3)787-12,670.0	-0. (3)25645-i686.0	-0.03452+U6.77
	1.2	0.28480-i35.790	0.02088-i78.920	0.001507-il, 083.7	-0. (3)666-i429.4	-0.0337+i9,81
	1.3	0. 34550-i24. 618	0.02925-i49.730	0.00247-i602.00	-0.00125-i297.0	-0.0327+i7.264
0.6	1.1	0.33460-i30.090	0.02683-i48.50	0.003047-i535.0	-0.00104-i120.0	-0.04989+i7.337
	1.2	0.41170-i15.616	0.04684-i23.06	0.0050-i217.5	-0.00225-i83.54	-0.04749+14.342
	1.3	0.49480-i10.768	0.0805-i14.540	0.00762-i121.0	-0.00424-i55.6	-0.0450+13.263
0.8	1.1	0,42920-i16.847	0.0514-i20.020	0.00463-i176.01	-0.00214-i40.56	-0.0626+14.101
	1.2	0.51990-i8.6890	0.0753-i9.5300	0.01196-i71.86	-0.00536-i26.44	-0.0580+i2.440
	1.3	0.60950-i6.0228	0. 105-i6.02000	0.0207-i39.70	00.0117-i19.63	-0.051+il. 865

TABLE XIV

SCATTERING COEFFICIENTS (REAL AND IMMAGINARY PARTS)

$\xi = 1.1$

c	$Re(\alpha_{00})$	$Im(\alpha_{00})$	$Re(\alpha_{01})$	$Im(\alpha_{01})$	$Re(\alpha_{02})$	$Im(\alpha_{02})$
0.1	.(2)1133*	.(6)1014	-.(6)1935	-. (2)1620	. (5)1360	.(10)1900
0.2	.(2)4843	.(5)3420	-.(5)6224	-.(2)6530	.(4)3019	.(8)2953
0.4	.(1)1883	.(3)1018	-.(4)5129	-. (1)2509	.(3)4771	.(6)3155
0.6	.(1)4001	.(3)6766	-.(2)1383	-.(1)5408	.(2)2 338	.(5)3705
0.8	.(1)6691	.(2)2221	-.(2)5321	-.(1)8841	.(2)7225	.(4)1566

$\xi = 1.2$

0.1	.(2)2450	.(6)5834	-. (5)1068	-.(2)3652	.(5)5092	.(9)3210
0.2	.(2)9635	.(4)1480	-.(4)4332	-.(1)1714	.(4)8199	. (7)1115
0.4	.(1)3675	.(3)4219	-.(2)1074	-.(1)5697	.(2)1194	.(5)1127
0.6	.(1)7763	.(2)2690	-.(2)7755	-. (0)1225	.(2)6762	. (5)5861
0.8	.(0)1419	.(2)9847	-.(1)3026	-. (0)2062	. (1)1937	. (3)1067

$\xi = 1.3$

0.1	.(2)3757	.(5)1174	-.(5)3055	-.(2)5915	.(4)102 5	.(9)2917
0.2	.(1)1472	.(4)3724	-.(4)9788	-.(1)2361	. (3)1613	.(7)2998
0.4	.(1)5530	.(2)1020	-.(2)3018	-.(1)9121	.(2)2518	.(5)2 042
0.6	. (0)1141	.(2)6150	-.(1)2339	-. (0)1980	.(1)1256	.(4)1328
0.8	.(0)1759	.(1)1801	-.(1)8032	-.(0)3140	. (1)3670	'.(3)5219

* The numbers within the parentheses denote the number of zeros between the decimal point and the first significant figure. Thus . (2)1133 = . 001133.

TABLE XIV A

DENOMINATOR DETERMINANTS G, H
(REAL AND IMMAGINARY PARTS)

ξ =1.1

c	Re (G)	Im (G)	Re (H)	Im (H)
0.1	5.7232(5)*	6.3958(9)	-3.4958(8)	2.9285(12)
0.2	2.9706(4)	4.2105(7)	-1.0594(6)	1. 1143(9)
0.4	1.8004(3)	3.3402(5)	-8.6227(3)	4.4125(6)
0.6	3.3424(2)	1.9920(4)	-4.2051(3)	1. 6853(5)
0.8	8.8926(1)	2.7191(3)	-9.9284(2)	1.7275(4)

ξ =1.2

0.1	2.2292(5)	9.3609(8)	-1.1703(8)	4.0047(11)
0.2	1.1341(4)	7.3941(6)	-3.9035(5)	1.5630(8)
0.4	6.8297(2)	5.9905(4)	-1.1093(4)	5.9830(5)
0.6	1.2358(2)	3.6236(3)	-1.4115(3)	2.2937(4)
0.8	3.4907(1)	5.1604(2)	-3.3295(2)	2. 3414(3)

ξ =1.3

0.1	9.5443(4)	3.0538(8)	-5.9198(7)	1.1478(11)
0.2	6.1140(3)	2.4215(3)	-1.8059(5)	4.3801(7)
0.4	3.6592(2)	2.0014(4)	-5.5793(3)	1.7185(5)
0.6	6.3943(1)	1.2260(3)	-7.2291(2)	6.5517(3)
0.8	1.7900(1)	1.8206(2)	-1.6989(2)	6.9386(2)

* The number within the parentheses at the end denote the powers of ten by which the whole number is to be multiplied. Thus 5. 7232(5) = 572320.

TABLE XV

DERIVATIVES OF BESSEL FUNCTIONS

ξ	c	$c\xi$	j_0'	j_1'	j_2'	j_3'	j_4'
1.1	.1	.11	-.00366	+.033212	+.001463	+,(4)345	+.(6)5631
	.2	.22	-.014594	+.06570	+.005826	+.(3)276	+.(5)8978
	. 4	.44	-.05752	+.12565	+.022911	+. (2)2167	+.(3)1422
	.6	.66	-.12636	+.17452	+.049584	+.(2)7158	+.(3)7056
	.8	.88	-.2168	+.20758	+.08374	+.01645	+.(2)2174
1.2	.1	.12	-.(2)399	+.033186	+.001596	+.(4)411	+.(6)7289
	. 2	.24	-.0159	+.065514	+.00634	+.(3)326	+. (4)l166
	. 4	.48	-.06252	+.12437	+.02476	+.(2)2575	+.(3)1840
	.6	.72	-.13668	+.16986	+.05455	+.(2)8466	+.(3)9102
	.8	.96	-.23320	+.196850	+.08944	+.019320	+.(2)37904
1.3	.1	.13	-.00433	+.033165	+.0017307	+.(4)4843	+.(6)9333
	.2	.26	-.01722	+.0653	+.00686	+.(3)384	+.(4)14844
	.4	.52	-.067480	+.12268	+.02668	+.(2)3017	+.(3)2334
	.6	.78	-.14670	+.164778	+.058524	+.(2)98466	+.(2)11508
	.8	.104	-.24848	+.18522	+.09454	+.02182	+.(2)35136

TABLE XVI

NUMERICAL VALUES OF N_{ml} and A_{ml} for m = 0; l= 0, 1 and 2

c	N_{0l}			A_{ol}		
	l=0	1	2	0	1	2
.1	1.9978	.66590	.40024	.99944	3.0004i	-5.0005
.2	1.9911	.66347	.40080	.99770	3.0024i	-4.9950
.4	1.9652	.65408	.40339	.99100	3. 009li	-4.9768
.6	1.9234	.63879	.40762	.97989	3.0201i	-4.9477
.8	1.8684	.61777	.41360	.96288	3.036li	-4.9062

TABLE XVII

SCATTERING COEFFICIENTS OF STEVENSON'S THEORY (Eq. 38)

ξ	b/a	K_1/b^2a	$\bar{K}_2/b^2a$	L_1/a^3b^2	N_2/a^3b^2	$\bar{L}_2/a^3b^2$	$\bar{N}_1/a^3b^2$	A	B
1.005	.1000	.6804	-.6533	-.1528	.0890	.2490	.0227	1.3338	-.5792
1.10	.4167	.7767	-.5839	-.0916	.0886	.2197	.0259	1.3601	-.4861
1.20	.5528	.8261	-.5588	-.0354	.0873	.2108	.0275	1.3848	-.4174
1.30	.6390	.8591	-.5446	+.0129	.0870	.2052	.0286	1.4036	-.3602

TABLE XVIII

REAL AND IMAGINARY PARTS OF THE SCATTERING COEFFICIENTS FOR PROLATE DROPS AT 3 cm (Horizontal Polarization)

b/c	$Re(K_1')$	$Im(K_1')$	$Re(L_1')$	$Im(L_1')$	$Re(\bar{L}_3')$	$Im(\bar{L}_3')$	$Re(N_3')$	$Im(N_3')$	$Re(\bar{N}_1')$	$Im(\bar{N}_1')$
.95	.(0)9418	-.(1)1750	.(0)6895	-.(1)3610	.1929(1)	-.(0)9050	.(1)9257	-.(2)1520	.(2)4780	-.(4)9306
.90	.(0)9257	-.(1)1690	.(0)6217	-.(1)3090	.1730(1)	-.(0)8120	.(1)7950	-.(2)1230	.(2)9010	-.(4)4910
.85	.(0)9082	-.(1)1630	.(0)5569	-.(1)2740	.1544(1)	-.(0)7250	.(1)6994	-.(2)1080	.(1)1204	-.(4)6700
.80	.(0)8828	-.(1)1560	.(0)4961	-.(1)2440	.1366(1)	-.(0)6400	.(1)6098	-.(2)1074	.(1)1673	-.(4)8300
.75	.(0)8710	-.(1)1500	.(0)4401	-.(1)2120	.1205(1)	-.(0)5650	.(1)5185	-.(3)7900	.(1)1990	-.(4)8200
.70	.(0)8528	-.(1)1430	.(0)3777	-.(1)1830	.1044(1)	-.(0)4900	.(1)4545	-.(3)6700	.(1)2190	-.(3)3300
.60	.(0)8172	-.(1)1320	.(0)2965	-.(1)1380	.(0)7690	-.(0)3610	.(1)3250	-.(3)4700	.(1)2770	-.(3)1100
.40	.(0)7465	-.(1)1100	.(0)1587	-.(2)7400	.(0)3410	-.(0)1600	.(1)1380	-.(3)1900	.(1)3280	-.(3)5500
.20	.(0)6874	-.(2)9300	.(1)7350	-.(2)4100	.(1)8520	-.(1)4000	.(2)3300	-.(4)4300	.(1)3220	+.(4)6700
.10	.(0)6500	-.(2)5000			.(1)2130	-.(1)1000				

TABLE XIX

REAL AND IMAGINARY PARTS OF THE SCATTERING COEFFICIENTS FOR OBLATE DROPS AT 3 cm (Horizontal Polarization)

c/b	$Re(K_1')$	$Im(K_1')$	$Re(L_1')$	$Im(L_1')$	$Re(\bar{L}_3')$	$Im(\bar{L}_3')$	$Re(N_3')$	$Im(N_3')$	$Re(\bar{N}_1')$	$Im(\bar{N}_1')$
.95	.(0)9830	-.(1)1890	.(0)8958	-.(1)4870	.2371(1)	-.1113(1)	.(1)8852	-.(2)1310	.(2)3010	.(2)2270
.90	.1003(1)	-.(1)1990	.(0)9261	-.(1)5840	.2633(1)	-.1236(1)	.(0)1021	-.(2)1660	.(2)6320	.(2)2920
.85	.1030(1)	-.(1)2090	.1071(1)	-.(1)6290	.2954(1)	-.1386(1)	.(0)1215	-.(2)2060	.(1)1290	.(2)4800
.75	.1087(1)	-.(1)2320	.1387(1)	-.(1)9430	.3793(1)	-.1780(1)	.(0)1581	-.(2)2740	.(1)2310	.(2)9640
.70	.1124(1)	-.(1)2470	.1622(1)	-.(0)1032	.4357(1)	-.2045(1)	.(0)1856	-.(2)3320	.(1)3230	.(1)1280
.60	.1212(1)	-.(1)2860	.2303(1)	-.(0)1737	.5933(1)	-.2784(1)	.(0)2678	-.(2)2678	.(1)6040	.(1)2170
.40	.1541(1)	-.(1)4630	.5376(1)	-.(0)4914	.1333(2)	-.6255(1)	.(0)7308	-.(1)1680	.(0)2373	.(1)6100
.20	.2419(1)	-.(0)1180	.3038(2)	-.4188(1)	.5337(2)	-.2505(2)	.4445(1)	-.(0)1564	.(0)7970	.(0)2074
.10	.3990(1)	-.(0)3160	.1909(3)	-.4000(2)	.2135(3)	-.1002(3)				

TABLE XX

REAL AND IMAGINARY PARTS OF THE SCATTERING COEFFICIENTS FOR PROLATE DROPS AT 3 cm (Vertical Polarization)

b/c	$Re(K_3')$	$Im(K_3')$	$Re(\bar{L}_1')$	$Im(\bar{L}_1')$	$Re(L_3')$	$Im(L_3')$	$Re(\bar{N}_3')$	$Im(\bar{N}_3')$	$Re(N_1')$	$Im(N_1')$
.80	.1156(1)	-.(1)2570	.1766(1)	-.(0)9180	.5529(1)	-.2533(1)	.0000(0)	.0000(0)	.(1)8250	-.(2)1060
.60	.1497(1)	-.(1)4480	.1690(1)	-.(0)8870	.5055(1)	-.1961(1)	.0000(0)	.0000(0)	.(1)8280	-.(2)1000
.20	.4814(1)	-.(0)4630	.1941(1)	-.1028(1)	.2320(2)	-.7327(1)	.0000(0)	.0000(0)	.(1)7290	-.(3)1710

TABLE XXI

REAL AND IMAGINARY PARTS OF THE SCATTERING COEFFICIENTS FOR OBLATE DROPS AT 3 cm (Vertical Polarization)

c/b	$Re(K_3')$	$Im(K_3')$	$Re(\bar{L}_1')$	$Im(\bar{L}_1')$	$Re(L_3')$	$Im(L_3')$	$Re(\bar{N}_3')$	$Im(\bar{N}_3')$	$Re(N_1')$	$Im(N_1')$
1.25	.(0)8160	-.(1)1290	.2539(1)	-.1325(1)	.8459(1)	-.4245(1)	.0000(0)	.0000(0)	-.(1)5130	-.(3)2910
1.667	.(0)6820	-.(2)9000	.3541(1)	-.1852(1)	.1220(2)	-.6256(1)	.0000(0)	.0000(0)	-.(1)2620	-.(3)2110
5.0	.(0)4370	-.(2)3890	.2556(2)	-.1342(2)	.6830(2)	-.3570(2)	.0000(0)	.0000(0)	-.(2)1380	.(3)3200

TABLE XXII

REAL AND IMAGINARY PARTS OF THE SCATTERING COEFFICIENTS FOR PROLATE DROPS AT 10 cm (Horizontal Polarization)

b/c	$Re(K_1')$	$Im(K_1')$	$Re(L_1')$	$Im(L_1')$	$Re(\bar{L}_3')$	$Im(\bar{L}_3')$	$Re(N_3')$	$Im(N_3')$	$Re(\bar{N}_1')$	$Im(\bar{N}_1')$
.95	.(0)9450	-.(2)5820	.(0)7060	-.(2)8550	.2400(1)	-.(0)3700	.(1)7490	-.(3)3690	.(3)1800	.(4)1771
.90	.(0)9290	-.(2)5440	.(0)6330	-.(2)6450	.2153(1)	-.(0)3320	.(1)6380	-.(3)2990	.(3)4500	.(4)3350
.85	.(0)9080	-.(2)4760	.(0)5660	-.(2)5860	.1922(1)	-.(0)2960	.(1)5610	-.(3)2590	.(3)8700	.(4)4480
.80	.(0)8920	-.(2)4890	.(0)5050	-.(2)5220	.1698(1)	-.(0)2620	.(1)4900	-.(3)2220	.(2)1310	.(4)5690
.75	.(0)8700	-.(2)4210	.(0)4450	-.(2)3720	.1499(1)	-.(0)2310	.(1)4260	-.(3)1920	.(2)1890	.(4)6360
.70	.(0)8540	-.(2)4340	.(0)3950	-.(2)3640	.1300(1)	-.(0)2000	.(1)3650	-.(3)1610	.(2)2500	.(4)7290
.60	.(0)8170	-.(2)3790	.(0)3030	-.(2)2620	.(0)9570	-.(0)1470	.(1)2610	-.(3)1120	.(2)3930	.(4)8540
.50	.(0)7850	-.(2)4060	.(0)2270	-.(2)2020	.(0)6320	-.(1)9200	.(1)1770	-.(4)7430	.(2)5380	.(4)9550
.40	.(0)7480	-.(2)3510	.(0)1610	-.(3)9700	.(0)4250	-.(1)6550	.(1)1110	-.(4)4530	.(2)7060	.(4)9480
.30	.(0)7170	-.(2)3260	.(0)1140	-.(3)7030	.(0)2390	-.(1)3680	.(2)6060	-.(4)2430	.(2)9410	.(4)9400
.20	.(0)6900	-.(2)3320	.(1)7850	-.(3)4030	.(0)1060	-.(1)1630	.(2)2650	-.(4)1040	.(2)9920	.(4)9520
.10	.(0)6640	-.(2)2850	.(1)5540	_.(3)3420	.(1)2660	-.(2)4090	.(3)6540	-.(5)2540	.(1)1079	.(4)8790

TABLE XXIII

REAL AND IMAGINARY PARTS OF THE SCATTERING COEFFICIENTS FOR OBLATE DROPS AT 10 cm (Horizontal Polarization)

c/b	$Re(K_1)$	$Im(K_1)$	$Re(L_1)$	$Im(L_1)$	$Re(\bar{L}_3)$	$Im(\bar{L}_3)$	$Re(N_3)$	$Im(N_3)$	$Re(\bar{N}_1)$	$Im(\bar{N}_1)$
.95	.(0)9840	-.(2)5770	.(0)8640	-.(1)1620	.2950(1)	-.(0)4540	.(1)9160	-.(3)4510	.(2)1740	-.(4)2110
.90	.1004(1)	-.(2)5890	.(0)9620	-.(1)1060	.3277(1)	-.(0)5050	.(0)1020	-.(3)5040	.(2)3950	-.(4)4660
.85	.1030(1)	-.(2)6310	.1084(1)	-.(1)1080	.3676(1)	-.(0)5660	.(0)1180	-.(3)5960	.(2)6800	-.(4)8020
.80	.1056(1)	-.(2)6440	.1233(1)	-.(1)1510	.4154(1)	-.(0)6400	.(0)1360	-.(3)7020	.(1)1060	-.(3)1280
.75	.1072(1)	-.(2)7370	.1508(1)	-.(1)3260	.4720(1)	-.(0)7270	.(0)1580	-.(3)8340	.(1)1490	-.(3)2020
.70	.1135(1)	-.(2)7760	.1651(1)	-.(1)2140	.5422(1)	-.(0)8350	.(0)1860	-.(2)1010	.(1)2210	-.(3)2730
.60	.1215(1)	-.(2)8720	.2332(1)	-.(1)3500	.7383(1)	-.1137(1)	.(0)2680	-.(2)1540	.(1)4240	-.(3)5200
.50	.1337(1)	-.(1)1045	.3530(1)	-.(1)5470	.1060(2)	-.1634(1)	.(0)4180	-.(2)2600	.(1)8410	-.(3)7510
.40	.1528(1)	-.(1)1400	.6028(1)	-.(0)1130	.1658(2)	-.2555(1)	.(0)732	-.(2)5130	.(0)1800	-.(2)2470
.30	.1835(1)	-.(1)2000	.1220(2)	-.(0)2580	.2950(2)	-.4544(1)	.1532(1)	-.(1)1260	.(0)4500	-.(2)6760
.20	.2427(1)	-.(1)3510	.3397(2)	-.(0)9980	.6642(2)	-.1023(2)	.4473(1)	-.(1)4770	.1540(1)	-.(1)2810
.10	.4022(1)	-.(1)9370	.2052(3)	-.1136(2)	.2658(3)	-.4094(2)	.2924(2)	-.(0)5090	.1164(2)	-.(0)3110

REPORTS OF INVESTIGATIONS
ISSUED BY THE STATE WATER SURVEY

No. 1. Temperature and Turbidity of Some River Waters in Illinois. 1948*
No. 2. Groundwater Resources in Winnebago County, With Specific Reference to Conditions at Rockford. 1948
No. 3. Radar and Rainfall. 1949*
No. 4. The Silt Problem at Spring Lake, Macomb, Illinois. 1949*
No. 5. Infiltration of Soils in the Peoria Area. 1949
No. 6. Groundwater Resources in Champaign County. 1950
No. 7. The Silting of Ridge Lake, Fox Ridge State Park, Charleston, Illinois. 1951*
No. 8. The Silting of Lake Chautauqua, Havana, Illinois. 1951
No. 9. The Silting of Carbondale Reservoir, Carbondale, Illinois. 1951*
No. 10. The Silting of Lake Bracken, Galesburg, Illinois. 1951
No. 11. Irrigation in Illinois. 1951*
No. 12. The Silting of West Frankfort Reservoir, West Frankfort, Illinois. 1951
No. 13. Studies of Thunderstorm Rainfall with Dense Raingage Networks and Radar. 1952*
No. 14. The Storm of July 8, 1951, in North Central Illinois. 1952
No. 15. The Silting of Lake Calhoun, Galva, Illinois. 1952
No. 16. The Silting of Lake Springfield, Springfield, Illinois. 1952
No. 17. Preliminary Investigation of Groundwater Resources in the American Bottom. 1953
No. 18. The Silting of Lake Carthage, Carthage, Illinois. 1953
No. 19. Rainfall-Radar Studies of 1951. By G. E. Stout, J. C. Neill, and G. W. Farnsworth. 1953
No. 20. Precipitation Measurements Study by John C. Kurtyka. 1953
No. 21. Analysis of 1952 Radar and Raingage Data by J. C. Neill. 1953
No. 22. Study of an Illinois Tornado Using Radar, Synoptic Weather and Field Survey Data by F. A. Huff, H. W. Hiser and S. G. Bigler. 1954
No. 23. Bubbler System Instrumentation for Water Level Measurement by G. H. Nelson. 1955
No. 24. The Storm of July 18-19, 1952 Rockford, Illinois, and Vicinity by Bernt O. Larson, Homer W. Hiser and Warren S. Daniels. 1955
No. 25. Selected Methods for Pumping Test Analysis. By Jack Bruin and H. E. Hudson, Jr. 1955
No. 26. Groundwater Resources in Lee and Whiteside Counties. By Ross Hanson. 1955
No. 27. The October 1954 Storm in Northern Illinois. By F. A. Huff, H. Hiser and G. E. Stout 1955

*Out of print